

CHALMERS



Impact of PAPR on link adaptation strategies of OFDM based systems

Master of Science Thesis

FAISAL TARIQ

Department of Signals and Systems
Division of Communication Systems
CHALMERS UNIVERSITY OF TECHNOLOGY
Göteborg, Sweden, 2007
Report No. EX067/2007



Department of Signals and Systems

Impact of PAPR on Link Adaptation Strategies of OFDM Based Systems

by

Faisal Tariq,

Thesis

Presented to the Chalmers University of Technology

in Partial Fulfillment of the Requirements for the Degree of

Master of Science

Chalmers University of Technology

May 2007

Copyright

by

Faisal Tariq

2007

The Dissertation Committee for Faisal Tariq
certifies that this is the approved version of the following dissertation:

Impact of PAPR on Link Adaptation Strategies of OFDM Based Systems

Committee:

Prof. Thomas Eriksson, Examiner

Impact of PAPR on Link Adaptation Strategies of OFDM Based Systems

Faisal Tariq, M.Sc.

Chalmers University of Technology, 2007

Supervisor:

In this work, the impact of non linear distortion due to High Power Amplifier (HPA) on the performance of Orthogonal Frequency Division Multiplexing (OFDM) based wireless system has been analyzed for both coded and uncoded system when Link Adaptation (LA) is used. LA maximizes the throughput while maintaining a certain QoS constraint. It is found that when OFDM signal with high PAPR suffers non linear distortion due to non ideal HPA, LA fails to meet the target Block Error Rate (BLER). Detailed analysis of the distortion and effects on Link Adaptation is presented in this work. Difference in the effect on the performance of uncoded and FEC coded systems is also described. It is shown in this work that the Adaptive Modulation and Coding (AMC) threshold for switching modulation and coding rates must be updated to make the LA system satisfy the target BLER constraint. It is also shown that the impairment has severe impact on uncoded system while it is reduced in coded systems.

Dedicated To My Parents

Acknowledgement

I am deeply indebted to my supervisor Prof. Ramjee Prasad, for inviting me to carry out the research work at CTIF and for giving me the opportunity to learn from his vast knowledge and experience. Without the careful guidance of my co-supervisor Suvra Sekhar Das it was not possible for me to complete the project. He has been everything a student want in his supervisor. Muhammad Imadur Rahman, my other co-supervisor, for whom no word is enough to express his contribution both to the project and to my career. Whenever I was in trouble, it was him who always stood beside me selflessly.

I am grateful to my examiner Prof. Thomas Eriksson for managing time to evaluate my thesis which took considerable amount of his vacation time. Thanks also to Nima Seifi for his valuable insights and suggestions. I am indebted to Fakhru Alam of Massey University for introducing me to wireless arena. My special thanks to Muhammad Sajjadur Rahim, Sabbir Ahmed and Dua Idris for managing time to read the manuscript despite there busy schedule. Their valuable comments certainly helped a lot to improve the quality of the report.

I can never forget the motherly care of Maizura Ailin, specially when I was sick after an accident. Nurul Huda Mahmood helped me selflessly in every possible way. I am grateful to him for his tremendous support and encouragement throughout my stay there in Aalborg. The vibrant MS@AAU members and the activities we did together was the source of all joy and happiness. Finally, it is my parents, brothers and sisters whose unconditional love and support give me the strength to stay aborad for carrying out the Masters Studies.

FAISAL TARIQ

Chalmers University of Technology

May 2007

Contents

Abstract	iv
Acknowledgments	vi
Acknowledgement	vii
List of Figures	xi
List of Tables	xv
Abbreviations	xv
Chapter 1 Introduction	1
1.1 Background	1
1.2 Motivation	2
1.3 Goal of the Project	3
1.4 Scope of the project	4
1.5 Organization of Report	5
Chapter 2 Wireless Channel, Baseband Modulation and OFDM	7
2.1 Wireless Channel Characteristics	7
2.1.1 Propagation Loss	8
2.1.2 Small Scale Fading	9
2.1.3 Time Varying Channel	10
2.2 Quadrature Amplitude Modulation	11
2.2.1 Probability of Error in QAM	12

2.3	OFDM Basics	12
2.3.1	Historical Background	13
2.3.2	Principle of Orthogonality	14
2.3.3	OFDM Analytical Model	14
2.3.4	OFDM System Design	17
2.3.5	Comparison of Single and Multi-Carrier Techniques	19
2.3.6	Advantages of OFDM	19
2.3.7	Disadvantages of OFDM	21
2.4	Wireless Broadband Standard	22
2.4.1	3GPP-LTE	23
2.4.2	WiMAX	24
Chapter 3 High Power Amplifier and PAPR in OFDM		27
3.1	Introduction	27
3.2	HPA Models	28
3.2.1	TWTA Model	28
3.2.2	SSPA Model	29
3.3	PAPR in OFDM	31
3.3.1	CDF of PAPR	32
3.4	Effect of HPA and BO Power	35
3.4.1	Effect on Constellation Points	35
3.4.2	Effect on Power Spectrum	35
3.4.3	SDNR Plot	37
3.5	Performance of Different Modulation and Coding	43
3.5.1	Performance in AWGN Channel	44
3.5.2	Performance in Fading Channel	52
3.6	Conclusion	60
Chapter 4 Influence of PAPR on Link Adaptation		62
4.1	Introduction	62
4.2	Link Adaptation Concept	63

4.2.1	LA with PAPR	66
4.3	Link Adaptation Algorithm	67
4.4	Performance of LA based OFDM System	69
4.4.1	CDF of PAPR for LA System	69
4.4.2	Performance in AWGN Channel	70
4.4.3	Performance in Fading Channel	73
4.5	Conclusion	78
Chapter 5 Conclusion		79
5.1	Summary	79
5.2	Further Work	80
Appendix A BLER and SE performance for Coded System		82
Appendix B BER performance of Coded System		99
Bibliography		109
Vita		113

List of Figures

2.1	QAM Constellation Diagram	11
2.2	Time domain view of principle of orthogonality	14
2.3	Frequency domain view of principle of orthogonality	15
2.4	Block Diagram of OFDM Transceiver Systems	17
2.5	Comparison between OFDM and Conventional FDM	20
3.1	Transfer Function and of Rapps model with BO scenario.	29
3.2	Relation between Amplifier Distortion and BO Power	30
3.3	Comparison of theoretical and simulated CDF of PAPR	33
3.4	Effect of Different Modulation Scheme on CDF of PAPR	34
3.5	Effect of FEC on CDF of PAPR	34
3.6	16QAM basic constellation points	35
3.7	Effect of BO on 16QAM constellation points	36
3.8	Subcarrier Organization for Spectrum plot	37
3.9	Spectrum plot of OFDM signal	37
3.10	SDNR plot for 4QAM modulation in AWGN Channel.	38
3.11	SDNR plot for 4QAM modulation in Fading Channel.	39
3.12	SDNR plot for 16QAM modulation in AWGN Channel	40
3.13	SDNR plot for 16QAM modulation in Fading Channel	40
3.14	SDNR plot for 64QAM modulation in AWGN Channel	42
3.15	SDNR plot for 64QAM modulation in Fading Channel	42
3.16	BER vs SNR curve for M= 4, Uncoded system in AWGN	44

3.17	BER vs SNR curve for M= 16, Uncoded system in AWGN	45
3.18	BER vs SNR curve for M= 64, Uncoded system in AWGN	46
3.19	BLER vs. SNR curve for $C = \frac{1}{2}$ and M= 4 in AWGN	47
3.20	Spectral Efficiency vs. SNR curve for $C = \frac{1}{2}$ and M= 4 in AWGN	47
3.21	BLER vs. SNR curve for $C = \frac{1}{2}$ and M= 16 in AWGN	48
3.22	Spectral Efficiency vs. SNR curve for $C = \frac{1}{2}$ and M= 16 in AWGN	48
3.23	BLER vs. SNR curve for $C = \frac{1}{2}$ and M= 64 in AWGN	49
3.24	Spectral Efficiency vs. SNR curve for $C = \frac{1}{2}$ and M= 64 in AWGN	49
3.25	TD plot for $FEC = \frac{1}{2}$ with BLER Threshold= 0.1 in AWGN	50
3.26	TD plot for $FEC = \frac{1}{2}$ with BLER Threshold= 0.05 in AWGN	50
3.27	BER vs SNR curve for M= 4, uncoded system in Fading Channel	53
3.28	BER vs SNR curve for M= 16, uncoded system in Fading Channel	54
3.29	BER vs SNR curve for M= 64, uncoded system in Fading Channel	55
3.30	BLER vs SNR curve for $C = \frac{1}{2}$ and M= 4 in Fading Channel	56
3.31	Spectral Efficiency vs SNR curve for $C = \frac{1}{2}$ and M= 4 in Fading Channel	56
3.32	BLER vs SNR curve for $C = \frac{1}{2}$ and M= 16 in Fading Channel	57
3.33	Spectral Efficiency vs SNR curve for $C = \frac{1}{2}$ and M= 16 in Fading Channel	57
3.34	BLER vs SNR curve for $C = \frac{1}{2}$ and M= 64 in Fading Channel	58
3.35	Spectral Efficiency vs SNR curve for $C = \frac{1}{2}$ and M= 64 in Fading Channel	58
3.36	TD plot for $FEC = \frac{1}{2}$ with BLER Threshold= 0.1 in Fading Channel	59
3.37	TD plot for $FEC = \frac{1}{2}$ with BLER Threshold= 0.05 in Fading Channel	59
4.1	Basic Link Adaptation system employing adaptive modulation	63
4.2	Pilot Subcarrier for CSI	64
4.3	BER Threshold Points for LA System	65
4.4	Spectral Efficiency Gain for LA System	65
4.5	Link Adaptation Algorithm	68
4.6	PAPR distribution for LA based OFDM system	70
4.7	Performance of LA system with basic LUT when no power amplifier is applied	71
4.8	Performance of LA system with basic LUT when power amplifier is applied	72
4.9	Performance of LA system with revised LUT when power amplifier is applied	72

4.10 Spectral Efficiency comparison for LA system with and without PAPR consideration	73
4.11 Performance of LA system with basic LUT for 6 dB of BO power	75
4.12 Performance of LA system with basic LUT for 4 dB of BO power	75
4.13 Performance of LA system with revised LUT for 6 dB of BO power	77
4.14 Performance of LA system with revised LUT for 4 dB of BO power	77
A.1 BLER vs SNR curve for $C = \frac{1}{3}$ and $M= 4$ in AWGN	83
A.2 Spectral Efficiency vs SNR curve for $C = \frac{1}{3}$ and $M= 4$ in AWGN	83
A.3 BLER vs SNR curve for $C = \frac{1}{3}$ and $M= 16$ in AWGN	84
A.4 Spectral Efficiency vs SNR curve for $C = \frac{1}{3}$ and $M= 16$ in AWGN	84
A.5 BLER vs SNR curve for $C = \frac{1}{3}$ and $M= 64$ in AWGN	85
A.6 Spectral Efficiency vs SNR curve for $C = \frac{1}{3}$ and $M= 64$ in AWGN	85
A.7 TD plot for $FEC = \frac{1}{3}$ with BLER Threshold= 0.1 in AWGN	86
A.8 TD plot for $FEC = \frac{1}{3}$ with BLER Threshold= 0.05 in AWGN	86
A.9 BLER vs SNR curve for $C = \frac{1}{3}$ and $M= 4$ in Fading Channel	87
A.10 Spectral Efficiency vs SNR curve for $C = \frac{1}{3}$ and $M= 4$ in Fading Channel	87
A.11 BLER vs SNR curve for $C = \frac{1}{3}$ and $M= 16$ in Fading Channel	88
A.12 Spectral Efficiency vs SNR curve for $C = \frac{1}{3}$ and $M= 16$ in Fading Channel	88
A.13 BLER vs SNR curve for $C = \frac{1}{3}$ and $M= 64$ in Fading Channel	89
A.14 Spectral Efficiency vs SNR curve for $C = \frac{1}{3}$ and $M= 64$ in Fading Channel	89
A.15 TD plot for $FEC = \frac{1}{3}$ with BLER Threshold= 0.1 in Fading Channel	90
A.16 TD plot for $FEC = \frac{1}{3}$ with BLER Threshold= 0.05 in Fading Channel	90
A.17 BLER vs SNR curve for $C = \frac{2}{3}$ and $M= 4$ in AWGN	91
A.18 Spectral Efficiency vs SNR curve for $C = \frac{2}{3}$ and $M= 4$ in AWGN	91
A.19 BLER vs SNR curve for $C = \frac{2}{3}$ and $M= 16$ in AWGN	92
A.20 Spectral Efficiency vs SNR curve for $C = \frac{2}{3}$ and $M= 16$ in AWGN	92
A.21 BLER vs SNR curve for $C = \frac{2}{3}$ and $M= 64$ in AWGN	93
A.22 Spectral Efficiency vs SNR curve for $C = \frac{2}{3}$ and $M= 64$ in AWGN	93
A.23 TD plot for $FEC = \frac{2}{3}$ with BLER Threshold= 0.1 in AWGN	94
A.24 TD plot for $FEC = \frac{2}{3}$ with BLER Threshold= 0.05 in AWGN	94

A.25 BLER vs SNR curve for $C = \frac{2}{3}$ and $M= 4$ in Fading Channel	95
A.26 Spectral Efficiency vs SNR curve for $C = \frac{2}{3}$ and $M= 4$ in Fading Channel	95
A.27 BLER vs SNR curve for $C = \frac{2}{3}$ and $M= 16$ in Fading Channel	96
A.28 Spectral Efficiency vs SNR curve for $C = \frac{2}{3}$ and $M= 16$ in Fading Channel	96
A.29 BLER vs SNR curve for $C = \frac{2}{3}$ and $M= 64$ in Fading Channel	97
A.30 Spectral Efficiency vs SNR curve for $C = \frac{2}{3}$ and $M= 64$ in Fading Channel	97
A.31 TD plot for $FEC = \frac{2}{3}$ with BLER Threshold= 0.1 in Fading Channel	98
A.32 TD plot for $FEC = \frac{2}{3}$ with BLER Threshold= 0.05 in Fading Channel	98
B.1 BER vs SNR curve for $C = \frac{1}{3}$ and $M= 4$ in AWGN	100
B.2 BER vs SNR curve for $C = \frac{1}{3}$ and $M= 16$ in AWGN	100
B.3 BER vs SNR curve for $C = \frac{1}{3}$ and $M= 64$ in AWGN	101
B.4 BER vs SNR curve for $C = \frac{1}{2}$ and $M= 4$ in AWGN	101
B.5 BER vs SNR curve for $C = \frac{1}{2}$ and $M= 16$ in AWGN	102
B.6 BER vs SNR curve for $C = \frac{1}{2}$ and $M= 64$ in AWGN	102
B.7 BER vs SNR curve for $C = \frac{2}{3}$ and $M= 4$ in AWGN	103
B.8 BER vs SNR curve for $C = \frac{2}{3}$ and $M= 16$ in AWGN	103
B.9 BER vs SNR curve for $C = \frac{2}{3}$ and $M= 64$ in AWGN	104
B.10 BER vs SNR curve for $C = \frac{1}{3}$ and $M= 4$ in Fading Channel	104
B.11 BER vs SNR curve for $C = \frac{1}{3}$ and $M= 16$ in Fading Channel	105
B.12 BER vs SNR curve for $C = \frac{1}{3}$ and $M= 64$ in Fading Channel	105
B.13 BER vs SNR curve for $C = \frac{1}{2}$ and $M= 4$ in Fading Channel	106
B.14 BER vs SNR curve for $C = \frac{1}{2}$ and $M= 16$ in Fading Channel	106
B.15 BER vs SNR curve for $C = \frac{1}{2}$ and $M= 64$ in Fading Channel	107
B.16 BER vs SNR curve for $C = \frac{2}{3}$ and $M= 4$ in Fading Channel	107
B.17 BER vs SNR curve for $C = \frac{2}{3}$ and $M= 16$ in Fading Channel	108
B.18 BER vs SNR curve for $C = \frac{2}{3}$ and $M= 64$ in Fading Channel	108

List of Tables

2.1	General WiMAX Parameters	25
3.1	Table for Calculation of Total Degradation in dB	51
4.1	Switching Threshold for Link Adaptation	64
4.2	LUT with basic and updated values for system with FEC= $\frac{1}{2}$ in AWGN Channel(Values in dB)	71
4.3	LUT with basic values for system with FEC = $\frac{1}{2}$ in Fading Channel(Values in dB)	74
4.4	LUT with updated values for system with FEC = $\frac{1}{2}$ and PRE-SNR of 10 dB in Fading Channel(Values in dB)	76
4.5	LUT with updated values for system with FEC = $\frac{1}{2}$ and PRE-SNR of 20 dB in Fading Channel(Values in dB)	77
4.6	LUT with updated values for system with FEC = $\frac{1}{2}$ and PRE-SNR of 25 dB in Fading Channel(Values in dB)	78

Abbreviations

3GPP-LTE	Third Generation Partnership Project-Long Term Evolution
ACI	Adjacent Channel Interference
AMC	Adaptive Modulation and Coding
APDA	Adaptive Power Distribution Algorithm
ARQ	Automatic Repeat Request
AWGN	Adaptive White Gaussian Noise
BER	Bit Error Rate
BLER	Block Error Rate
BO	Back Off
BWA	Broadband Wireless Access
CDF	Cumulative Distribution Function
CIR	Channel Impulse Response
CP	Cyclic Prefix
CPE	Customer Premises Equipment
CSI	Channel State Information
FEC	Forward Error Correction

DFT	Discrete Fourier Transform
DL	DownLink
FFT	Fast Fourier Transform
FWA	Fixed Wireless Access
HPA	High Power Amplifier
HSDPA	High Speed Downlink Packet Access
HSUPA	High Speed Uplink Packet Access
ICI	Inter Carrier Interference
ISI	Inter Symbol Interference
LA	Link Adaptation
LUT	Look Up Table
MAC	Medium Access Control
MBWA	Mobile Broadband Wireless Access
MCM	Multi Carrier Modulation
MIMO	Multiple Input Multiple Output
NLOS	Non Line Of Sight
OFDMA	Orthogonal Frequency Division Multiple Access
OFDM	Orthogonal Frequency Division Multiplexing
PAM	Pulse Amplitude Modulation
PAPR	Peak to Average Power Ratio
PPM	Pulse Position Modulation

QAM	Quadrature Amplitude Modulation
QoS	Quality of Service
RSSI	Received Signal Strength Indication
SAMPDA	Simple Adaptive Modulation and Power Distribution Algorithm
SDNR	Signal to Distortion and Noise Ratio
SE	Spectral Efficiency
SNR	Signal to Noise Ratio
SSPA	Solid-State Power Amplifier
TD	Total Degradation
TWTA	Traveling Wave Tube Amplifier
UL	UpLink
VoIP	Voice over Internet Protocol
WCDMA	Wideband Code Division Multiple Access
WiMAX	Worldwide Interoperability for Microwave Access
WLAN	Wireless Local Area Network

Chapter 1

Introduction

1.1 Background

Wireless communication has gained momentum during past one and a half decade with invention of digital cellular system. Initially the focus of the wireless system was to enable voice communication and therefore data rate requirement was quite low. With the emergence of mobile multimedia service based on 3G and beyond technologies, there is a tremendous growth in demand of wireless services that contains more than just voice data [1][2]. Thus recent and future generation of wireless communication system is characterized by variety of application ranging from low rate voice data to very high rate real time streaming video data. There exists a strong trend of shifting towards *all in one* service, i.e. one system supporting many of the applications. Applications includes e-mail, web browsing, video conferencing, internet telephony, multimedia video streaming, IP TV etc. A significant growth of non-realtime file sharing applications through mobile system has also been found. To support seamless communication, i.e. *any time any where anything* service, a gradually increasing demand of ubiquitous wireless services at very high velocity is observed in recent days.

All these applications impose different QoS constraint to deliver the service appropriately. Some applications like internet telephony requires low delay service whereas web browsing or file sharing applications can tolerate a certain amount of delay. For applications like IP TV and video conferencing, both high data rate and low delay service is required.

OFDM is a special form of multicarrier technique where all the subcarriers are *orthogonal* to each other. OFDM promises higher data rate and great resilience to the the frequency selective fading at the reasonable cost and complexity in implementation. It is becoming more and more popular for broadband communication system for its high spectral efficiency and its capacity to combat multipath fading [3]. With many advantages like these, OFDM is expected to be the key physical layer technology for almost all future wireless systems. To further improve the spectral efficiency, **LA** is employed which adapts power and bit loading according to the channel condition. In short, **LA** in conjunction with **OFDM** promises to provide a massive improvement in system throughput.

1.2 Motivation

Since available frequency spectrum is very expensive and limited, wireless engineers are always looking for spectrally efficient transmission system. **OFDM**, being a spectrally efficient system, promises to provide quite high data rate. Dynamic behavior of wireless channel always act as a bottleneck for achieving higher data rate [4]. However, it also provides an option to exploit the dynamic nature to improve the link performance. **LA** is an advanced technique which changes power and bit loading adaptively to cope with the varying channel condition based on the information feedback by the receiver [5]. The strategy chooses the optimum power level, modulation order and coding rate, so that spectral efficiency is maximized and target **BLER** is maintained.

With the limited feedback (in the form of Received Signal Strength Indication (**RSSI**)) from the receiver, WLAN systems (IEEE 802.11a) uses same modulation and power across all the subcarrier for each transmission. Although this technique provides some sort of power and spectral efficiency, further improvement is also possible by considering subchannels or subcarriers for adaptation instead of adapting the whole bandwidth together.

Prominent wireless technology standard like Third Generation Partnership Project-Long Term Evolution (**3GPP-LTE**), Worldwide Interoperability for Microwave Access (**WiMAX**) etc. promises data rate of several Mbps for pedestrian to highly mobile users. It proposes to use link adaptation per subcarrier or per subchannel to maximize the throughput. However,

Chalmers University of Technology

this also increases the overhead by sending large amount of feedback information. Adaptation for each subcarrier or for each subchannel increases the implementation complexity even more.

Despite many advantages that make OFDM system very popular, it suffers from large Peak to Average Power Ratio (PAPR) problem [6]. PAPR increases with number of subcarriers. Due to amplifier nonlinearity this may give rise to phenomenon like spectral regrowth and intermodulation among subcarrier causing significant performance degradation [7]. To mitigate the effect, the transmit power is reduced so that probability of high peaks of the signal is amplified in the linear region of the amplifier transfer function. This technique is referred to as power Back Off (BO). However it reduces the power efficiency. This problem becomes severe in link adaptation system since optimum back off power required for satisfactory operation varies on modulation and coding rate. Changing the BO power for each subcarrier or subchannel too frequently is extremely difficult if not impossible. This problem further extends the implementation complexity. Thus a trade off must be made among complexity, efficiency and performance improvement.

The effect of nonlinear distortion can again have severe impact on link adaptation system. Link adaptation studies so far had little attention on the combined effect of PAPR and link adaptation [8]. The link adaptation is done based on the measurement of the specially designed signal called training sequence which is sent from transmitter. However this training sequence is designed in such a way that PAPR remains low [9]. So the distortion due to high PAPR can not be captured in this way. Since existing link adaptation algorithms do not take care of the PAPR effect properly, the system may fail to maintain the QoS constraint. i.e. increase in BLER means decrease in Spectral Efficiency (SE), which is completely undesirable. Therefore it is important to consider the aspects of PAPR for any implementation of OFDM system.

1.3 Goal of the Project

Operating point of the HPA is usually selected based on average power. High power amplifier used in the transceiver circuit of OFDM system does not have linear transfer function.

So, even if we select the operating point of the HPA in the linear region, high peaks of the OFDM symbol may be amplified in the nonlinear region and thereby introduce some nonlinear distortion which in turn will degrade the system performance. To prevent this unexpected effect, the peak of the signal has to be accommodated in the linear operating region of the power amplifier. This means Amplifier has to operate with certain amount of back off power. However this is completely undesirable as increasing the BO power means decreasing the coverage of the cell. Larger the PAPR, higher is the back off power depending on the level of PAPR. But large BO's are totally undesirable since it leads to low power efficiency and reduced cell coverage [10].

If PAPR and the consequent nonlinear distortion are taken into account, the existing LA algorithms may not be able to achieve the target BLER since threshold for modulation and coding rates were fixed without considering PAPR. The goal of the project is to bring out the impact of PAPR on existing LA algorithm and to find a method to combat this effect and restore the performance of the LA system in terms of BLER and Spectral efficiency.

1.4 Scope of the project

The issue of PAPR in multicarrier system is being researched for quite some time and literature survey reveals several proposed approaches towards mitigating this problem e.g. predistortion, PAPR reduction etc. [7][11] [12][13]. But nonlinearity effect still exist. Moreover, very little measure has been taken so far from the link adaptation point of view. So basic focus of this project is to investigate how the PAPR affects the link adaptation system performance. And in that respect, if the system fails to maintain QoS constraint, we also find out ways to modify the existing LA algorithm to regain the spectral efficiency and thereby ensuring the the target BLER.

In this project, the LA based OFDM system will be implemented using the algorithm developed in [8]. 3GPP-LTE standard parameter will be used in our simulation which has shown huge potential for future wireless system. Both uncoded system and coded system (different FEC) will be investigated to bring out the impact of coding gain as well. Different QAM modulation scheme will be considered. Distortion for different modulation

with coding rate scenarios will be evaluated to find out the optimum BO power needed for a given modulation and code rate. For different optimum BO power for different scenarios, threshold for AMC will be modified to satisfy the target BLER. Analysis of performance of different modulation system, in the presence of PAPR, in terms of total degradation, Signal to Distortion plus Noise Ratio (SDNR) will be done.

Spectral efficiency performance before and after consideration of PAPR will also be compared. The system will initially be simulated for the AWGN channel to investigate the basic performance and then Fading channel will be incorporated to see the real environment performance. All the performance will be evaluated in terms of Bit Error Rate (BER), BLER, Total Degradation and Spectral Efficiency.

1.5 Organization of Report

The rest of the report is organized as follows:

Chapter 2 describes the system components. Starting with the wireless channel characteristics in brief, the baseband modulation techniques and fundamentals of OFDM systems are described. The comparison between single carrier and multi-carrier transmission system has been described in the form of pros and cons of OFDM system. The system design requirement and parameters are also outlined.

Chapter 3 represents the performance of the different modulation and coding rate. Coded and uncoded system performance is compared in the beginning. A detail treatment is provided to bring out the effect of HPA and BO power for different combination of modulation and coding rate. Performance in both Adaptive White Gaussian Noise (AWGN) and Fading channel has been described. SDNR and Total Degradation (TD) curves are also presented to address the problem from different angles.

Chapter 4 contains the performance of LA based system. The chapter begins with a brief discussion on the concept of LA. Then the performance of existing LA algorithm is presented with and without consideration of PAPR. Look Up Table (LUT) which is used to determine the threshold for AMC to meet the QoS constraint is presented. Updated LUT to meet the target BLER when PAPR is taken into account is also given. Finally

Faisal Tariq

performance of these different scenarios in terms of spectral efficiency is compared.

The report concludes with Chapter 5 which summarizes the whole project and gives some insight to the possible future work.

Chapter 2

Wireless Channel, Baseband Modulation and OFDM

In this chapter the basic system components will be discussed in brief. Hostility of wireless channel is considered as the main obstacle for achieving higher data rate and therefore a brief introduction to wireless channel and its characteristics is described here. Standard under investigation, 3GPP-LTE and also some other promising technology like WiMAX proposes to use Quadrature Amplitude Modulation (QAM) as modulation technique in the physical layer and hence included here. OFDM has been proposed as multiplexing as well as multiple access scheme. A detailed treatment to the OFDM is provided here.

2.1 Wireless Channel Characteristics

In wireless communication system, signal from transmitter to receiver travels through channel which has dynamic characteristics. Channel characteristics depends on different parameters like location, environment, mobility of user etc. Signal is reflected, diffracted or attenuated by the propagating media. The channel characteristics is random in nature and described by statistical properties which can be used to model the channel

2.1.1 Propagation Loss

Electromagnetic waves travel as spherical wave moving along its perimeter and the total energy of the waves get distributed across the surface. Available signal energy reduces exponentially with the distance from the source. Also there are many interfering objects in the environment which reflect, diffract and attenuate signal energy.

The received signal power is given by Friis free space equation [4]

$$P_r(d) = \frac{P_t G_t G_r \lambda^2}{(4\pi)^2 d^2 L} \quad (2.1)$$

where P_t is the transmit power, $P_r(d)$ is the received power which is the function of T-R separation, G_t is the transmitter antenna gain, G_r is the receiver antenna gain, d is the T-R separation distance in meters, L is the system loss factor not related to propagation ($L \geq 1$), and λ is the wavelength in meters and is related to the carrier frequency by [4]:

$$\lambda = \frac{c}{f} = \frac{2\pi c}{\omega_c} \quad (2.2)$$

where f is the carrier frequency in Hertz, ω_c is the carrier frequency in radian/second, and c is the speed of light in meter/second.

The Eq.(2.1) can be modified as [4]:

$$P_r(d) = P_r(d_0) \left(\frac{d_0}{d} \right)^2 \quad d \geq d_0 \geq d_f \quad (2.3)$$

where, d_0 is point close to the transmitter, known as received power reference point.

In general, the path loss (in dB) can be expressed as follows:

$$\overline{PL}(dB) = \overline{PL}(d_0) + 10n_p \log\left(\frac{d}{d_0}\right) \quad (2.4)$$

where n_p is the path loss exponent. The bars denote the ensemble average of the all possible path loss values for a given value of d .

Many practical model, based on simulations became popular. Okumura-Hata model is most widely used. Modified path loss is given by [4]:

$$PL_{mod} = PL + \Delta PL_f + \Delta PL_h \quad (2.5)$$

where,

- PL is path loss given by (2.4)
- ΔPL_f is frequency correction term given by $6 \log_{10}(f/2000)$, f is the frequency in MHz
- ΔPL_h is receiver antenna height correction factor and is given by $-10.8 \log_{10}(h/2)$, where h is the new receiver antenna height (m) such that $2 < h < 8$

2.1.1.1 Shadowing

Geographical structure of different positions are different. Variation is higher in the urban area and the measured signal between places at the same distance from the transmitter might be quite different. This variation is due to refraction and diffraction from different objects on the path of the traveling wave. This effect is called shadowing. From measurement it is found to be log normally distributed and hence referred to as *log normal shadowing*.

2.1.2 Small Scale Fading

Signal varies rapidly within a very short distance in small scale fading. The variation of the signal strength caused by multipath delay, doppler shift due to the relative motion between receiver and the transmitter etc. Due to the reflection, the receiver may receive some delayed version of the original signal. The Channel Impulse Response (CIR), $h(t, \tau)$ gives the nature of the channel and is given by[14]:

$$h(t, \tau) = \sum_{m=1}^{N_{SE}} A_{np,m} \delta(t - \tau_m) \exp(-j\theta_m) \quad (2.6)$$

where A_{np} is the amplitude of the different delayed version with phase θ_n , and arriving at a delay of τ_n .

2.1.2.1 Multi Path Fading

The time dispersion of the channel is measured by rms delay spread, τ_{RMS} and can be found from the following relation [4]:

$$\tau_{RMS} = \sqrt{\left[\frac{\sum_{n=1}^{N_{SE}} A_{np} \tau_n^2}{\sum_{n=1}^{N_{SE}} A_{np}} - \left(\frac{\sum_{n=1}^{N_{SE}} A_{np} \tau_n}{\sum_{n=1}^{N_{SE}} A_{np}} \right)^2 \right]} \quad (2.7)$$

Thus signal experiences different level of fading for different frequencies of the fading channel. Fading channel can be either flat fading or frequency selective fading depending on the bandwidth of the system compared to the channel coherence bandwidth, B_c . This is inversely proportional to the rms delay spread, τ_{RMS} :

$$B_c \propto \frac{1}{\tau_{RMS}} \quad (2.8)$$

If the system bandwidth is smaller than the coherence bandwidth then the channel is said to flat fading channel, otherwise it is referred to as frequency selective channel.

2.1.3 Time Varying Channel

There is channel variation in time domain too. This variation is mainly due to relative motion between transmitter and receiver which gives rise to a phenomenon called doppler effect. This effect is expressed by doppler frequency:

$$f_d = \frac{1}{2\pi} \frac{\Delta\phi}{\Delta t} = \frac{v}{\lambda} \cos\theta \quad (2.9)$$

where v is the velocity and $\Delta\phi$ is the phase change:

$$\Delta\phi = \frac{2\pi\Delta l}{\lambda} = \frac{2\pi v\Delta t}{\lambda} \cos(\theta) \quad (2.10)$$

Here, θ is the arrived angle of the signal component. The maximum doppler shift is

$$f_m = \frac{v}{\lambda}.$$

2.2 Quadrature Amplitude Modulation

In Digital modulation scheme the modified parameter of the carrier signal, which carries the information, can take only discrete values. This type of modulation is also referred to also as discrete modulation. When information to be conveyed is carried on the varying amplitude of the carrier wave, then the modulation is called Pulse Amplitude Modulation (PAM). And if the information is carried on the phase of the modulated signal then it is referred to as Pulse Position Modulation (PPM). QAM is the combination of the above two methods and carries information on phase as well as on Amplitude of the modulated signal. This can also be seen as embedding two simultaneous sequence of k bits information signal on two quadrature carriers $\cos 2\pi f_c t$ and $\sin 2\pi f_c t$. The corresponding modulated waveform can be written as [14]:

$$s_m(t) = (A_{mc} + jA_{ms})g(t)e^{j2\pi f_c t} \quad m = 1, 2, \dots, M \quad (2.11)$$

where A_{mc} and A_{ms} are the information-bearing signal amplitudes of the quadrature carrier and $g(t)$ is the signal pulse.

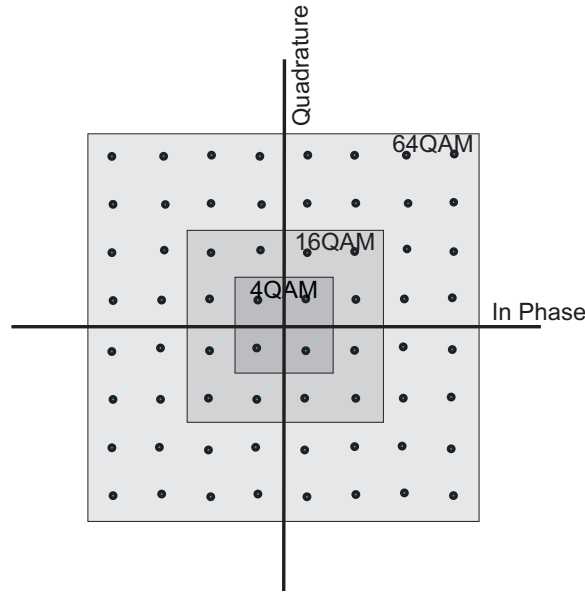


Figure 2.1: QAM Constellation Diagram

The Figure 2.1 shows the constellation diagram for QAM modulation scheme.

It is common practice to have rectangular QAM where $M = 2^{2k}$, with each symbol representing $2k$ information bits. The symbol is generated as a superposition of two PAM signal on quadrature carriers.

2.2.1 Probability of Error in QAM

Since rectangular M-ary QAM can be treated as the superposition of two \sqrt{M} -ary PAM signals, the probability of the a correct decision in the case of M-ary QAM system is as given by [14]:

$$P_c = (1 - P_{\sqrt{M}})^2 \quad (2.12)$$

$P_{\sqrt{M}}$ is the probability of error of a \sqrt{M} -ary PAM signal and is given by [14]:

$$P_{\sqrt{M}} = 2\left(1 - \frac{1}{\sqrt{M}}\right)Q\left(\sqrt{\frac{3}{M-1}}\gamma\right) \quad (2.13)$$

where γ is the average SNR. The probability of symbol error is then given by [14]:

$$P_M = 1 - (1 - P_{\sqrt{M}})^2 \quad (2.14)$$

Since the channel behavior has no deterministic nature, it introduces uncertainty in the position of the received points in constellation. With the increase of the level of modulation, the phase state distance is reduced, i.e. decision boundaries on the constellation diagram become more dense which results in higher BER at a given signal-to-noise ratio. In order to increase the spectral efficiency more information bits are required to be conveyed on one symbol and hence more states have to be allocated in the constellation diagram. However greater the number of states, denser the constellation points. This makes the detection more difficult in the receiver side.

2.3 OFDM Basics

Orthogonal Frequency Division Multiplexing (OFDM) is a special form of Multi Carrier Modulation (MCM) which is specially suitable for high data rate wireless communication.

It converts a single high rate stream of bits in to a number of parallel low rate streams that are transmitted over a number of narrow band channels, called subcarriers, which can be easily equalized[15]. OFDM is widely used as physical layer technology for its tolerance to harsh wireless channel conditions as well as for its high spectral efficiency [2].

2.3.1 Historical Background

Although interest to OFDM technique is recent [16], the basic concept of OFDM appeared in literature as early as in 1966 where Robert W. Chang in [17] outlined a theoretical way to transmit simultaneous data stream through linear band limited channel without Inter Symbol Interference (ISI) and Inter Carrier Interference (ICI). Subsequently, he obtained the first US patent on OFDM in 1970.

Performance analysis of OFDM was done in [18]. Until then, a large number of subcarrier oscillators were needed to perform parallel modulations and demodulations.

A major breakthrough in the history of OFDM came in 1971 when Weinstein and Ebert used Discrete Fourier Transform (DFT) to perform baseband modulation and demodulation which eliminated the need of bank of subcarrier oscillators thus making the operation efficient and simpler [19].

All the proposals of OFDM systems used guard spaces in frequency domain and a raised cosine windowing in time domain to combat ISI and ICI. Another milestone for OFDM history was when Peled and Ruiz introduced *Cyclic Prefix* (CP) or cyclic extension in 1980 [20]. This solved the problem of maintaining orthogonal characteristics of the transmitted signals at severe transmission conditions. The generic idea that they placed was to use cyclic extension of OFDM symbols instead of using empty guard spaces in frequency domain. This effectively turns the channel as performing cyclic convolution, which provides orthogonality over dispersive channels when CP is longer than the channel impulse response [2].

Inclusion of FFT and Cyclic Prefix (CP) in OFDM system and substantial advancements in *Digital Signal Processing* (DSP) technology made it an important part of telecommunications arena. *Digital Audio Broadcasting* (DAB) was the first commercial use of OFDM technology. DAB services came to reality in 1995 in UK and Sweden. At the

beginning of 21st century, several Wireless Local Area Network (WLAN) standard such as IEEE 802.11, HIPERLAN/2 adopted OFDM as their PHY technology.

The future generation of wireless system, most popularly known as 4G system and WiMAX, which has huge market potential, are likely to chose OFDM as there PHY technology. This is becoming more and more evident that OFDM will be the technology of choice in most wireless links world wide.

2.3.2 Principle of Orthogonality

The subcarrier spacing is chosen so that the waveforms transmitted on different sub carriers are orthogonal in time, but overlap in frequency. The orthogonality is achieved by making the peak of each subcarrier signal coincide with the null of the other subcarrier signals resulting in a perfectly aligned and spaced subcarrier signal. The Eq.2.15 gives the mathematical relation among the subcarriers.

$$\int_{t=t_0}^{t_0+T} f_1(t) \cdot f_2(t) dt = 0 \quad (2.15)$$

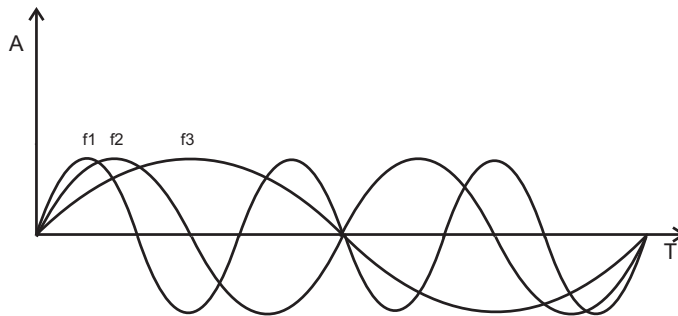


Figure 2.2: Time domain view of principle of orthogonality

This is achieved by having subcarriers which are integer multiple of a basic frequency. The time domain representation of the orthogonality principle is shown in Figure 2.2 and the frequency domain view of orthogonality is shown in Figure 2.3

2.3.3 OFDM Analytical Model

A good description of OFDM analytical model is presented in [5].

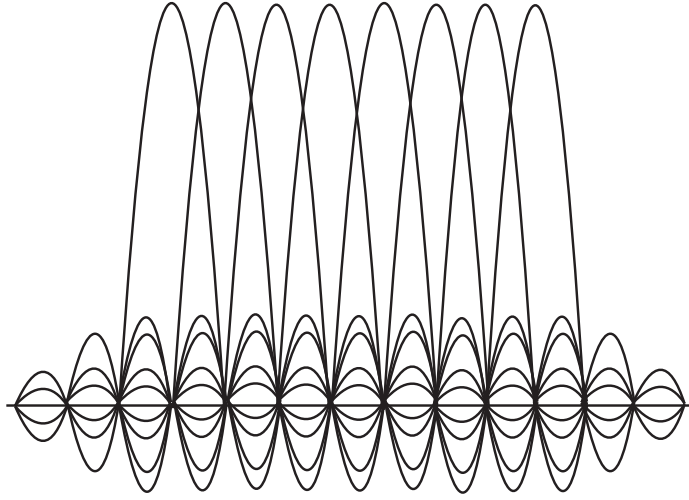


Figure 2.3: Frequency domain view of principle of orthogonality

Each OFDM symbol contains N subcarriers, where N is an even number. OFDM symbol duration is given by [5]:

$$T_u = \frac{2\pi}{\Delta w} \quad (2.16)$$

where w is the subcarrier spacing. Based on (2.16), the spectrum of the Fourier series for the duration of the s^{th} OFDM symbol is [5]:

$$X_s(w) = \sum_{k=-N/2}^{N/2-1} X_s[k] \delta_c(w - k\Delta w) \quad (2.17)$$

IFFT is applied to transform the OFDM symbol from frequency domain to time domain and to limit it to a time interval $0 \leq t < T_u$. The time domain signal $\tilde{x}_s(t)$ is then written as [5]:

$$\tilde{x}_s(t) = F\{X_s(w)\} \Xi_{T_u}(t) = \frac{1}{\sqrt{T_u}} \sum_{k=-N/2}^{N/2-1} X_s[k] e^{j\Delta w k t} \quad (2.18)$$

where Ξ_{T_u} is a rectangular pulse with duration T_u and amplitude of one. After the frequency domain conversion, the cyclic prefix is added [5]:

$$x_s'(t) = \begin{cases} \tilde{x}_s(t + T_u - T_g), & 0 \leq t < T_g \\ \tilde{x}_s(t - T_g), & T_g < t < T_u \\ 0, & \textit{otherwise} \end{cases} \quad (2.19)$$

where T_g is the cyclic prefix duration and $T_s = T_u + T_g$ is the total OFDM symbol duration.

The transmitted complex baseband signal $\tilde{x}_s(t)$ is formed by concatenating all OFDM symbols in the time-domain [5]:

$$\tilde{s}(t) = \sum_{s=0}^{S-1} x_s'(t - sT_s) \quad (2.20)$$

The signal is finally upconverted to a carrier frequency and transmitted [5]:

$$s(t) = \text{Re}\{s(t)e^{j2\pi f_c t}\} \quad (2.21)$$

The following Figure 2.4 shows the block diagram of the OFDM system.

The raw bit stream is first coded with Forward Error Correction (FEC) and then fed to the interleaver where they are interleaved so that the error introduced in the channel get spread over time. Then it is converted from serial to parallel and mapped by QAM modulator. IFFT is done to get the signal in time domain where CP is added. The next block is optional and added only if any peak reduction method is employed in the system. Finally the signal is up converted, amplified and transmitted through the antenna. At the receiver reverse order is followed. The received signal is down converted to get back the base band signal. Cyclic prefix is removed before feeding the signal to FFT. Then channel equalization and estimation is done. This estimation is done on the known pilot signal sent by the transmitter and the obtained information is used to feedback in the form of CSI, if link adaptation system is employed. Then the signal is demapped by QAM demodulator and the bits are de-interleaved and decoded to get back the original signal.

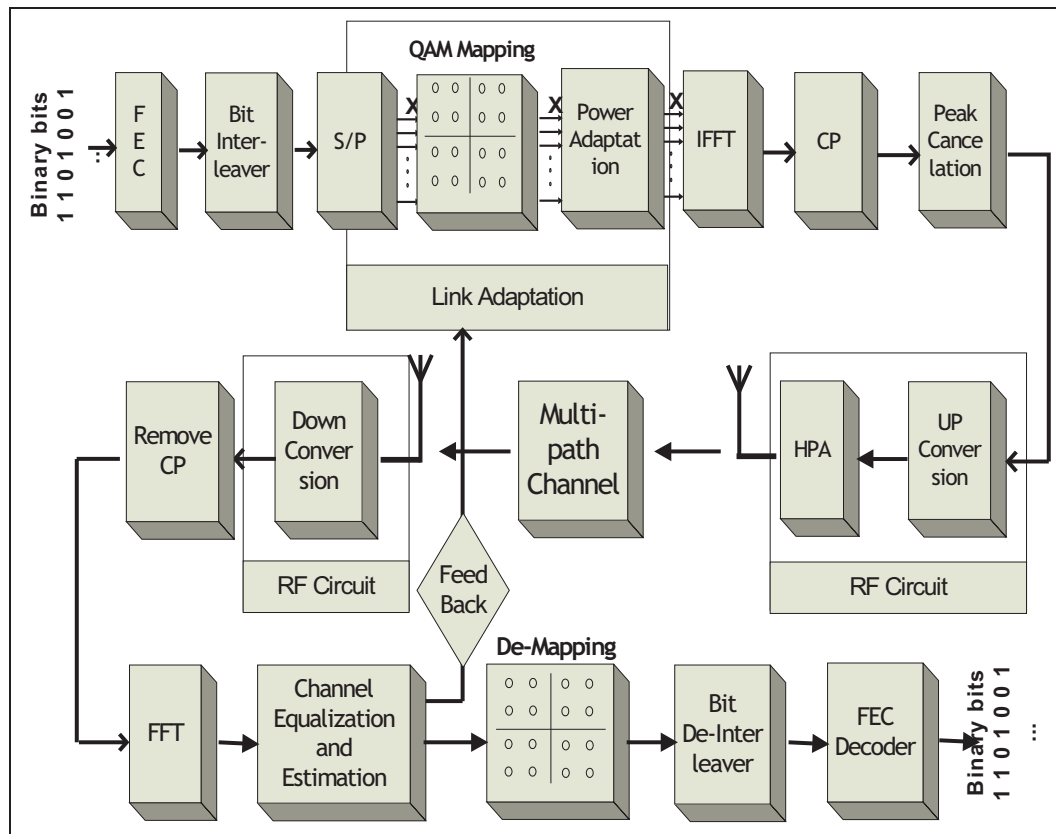


Figure 2.4: Block Diagram of OFDM Transceiver Systems

2.3.4 OFDM System Design

System design always needs sound and comprehensive understanding and consideration of crucial parameters. Basic OFDM philosophy is to decrease data rate at the subcarriers, so that the symbol duration increases, thus the multipath effects are removed. This poses a challenging problem, as higher value for CP interval will give better result, but it will increase the loss of energy due to insertion of CP. Thus, a tradeoff between these two must be made for a reasonable design.

2.3.4.1 OFDM System Design Requirements

OFDM systems depend on four system design requirement:

- **Bandwidth:** Bandwidth is always the scarce resource. The amount of bandwidth will play a significant role in determining number of subcarriers, because with a large

bandwidth, we can easily fit in large number of subcarriers with reasonable guard space.

- **Bit Rate:** The overall system should be able to meet the data rate required by the users.
- **Delay Spread:** Delay spread will depend on the user environment. For indoor environment maximum delay spread is around few hundreds of $nsec$ at most, whereas for outdoor environment it is up to $10\mu s$. So the length of CP should be determined according to the tolerable delay spread.
- **Doppler values:** The doppler value increases with the increase in velocity of the user. So velocity of expected users must be considered carefully.

2.3.4.2 OFDM System Design Parameters

The design parameters are derived according to the system requirements [1]:

- **Number of subcarriers:** Increasing number of subcarriers will reduce the data rate per subcarrier, which will make sure that the relative amount of dispersion in time will be decreased. But when there are large numbers of subcarriers, the synchronization at the receiver side will be extremely difficult.
- **Guard time (CP interval) and symbol duration:** A good ratio between the CP interval and symbol duration should be found, so that all multipaths are resolved and not significant amount of energy is lost due to CP. As a rule of thumb, the CP interval must be two to four times larger than the *Root-Mean-Square* (RMS) delay spread.
- **Subcarrier spacing:** Subcarrier spacing must be kept at a level so that synchronization is achievable. This parameter will largely depend on available bandwidth and the required number of subchannels.
- **Modulation type per subcarrier:** This is of immense importance, because different modulation scheme will give different performance in terms of BLER and throughput. Adaptive modulation and bit loading can be implemented depending on the requirement.

- **FEC coding:** Choice of FEC code will play a vital role also. A suitable FEC coding will make sure that the channel is robust to all the random errors. This is achieved at the cost of throughput reduction.

2.3.5 Comparison of Single and Multi–Carrier Techniques

There has been a long debate whether multicarrier technique is better than single carrier technique or not. Specially when PAPR and synchronization issue comes into consideration. In the following subsection the advantage and disadvantage of OFDM as a multicarrier technique has been described.

2.3.6 Advantages of OFDM

OFDM has many advantages over single carrier system which are summarized below:

2.3.6.1 Combating ISI and Reducing ICI

Time-dispersive channel jeopardizes the orthogonality of the signal. The guard interval must be chosen larger than the expected maximum delay spread, such that multi path reflection from one symbol would not interfere with another. In practice, the empty guard time introduces ICI. ICI is crosstalk between different subcarriers, which means they are no longer orthogonal to each other [1]. The cyclic extension of OFDM symbol or CP, which is a copy of the last part of OFDM symbol, is appended in front of the transmitted OFDM symbol [21].

CP still occupies the same time interval as guard period, but it ensures that the delayed replicas of the OFDM symbols will always have a complete symbol within the FFT interval. So, in short, by providing periodicity to the OFDM source signal, CP makes sure that subsequent subcarriers are orthogonal to each other.

For the insertion of CP, a part of the signal energy is lost since it carries no information. The loss is measured as

$$SNR_{loss_CP} = -10 \log_{10} \left(1 - \frac{T_{CP}}{T_{sym}} \right) \quad (2.22)$$

Here, T_{CP} is the interval length of CP and T_{sym} is the OFDM symbol duration.

CP gives two fold advantages, first, by occupying the guard interval it removes the effect of ISI and second, by maintaining orthogonality it completely removes the ICI. The cost in terms of signal energy loss is not too significant.

2.3.6.2 Spectral Efficiency

This is one of the main reason why OFDM gain this tremendous popularity over conventional single carrier system. Figure 2.5 illustrates the difference between conventional FDM and OFDM systems. In the case of OFDM, a better spectral efficiency is achieved by maintaining orthogonality between the subcarriers. If orthogonality is maintained properly then detection and separation at receiver becomes very easy. Conventional FDM requires guard band to ensure orthogonality between sub channels which results in inefficient use of spectral resources.

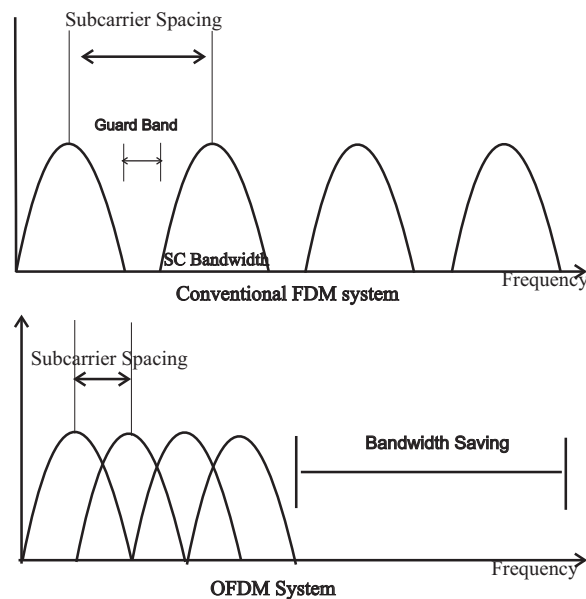


Figure 2.5: Comparison between OFDM and Conventional FDM

Orthogonality makes it possible in OFDM to arrange the subcarriers in such a way that the sidebands of the individual carriers overlap and still the signals are received without being interfered by ICI. At the receiver the signal is integrated over a symbol period to recover raw data. If the other subcarriers all down converted to the frequencies that, in the

Chalmers University of Technology

time domain, have a whole number of cycles in a symbol period T_{sym} , then the integration process results in zero contribution from all other carriers [22].

2.3.6.3 Some Other Benefits of OFDM System

1. Implementation of OFDM is very simple since mapping of bits to unique carriers is done via the use of IFFT.
2. Since OFDM receiver collects signal energy in frequency domain, there is no energy loss in frequency domain.
3. OFDM is more resistant to frequency selective fading than single carrier systems.
4. The orthogonality preservation procedures in OFDM are much simpler compared to CDMA or TDMA techniques even in very severe multipath conditions.[23]
5. It is possible to use maximum likelihood detection with reasonable complexity
6. OFDM can be used for high-speed multimedia applications with lower service cost.
7. Single frequency networks are possible in OFDM, which is especially attractive for broadcast applications.
8. Smart antennas can be integrated with OFDM [24]. MIMO systems and space-time coding can be incorporated with OFDM and all the benefit of MIMO can be achieved.

2.3.7 Disadvantages of OFDM

Despite many advantages that made OFDM system popular for many recent and future high data rate applications, it suffers from some drawback which are briefly described below.

2.3.7.1 Strict Synchronization Requirement

OFDM is highly sensitive to time and frequency synchronization errors, especially due to frequency synchronization errors, OFDM signal loses orthogonality which can lead to a high bit error rate.

This frequency synchronization error can happen due to two reasons. Firstly, mismatch in local oscillator frequency of transmitter and receiver and secondly, relative motion between transmitter and receiver which shifts the frequency of the received signal due to Doppler effect. OFDM system may show significant performance degradation at high velocity.

2.3.7.2 Peak-to-Average Power Ratio(PAPR)

Peak to Average Power Ratio (PAPR) is one of the key disadvantages as compared to the single carrier system. PAPR is proportional to the number of sub-carriers used for OFDM systems. An OFDM system with large number of sub-carriers will thus have a very large PAPR when the sub-carriers add up coherently. When the signal with high PAPR passes through HPA, due to nonlinearity of HPA, it gives rise to in band and out of band intermodulation. Thus the design of RF amplifier becomes increasingly difficult with the increase in PAPR. A detail treatment of PAPR will be provided in the Chapter 3.

2.3.7.3 Co-Channel Interference in Cellular OFDM

In cellular systems, CCI is combated by combining adaptive antenna techniques, such as sectorization, directional antenna, antenna arrays, etc. If OFDM is used in the cellular systems it will give rise to CCI. Similarly with the traditional techniques, with the aid of beam steering, it is possible to focus the receiver's antenna beam on the served user, while attenuating the co-channel interferers. This is significant since OFDM is sensitive to CCI.

2.4 Wireless Broadband Standard

Broadband wireless access is aiming to provide high data rate wireless access over wide area at vehicular speed and to support variety of applications such as personal computers to data networks. According to the 802.16-2004 standard, broadband means *having instantaneous bandwidth greater than around 1 MHz and supporting data rates greater than about 1.5 Mbit/s*. In terms of connectivity broadband wireless access is equivalent to broadband wired access, such as ADSL or cable modems. It is planned to be used in the next few years

and is estimated to have a range of 50km.

Several standard for Broadband Wireless Access ([BWA](#)) has been proposed so far. Among those, the most prominent broadband wireless access standard, 3GPP-LTE has been briefly described below.

2.4.1 3GPP-LTE

Aiming on meeting future needs, 3GPP has initiated activity on the long term evolution of UTRAN (Universal Terrestrial Radio Access Network), which is clearly targeting system performance beyond Wideband Code Division Multiple Access ([WCDMA](#)), High Speed Downlink Packet Access ([HSDPA](#)) and High Speed Uplink Packet Access ([HSUPA](#)). The UTRAN long-term evolution work is looking for the market introduction of Evolved UTRAN (EUTRAN) around 2010, with specification availability planned toward end of 2007. The feasibility study is currently on going and key decisions on the multiple access as well as on the protocol architecture have recently been finalized. Feasibility study is finalized for September 2006 time frame, after which actual specification development would start [[25](#), [26](#)]. Three basic concepts are proposed for DownLink ([DL](#)) [[25](#)]:

- OFDMA (FDD / [TDD])
- MC-WCDMA (FDD)
- MC-TD-SCDMA (TDD)

[OFDM](#) is chosen for the [DL](#) mainly due to the simplicity of the terminal receiver in case of large bandwidths in difficult environment. To support different bandwidth options, Orthogonal Frequency Division Multiple Access ([OFDMA](#)) has been adopted which gives better flexibility. Several advanced techniques are being considered on top of the basic [OFDMA](#) operation which includes advanced Automatic Repeat Request ([ARQ](#)) techniques, frequency domain scheduling, Multiple Input Multiple Output ([MIMO](#)) antenna technologies and variable coding and modulation [[26](#)].

A scalable solution for air interface is adopted to support a number of different bandwidths, starting from 1.25 MHz to 20 MHz. The single set of parameters for sub-carrier spacing etc. provide support for different bandwidths by only changing the number

of sub-carriers while keeping the frame length as well as symbol length constant. The parameters defined during the feasibility study can be found from [25, 26].

For the UpLink (UL) direction the Single Carrier FDMA (SC-FDMA) has been chosen due to the good performance in general and superior properties in terms of UL signal PAPR as compared to OFDM UL [26, 27].

2.4.2 WiMAX

The term Worldwide Interoperability for Microwave Access (WiMAX) is generally used to refer to IEEE 802.16 group of standards. This working group works towards defining a common standard for BWA. The PHY and Medium Access Control (MAC) Layer is addressed in this standardization, and defines a common MAC layer and a number of different PHY! (PHY!) options. The latest amendment, IEEE 802.16e, published in February 2006, covers "Physical and Medium Access Control Layers for Combined Fixed and Mobile Operation in Licensed Bands"

Recently, IEEE 802.16e, standard announced specification for mobile BWA which is one of the greatest promises of future wireless technologies for providing *Anytime, Anywhere, Anything* service.

The main advantage of WiMAX over other standards is that it offers a single standard approach while other technologies have several vendor specific proprietary solutions which prohibits seamless inter-operation. This means manufacturers can take advantage of economies of scale, while operators will have a wider range of choice. The WiMAX forum is a body of WiMAX related industry members that take care of the standardization process.

Roll out of WiMAX network is divided into three stages [28][29]:

1. Fixed Wireless Access (FWA): Here WiMAX technology acts as the backhaul connecting a local network through externally mounted fixed antennas. The first IEEE 802.16 standard defines this operation which requires LOS and operates in the 10-66 GHz frequency range. 11 GHz band was also included on later standard IEEE 802.16 a. Theoretically the data rate is up to 75Mbps on a single channel and 350 Mbps using multiple channel on both uplink and downlink. The coverage area was up to 50 km.

2. Nomadic Mobility through Customer Premises Equipment (**CPE**): This was introduced with the IEEE 802.16-2004 version, when sub 11 GHz band was included to support Non Line Of Sight (**NLOS**) operation. The standard allows nomadic users with **WiMAX** access points to connect to a **WiMAX** base station. P2MP service is provided with data rate of 10 Mbps or more. 5-10 km area can be covered depending on the data rate and other specifications.
3. Mobile Broadband Wireless Access (**MBWA**): The third stage of **WiMAX** implementation is the final state for which everyone is looking forward. Full mobility (vehicular speed) will be supported over a base station coverage range of several kilometers offering data rates of up to 15 Mbps operating at 2 - 6 GHz carrier frequencies with a channel bandwidth of 5 MHz. IEEE 802.16e standard includes this specification, and it is expected to be commercially available by 2007.

Operating Frequency	2-11 GHz and 10-66 GHz
Coverage area	Maximum 50 km(FWA) and 5 km (mobile)
Data rate	Up to 70 Mbps (Single Carrier, LOS) and 15 Mbps (mobile)
Channel bandwidth	Variable. From 1.75 MHz to 28 MHz
Key technology	OFDM and scalable OFDMA (mobile)

Table 2.1: General WiMAX Parameters

WiMAX allows channel bandwidth from 1.75 MHz to 28 MHz at almost any carrier. The PHY mode supported at 10-66GHz is only Single Carrier while at sub 11GHz, both Single Carrier and Multi-Carrier are supported, with various options for the MC mode, from **OFDM** (256 point FFT) to **OFDMA** (2048 point FFT). Modulation level of 64-QAM is supported by all PHY whereas the Single Carrier PHY mode supports 256-QAM. IEEE 802.16e specifies the option for scalability at the PHY **OFDMA**. This scalable sub-channelization structure and variable Fast Fourier Transform (**FFT**) size enables optimum ensures optimum performance.

A unique connection ID **MAC** is used to identify the links between BS and the subscriber. This allows for different Quality of Service (**QoS**), and hence providing support for wider range of applications, especially those requiring low latency and faster response,

such as Voice over Internet Protocol ([VoIP](#)) . Number of different transport technologies, such as IPv4, IPv6, ATM, Ethernet is also supported at the [MAC](#) layer, giving it a greater flexibility for seamless operation [[30](#), [28](#)].

Chapter 3

High Power Amplifier and PAPR in OFDM

3.1 Introduction

In contrast to its appealing properties, OFDM suffers from high Peak to Average Power Ratio (PAPR) problem. When the signal with high PAPR passes through the HPA, which has nonlinear transfer function, spectral regrowth occurs that can be separated as in band intermodulation and out band intermodulation [31]. This in turn causes Block Error Rate (BLER) degradation and Adjacent Channel Interference (ACI) [1], [15].

To reduce the non linear distortion effect, signal power is reduced before applying to the HPA input so that the probability of the signal peaks to be amplified in the linear region of the amplifier transfer function increases. This reduction of signal power is referred to as Back Off (BO). The larger the Back Off (BO), higher the reduction of the distortion effect. However, It reduces the total available transmit power which eventually reduces the coverage area of the system. Therefore it is aimed that minimum BO is used while optimizing the Block Error Rate (BLER) performance by limiting the signal distortion due to PAPR problem. It is also found that the amount of BO needed for optimum performance varies for different modulation schemes [8]. Since LA employs varying modulation, power and coding rate, fixed value of power BO will not optimize the performance. So, it becomes important to analyze the impact of nonlinearity in OFDM system using rate, modulation

and power adaptation.

3.2 HPA Models

Several **HPA** models are available in the literature mainly for two types of amplifier. One is relatively older and is known as Traveling Wave Tube Amplifier (**TWTA**) and another is Solid-State Power Amplifier (**SSPA**). The models developed so far can mainly be divided into two categories. One exhibits nonlinear distortion in both amplitude (*AM/AM*) and phase (*AM/PM*). Other exhibits nonlinear distortion in amplitude (*AM/AM*) only. A brief description of two models that are widely employed for wireless communication related studies has been given below.

3.2.1 TWTA Model

The most widely used model for TWTA is known as Saleh model. It considers nonlinear distortion in both amplitude (*AM/AM*) and phase (*AM/PM*). The model is extensively used in nonlinear distortion analysis related to OFDM system [31][32].

In Saleh model, input signal is defined as [33]

$$x(t) = r(t) \cdot \cos[w_0 t + \psi(t)] \quad (3.1)$$

where w_0 is the carrier frequency, $r(t)$ and $\psi(t)$ are modulated envelope and phase respectively.

The corresponding output can be written as [33]

$$y(t) = A[r(t)] \cdot \cos\{w_0 t + \psi(t) + \Phi[r(t)]\} \quad (3.2)$$

where $A(r)$ is an odd function of r , with a linear leading term representing *AM/AM* conversion and $\Phi(r)$ is an even function of r , with a quadratic leading term representing *AM/PM* conversion.

3.2.2 SSPA Model

For SSPA, nonlinear distortion has been analyzed using Rapp's Model [34]. This HPA model is simulated using the following relation considering distortion in amplitude only [1].

$$g(x) = \frac{|x|}{(1 + |x|^{2p})^{\frac{1}{2p}}} \quad (3.3)$$

Here x is the signal amplitude and the variable p is used to tune the amount of nonlinearity. A good approximation of existing HPA can be obtained by choosing p in the range of 2 to 3. For large values of p , the model converges to a clipping amplifier and is perfectly linear until it reaches the maximum output power level. This is however very hard to achieve in practical system. Available literatures suggests that the AM/PM distortion is small enough to be neglected [1].

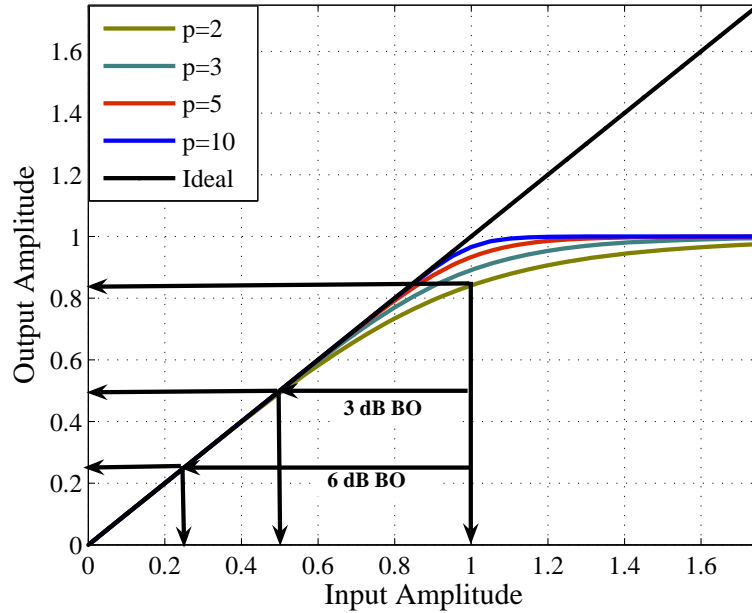


Figure 3.1: Transfer Function and of Rapps model with BO scenario.

Figure 3.1 represents the transfer function of the Rapp's model. It also explains the influence of BO on nonlinearity. When no BO is applied, the signal is more likely to be amplified in the nonlinear region of the transfer function. To increase the possibility

of amplifying in the linear region, operating point needs to be shifted to the left of the horizontal axis of Figure 3.1. To shift the operating point 3 dB to the left, the signal needs to be reduced by a factor of half. In order to accommodate more signal peaks in the linear region, operating point needs to be shifted more left. To implement 6 dB BO, the signal should be reduced by a factor of $\frac{1}{4}$.

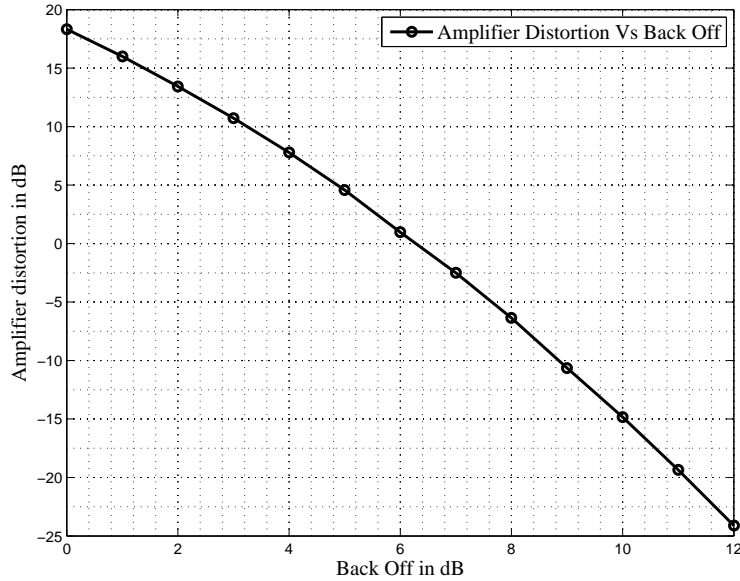


Figure 3.2: Relation between Amplifier Distortion and BO Power

Thus BO always gives some performance improvement in terms of BLER but at the cost to coverage reduction due to reduced output power. The amount of distortion caused by the amplifier is estimated by measuring the difference in signal power at the input and output of the amplifier. The distortion versus BO relation is shown in Figure 3.2 which again proves that with increasing BO, distortion decreases. i.e. the signal operates more in the linear region.

Selection of HPA model

Both TWTA and SSPA has advantages as well as disadvantages over one another. However, there have been a long debate whether tube based or solid state amplifier is better for wireless applications. For this work SSPA have been chosen due to some of its distinct advantages [35]

- No warm up time required.
- Inherently good linear performance for multicarrier, digital transmission
- Built in soft-fail capabilities in case of single device or module failure
- No expected RF section sparing requirements
- High volume production capability since the industry is growing exponentially.

And Rapp's model is used to model the SSPA.

3.3 PAPR in OFDM

OFDM symbol is generated by superimposing several narrow band subcarriers. These carriers may add up constructively resulting in high amplitude for some part of the signal. When power instead of amplitude of the signal is considered situation becomes even worse. This problem is widely known as Peak to Average Power Ratio (PAPR) problem. Large PAPR of a system makes the implementation of Digital-to-Analog Converter (DAC) and Analog-to-Digital Converter(ADC) extremely difficult. The design of RF amplifier also becomes more difficult with the increasing PAPR as it gives rise to the intermodulation in RF domain. Since the source of the problem is constructive addition of subcarriers, PAPR is proportional to the number of subcarrier in an OFDM symbol. PAPR can be defined mathematically as:

$$PAPR = \frac{\max |x(n)|^2}{E[|x(n)|^2]} \quad (3.4)$$

Several methods have been proposed to reduce nonlinear distortion due to high PAPR. Some techniques directly deal with nonlinearity of the amplifier such as predistortion, negative feedback, linear amplification with nonlinear component (LINC), feed forward etc. While some other techniques involve reduction of PAPR so that operating point does not fluctuate very much. Three category of techniques have been found in literature to reduce PAPR, namely *Signal Distortion Techniques*, *Coding Techniques* and finally the *Scrambling Technique*. A good comparison of these technique can be found in [7].

3.3.1 CDF of PAPR

OFDM signal is characterized by

$$x(t) = \frac{1}{\sqrt{N}} \sum_{n=1}^N a_n e^{jw_n t}. \quad (3.5)$$

Here a_n is the modulating signal. For large number of a_n both the real and imaginary parts tend to be Gaussian distributed, So the amplitude of the OFDM symbol has a Rayleigh distribution, while the power distribution is central chi squared with two degrees of freedom and zero mean with a cumulative distribution function given by:

$$F(z) = \int_0^z \frac{1}{2 \cdot \sigma^2} \cdot e^{-\frac{u}{2 \cdot \sigma^2}} du = 1 - e^{-z} \quad (3.6)$$

Assuming that the samples z to be mutually uncorrelated and the cumulative distribution function for the peak power per OFDM symbol is given by [10]:

$$P(PAPR \leq z) = F(z)^N = (1 - e^{-z})^N \quad (3.7)$$

where N is the number of subcarriers in one OFDM symbol.

3.3.1.1 PAPR and Number of Subcarrier

As stated earlier, high value of PAPR originates from the constructive addition of subcarriers, so PAPR increases with the increase in number of subcarriers. Figure 3.3 shows the theoretical and simulated *CDF* of PAPR for different number of subcarriers. Theoretical curve is generated using Eq.3.7. It is obvious that there is no difference between theoretical and simulated values except for the very low Cumulative Distribution Function (*CDF*) which probably occurs due to not enough number of simulation samples at that range. Here *CDF* for 128, 512 and 1024 subcarriers are shown and it shows that PAPR increases with the increase in number of subcarriers.

The *CDF* of PAPR reaches 90 percentile value, which is around 9 dB, very quickly and rest of the values span over wide range of SNR. There is very small difference between 90 percentile value and median value. Therefore, it can be concluded that high PAPR

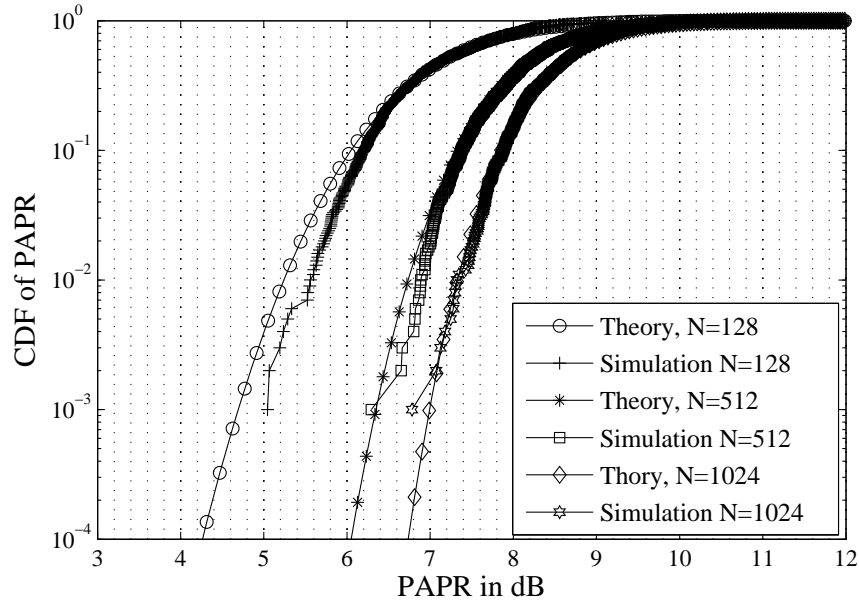


Figure 3.3: Comparison of theoretical and simulated CDF of PAPR

occurs very rarely. This, in fact, gives very useful information for system design. Since high PAPR occurs very rarely, for acceptable performance it is quite enough to accommodate high peaks up to median value in the linear region during amplification.

3.3.1.2 Effect Modulation and Coding Schemes on PAPR

The Figure 3.4 shows the CDF of PAPR when different modulation order were used while keeping number of subcarrier and code rate fixed to 512 and $\frac{1}{2}$ respectively. All the curve completely overlapped each other which proves that PAPR is completely independent of modulation scheme.

Figure 3.5 exhibits a very well known fact that PAPR does not depends on coding rate. Here modulation and number of subcarrier were fixed to 16QAM and 128 respectively while coding rate was varied. All the cdf curves again overlapped each other. So, it can be concluded that PAPR only depends on how the subcarriers are added together and their number. It is not influenced by the parameters like modulation, FEC coding etc.

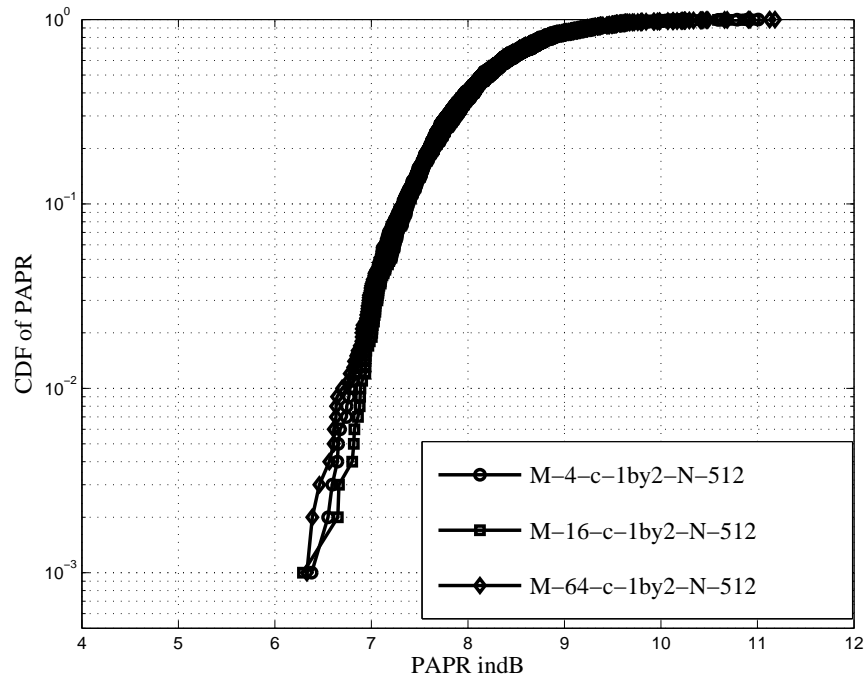


Figure 3.4: Effect of Different Modulation Scheme on CDF of PAPR

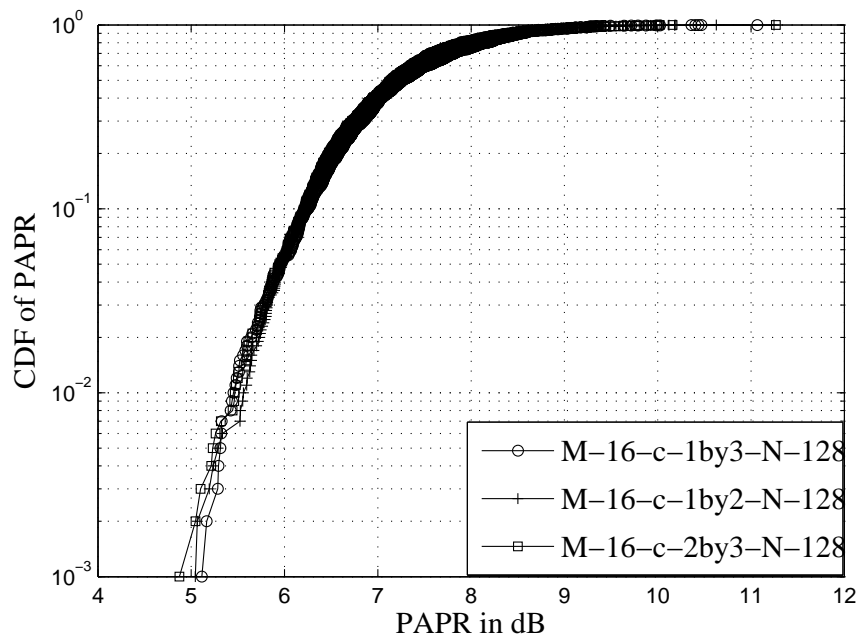


Figure 3.5: Effect of FEC on CDF of PAPR

3.4 Effect of HPA and BO Power

3.4.1 Effect on Constellation Points

The following Figure 3.6 shows the received constellation points for 16QAM modulation scheme when no power amplifier was used. The received constellation points for subsequent symbols are quite close to each other. However when power amplifier is plugged in to the system the received constellation points become affected by nonlinearity and therefore scattered.

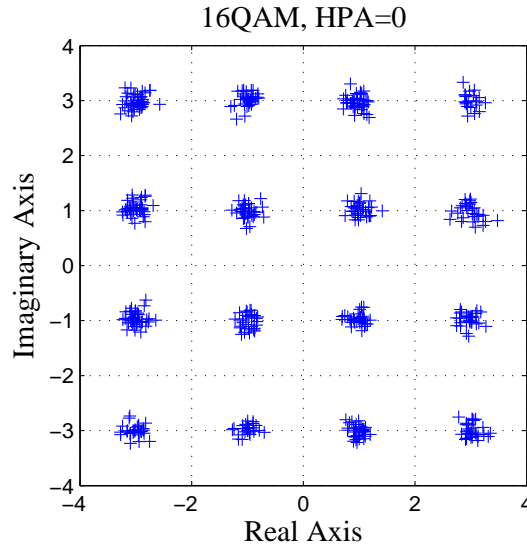


Figure 3.6: 16QAM basic constellation points

Figure 3.7 shows the received constellation diagram for 3 dB and 6 dB BO. It can be seen from the figures that for 3 dB BO, received constellation points are more scattered than that of 6 dB BO. Since with higher modulation order, decision boundaries in constellation diagram become more dense and so the impact of HPA and BO will surely become more severe. On the other hand, for low modulation rate like 4QAM, impact is much less since decision boundaries have comparatively wider space.

3.4.2 Effect on Power Spectrum

To investigate the effect of HPA on power spectrum, during generation of an OFDM symbol, subcarrier with high frequency components are forcefully set to zero to avoid ACI. The

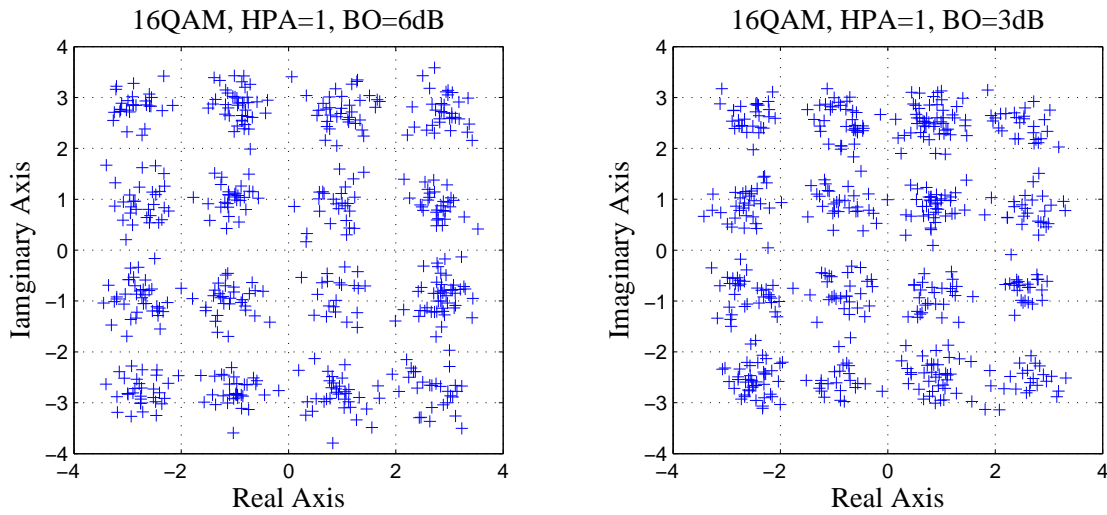


Figure 3.7: Effect of BO on 16QAM constellation points

Figure 3.8 shows the subcarrier arrangement at FFT output. The spectrum spans from $-\frac{N}{2}$ to $\frac{N}{2} - 1$. Frequencies higher than $-p$ and $p-1$ are set to zero, where p is chosen in a way that around 60 percent of the subcarriers are loaded. The 0 frequency is also set to zero to avoid unnecessary power wastage by DC transmission. The power spectrum of OFDM signal measured at the output of the power amplifier is shown in Figure 3.9 for different BO. The number of subcarriers were fixed to 512. It shows that with increasing BO power, out of band emission decreases, i.e. power leakage reduces. If a small BO of 1 dB is applied, it can be seen from the figure that high frequency leakage is few dB. However, with 10 dB of BO, out of band emission reduces to nearly -30 dB. Moreover, though DC component was set to zero, after power amplifier, DC value rises to -30 dB, -12 dB and 3 dB for BO power of 10 dB, 6dB and 1 dB respectively.

multipath fading effect etc.

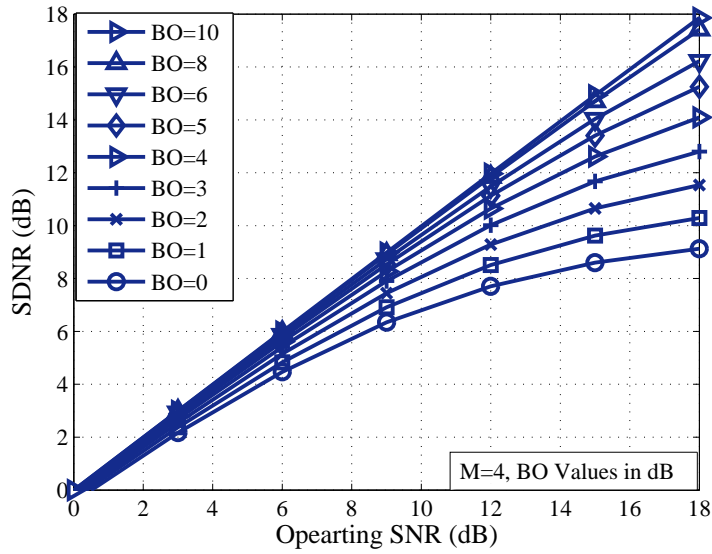


Figure 3.10: SDNR plot for 4QAM modulation in AWGN Channel.

SDNR at the receiver end can be expressed as follows:

$$SDNR = \frac{1}{N} \sum_{i=0}^{N-1} \frac{|X_i|^2}{|X_i - \hat{X}_i|^2} \quad (3.8)$$

Here, X_i is the transmitted signal,

\hat{X}_i is the received signal,

N is the number of subcarrier.

Amount of SDNR does not depend on the modulation scheme used. However, the decision boundary for higher modulation order in the constellation diagram is smaller as compared to the lower modulation order. Hence the probability of correct decision for the symbol will be much lower for higher modulation order than that of lower modulation order for the same amount of distortion. Therefore for the same amount of SDNR, the effect on BLER performance of different modulation will be different.

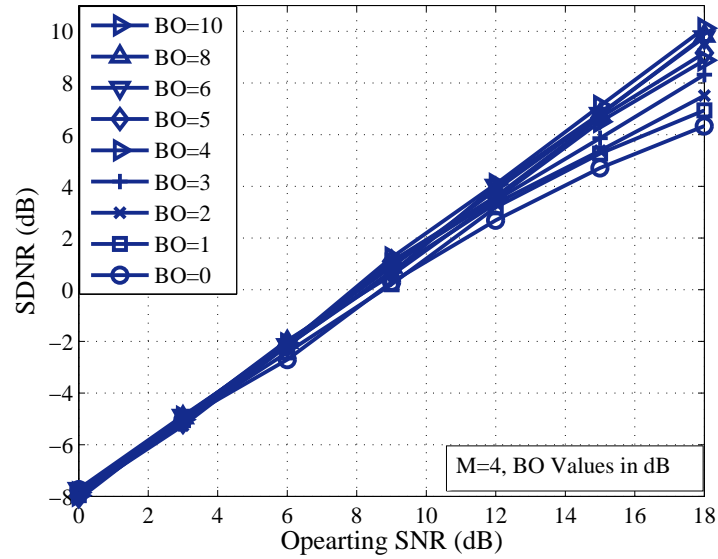


Figure 3.11: SDNR plot for 4QAM modulation in Fading Channel.

Since LA system usually selects modulation adaptively, it is more likely that at low SNR 4QAM modulation will be selected and then with increasing input SNR higher modulation will be selected gradually. So, even though the SDNR plots is independent of modulation, they are represented individually for each modulation in both AWGN and fading channel with emphasis on the different SNR range where they are more likely to operate. Thus for 4QAM modulation, SDNR is plotted against SNR range of 0 to 18 dB, while for 16QAM it ranges from 5 to 30 dB and for 64QAM the range is between 12 dB to 40 dB.

Figure 3.10, 3.12 and 3.14 shows plots for the modulation scheme of 4 16 and 64QAM respectively in AWGN channel while Figure 3.11, 3.13 and 3.15 shows the SDNR plots for 4, 16 and 64QAM respectively in Fading channel. For higher modulation level, it can be seen that, when the BO is reduced, then the SDNR is reaching the highest values quite speedily, i.e. with increasing transmit Signal to Noise Ratio (SNR), the SDNR increases until around 20 dB, after that the SDNR starts to saturate. This means increasing SNR after certain value will not give much gain.

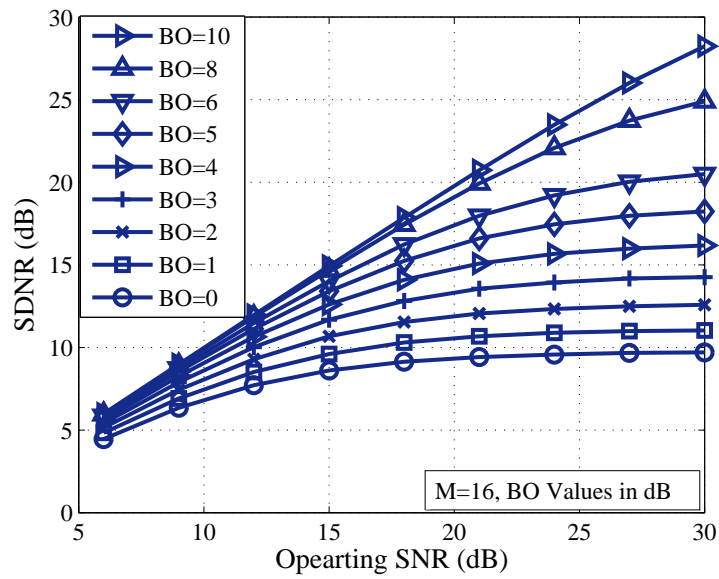


Figure 3.12: SDNR plot for 16QAM modulation in AWGN Channel

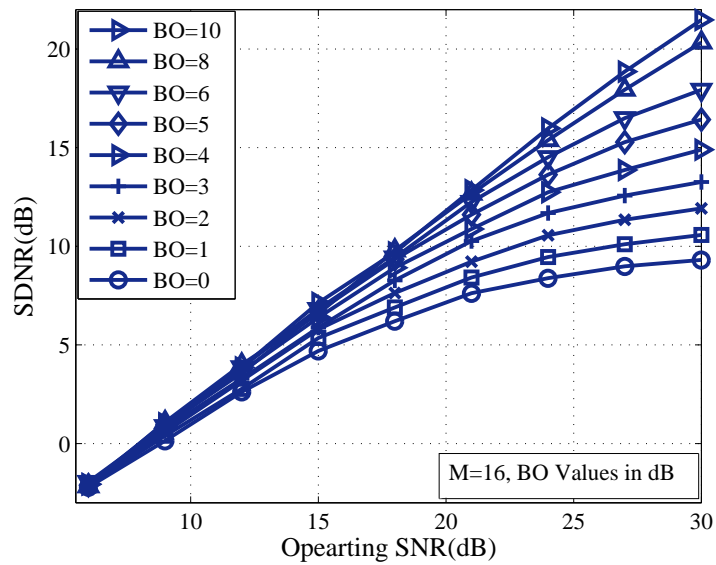


Figure 3.13: SDNR plot for 16QAM modulation in Fading Channel

Also it is evident from the figure that though the nature of SDNR curve is same for both AWGN and fading channel, the amount of SDNR for fading channel is much lower than that of AWGN channel since the SDNR for fading channel includes the distortion due to multipath fading. For example, in 4QAM system with BO power of 8 dB, if the input power is 18 dB then the output power is 17 dB and 9dB for AWGN and fading channel respectively. Similarly, for modulation scheme of 16QAM with the same BO power as above, if the input power is 24 dB then the out power is 22 dB and 15 dB for AWGN and fading channel respectively. This clearly shows the effect of multipath.

SDNR plots shows that with the increasing BO, distortion decreases and after 8dB of BO power, performance is more or less same since 8dB BO power is enough to accommodate most of the peaks in the linear region. So SDNR curve shows the optimum BO power as well. From the SDNR curve it is also possible to obtain the value at which it starts to saturate. Thus it helps to decide the operating SNR as well as the maximum SNR after which power will be wasted for different modulation scheme and thereby ensures optimum use of power.

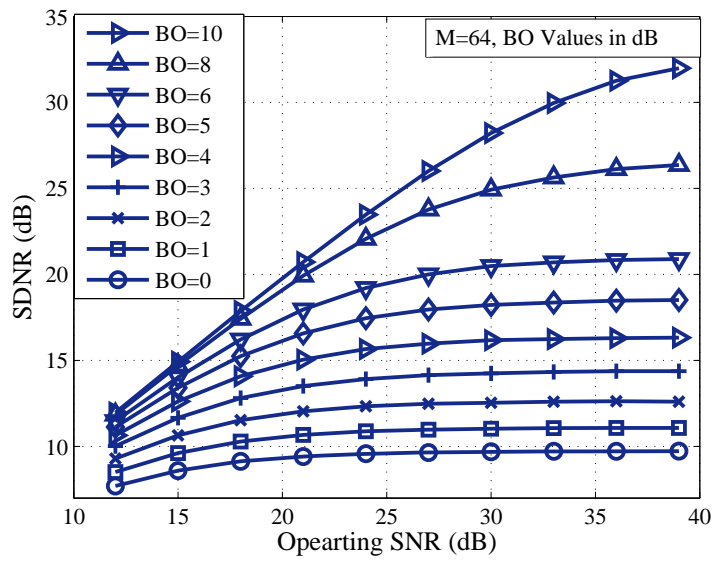


Figure 3.14: SDNR plot for 64QAM modulation in AWGN Channel

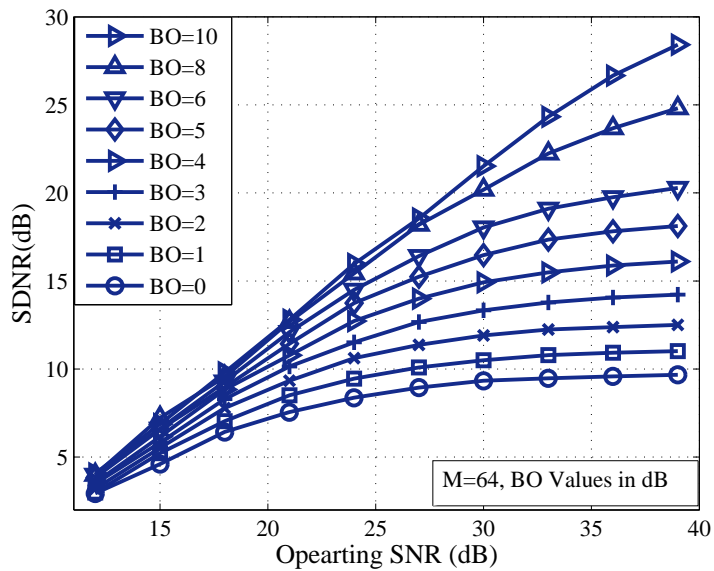


Figure 3.15: SDNR plot for 64QAM modulation in Fading Channel

3.5 Performance of Different Modulation and Coding

In this section system performance is presented for basic system with different modulation and coding rate. Number of subcarriers per OFDM symbol used in the simulation is 512. All the system parameters are selected as per 3GPP-LTE specification. Performance is studied initially for AWGN channel and then is extended for fading channel to realize how it will be affected in practical scenarios. Modulation schemes under investigation are 4QAM, 16QAM and 64QAM. BO power employed in the system simulation is from 0 dB to 10 dB. And as seen from the CDF curves presented in Section 3.3, 10 dB back off will accommodate almost all the high peaks and nonlinearity effect is mostly mitigated. Therefore, performance with 10 dB back off can also be considered as basic system performance. The doppler frequency for all the investigation was fixed at 50 Hz.

Block interleaver has been used in both AWGN and fading channel. However, it has no effect in AWGN channel but gives quite a good performance improvement in fading channel. Block interleaver spreads the errors in time and thereby converts frequency selective channel to the flat fading channel. So, even if the channel goes through deep fade at one instant, error due to this deep fade is distributed over time by the de-interleaver which makes the task of FEC decoder to recover the erroneous bit much easier.

Effect of HPA and BO power on all the modulation schemes are studied with FEC coding rate of $\frac{1}{3}$, $\frac{1}{2}$ and $\frac{2}{3}$. However in order to avoid repetitive information, only results for FEC = $\frac{1}{2}$ is presented here. Rest of the result is available in the Appendix A

The main parameters, that are usually used to characterize the impact of nonlinearities on digital communication systems are: EVM (Error Vector Magnitude), ACPR (Adjacent Channel Protection Ratio), power spectrum and BER or Block Error Rate (BLER). In this study the performance is shown in terms of BER for uncoded system. Since in all practical system FEC coding is employed and performance is measured in terms of Block Error Rate (BLER), it is used instead of BER to represent the performance of the coded system in order to keep our investigation close to the reality. Detail BER performance can be found in Appendix B. For coded system, performance is also presented in terms Spectral Efficiency (SE) and Total Degradation (TD).

It is worth mentioning that for convenience of using results obtained here in link

Faisal Tariq

adapted system, all the performance is plotted in terms of *POST-SNR* which is defined as the actual SNR measured at the receiver. For AWGN channel, there is no difference between *PRE-SNR* or the transmit SNR and *POST-SNR* or received SNR. However, in fading channel they are quite different due to the addition of multipath effect which reduces the SNR at the receiver.

3.5.1 Performance in AWGN Channel

3.5.1.1 Uncoded System

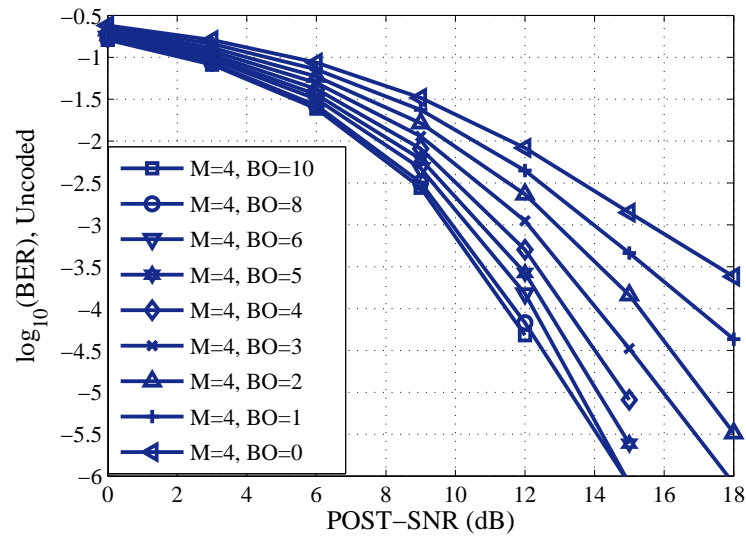


Figure 3.16: BER vs SNR curve for $M=4$, Uncoded system in AWGN

The Figure 3.16 3.17 and 3.18 shows the BER vs SNR performance for uncoded modulation of 4QAM, 16QAM and 64QAM respectively. For 4QAM modulation, backing off does not give that much performance improvement. However, impact of BO increases gradually with increasing modulation rate. For 4QAM, to achieve BER of 10^{-3} , the difference in required SNR with 10 dB and 5 dB BO is around 1 dB only. However if the same scenario is considered for 16 QAM, the required SNR will be 5 dB. For 64QAM it is even impossible to reach that BER level if 5 dB BO is used. This shows the importance of considering BO values carefully for different scenarios.

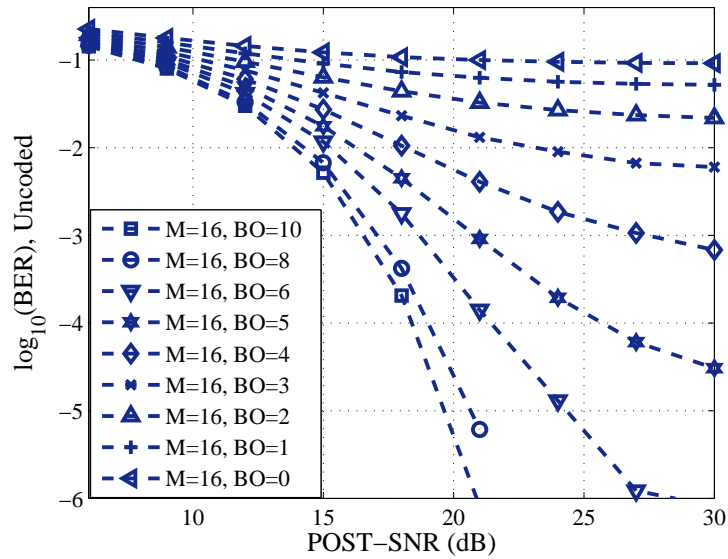


Figure 3.17: BER vs SNR curve for $M=16$, Uncoded system in AWGN

3.5.1.2 Coded System

The Figure 3.19, 3.21 and 3.23 shows the BLER vs. SNR performance for 4QAM, 16QAM and 64QAM modulation respectively with $FEC = \frac{1}{2}$. There is some performance improvement due to FEC coding gain. For 4QAM modulation, no significant difference in performance is observed between 5dB and 10 dB back off to reach the BLER threshold of 10^{-2} . Even though there is some difference in required SNR to reach the BLER level stated above, SE curves in Figure 3.20 shows that if the SNR is above 8 dB, there is no difference at all in spectral efficiency.

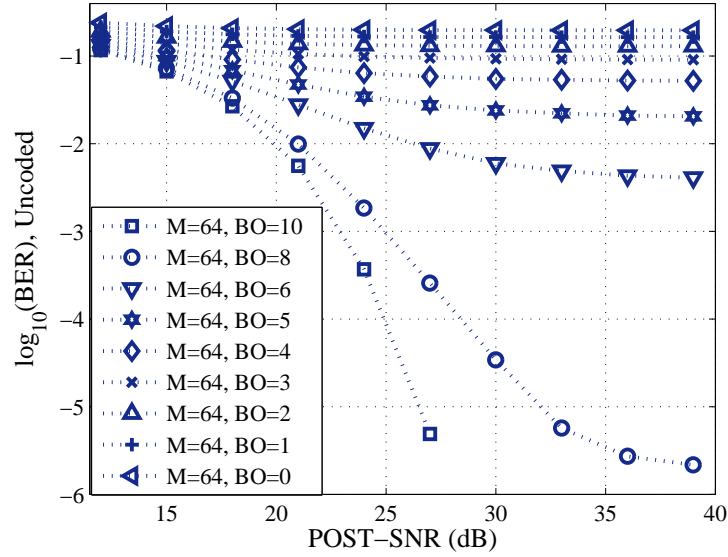


Figure 3.18: BER vs SNR curve for $M=64$, Uncoded system in AWGN

For the same scenario with 16 QAM, the required SNR difference is around 2.5 dB while the SE performance saturates after 15 dB of SNR. In case of 64QAM, the performance is worse and with 5dB BO power, it is almost impossible to reach the selected level and significant difference is observed for SE performance.

Even if the differences in BO between 10 dB and 6 dB and between 6dB and 2 dB are same (4 dB), the required SNR to reach the threshold level of 10^{-1} is not the same. For 16 QAM required SNR is 1 dB only for the first case while it is around 10 dB for the later case i.e. the same amount of BO will not always give same improvement. So BO should be carefully selected to get the optimum performance. As it is observed in the CDF curve, median and 90 percentile value of the PAPR is very close and concentrated around some value. Beyond that level, the rest of the high peaks span over a wide area of SNR values. However from the BLER curves it is obvious that the peaks with level higher than the median value do not have significant impact on BLER performance since implementing BO higher than 8 dB (which is the median value of cdf of PAPR for OFDM symbol used) do not give any performance improvement. Thus no performance improvement is achieved by using 10 dB of BO instead of 8 dB. Since the amount of BO is inversely proportional to the cell coverage, it is very important to keep BO as minimum as possible.

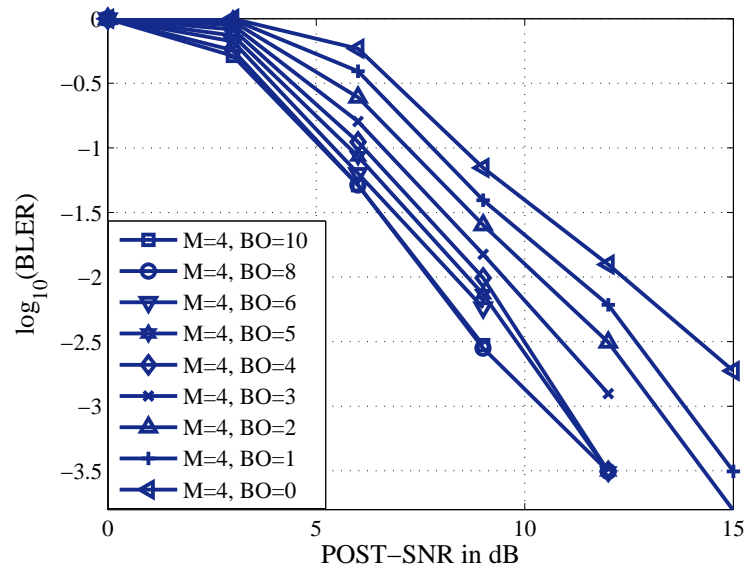


Figure 3.19: BLER vs. SNR curve for $C = \frac{1}{2}$ and $M = 4$ in AWGN

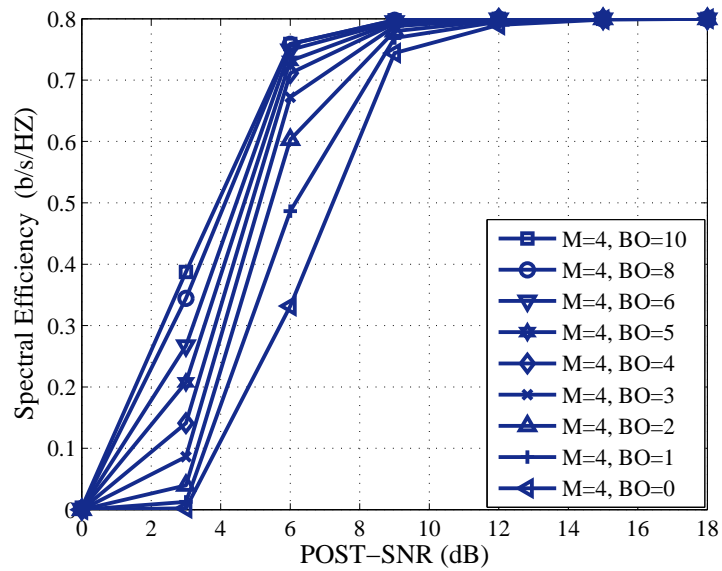


Figure 3.20: Spectral Efficiency vs. SNR curve for $C = \frac{1}{2}$ and $M = 4$ in AWGN

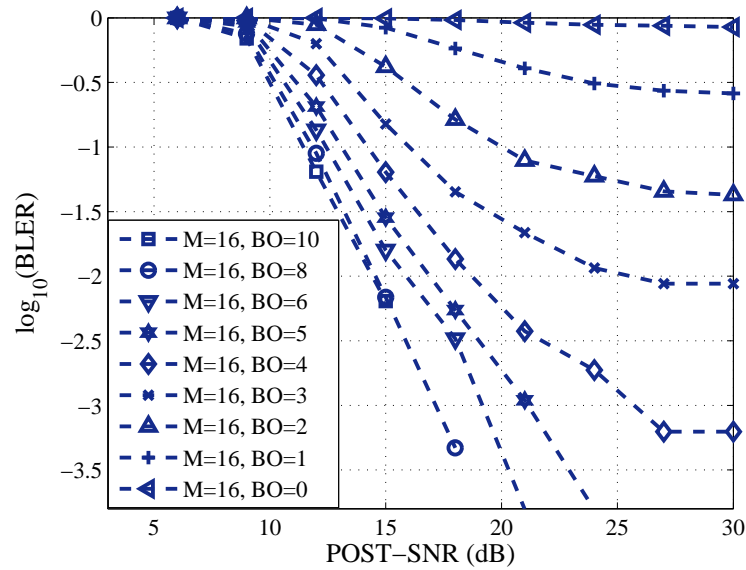


Figure 3.21: BLER vs. SNR curve for $C = \frac{1}{2}$ and $M = 16$ in AWGN

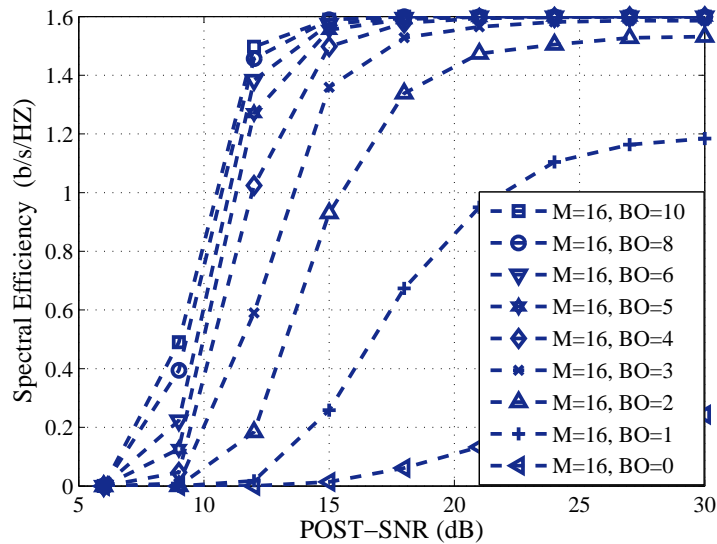


Figure 3.22: Spectral Efficiency vs. SNR curve for $C = \frac{1}{2}$ and $M = 16$ in AWGN

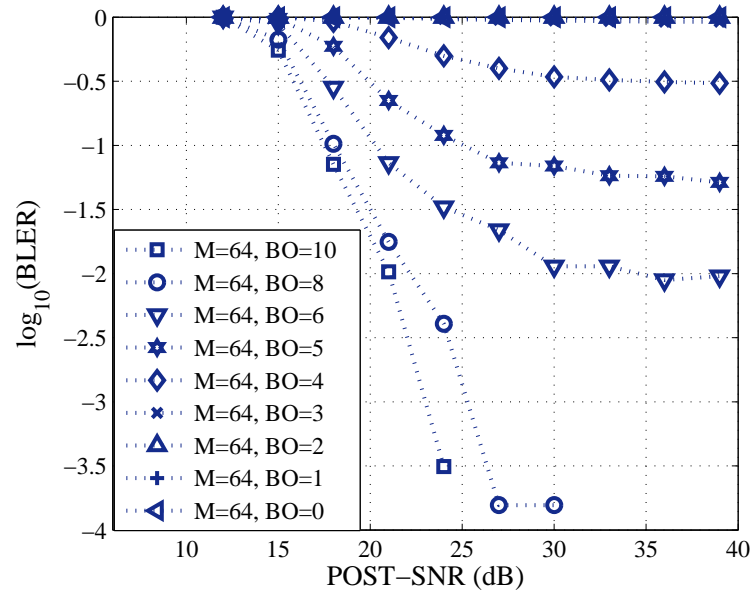


Figure 3.23: BLER vs. SNR curve for $C = \frac{1}{2}$ and $M = 64$ in AWGN

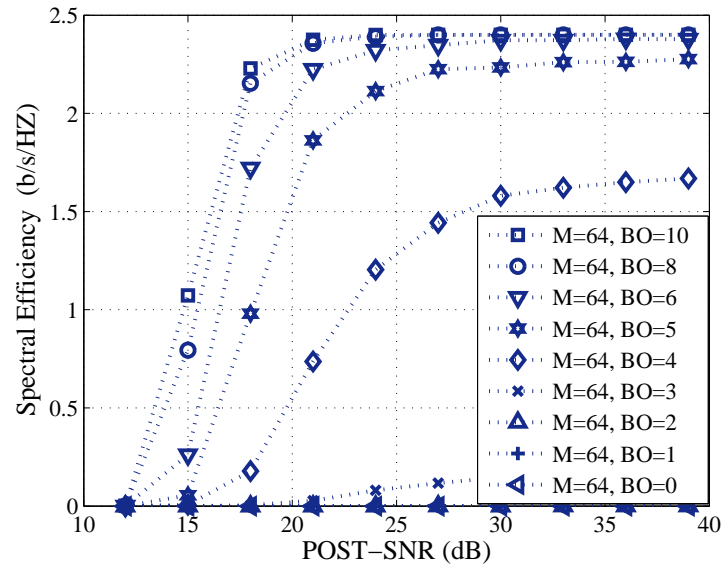


Figure 3.24: Spectral Efficiency vs. SNR curve for $C = \frac{1}{2}$ and $M = 64$ in AWGN

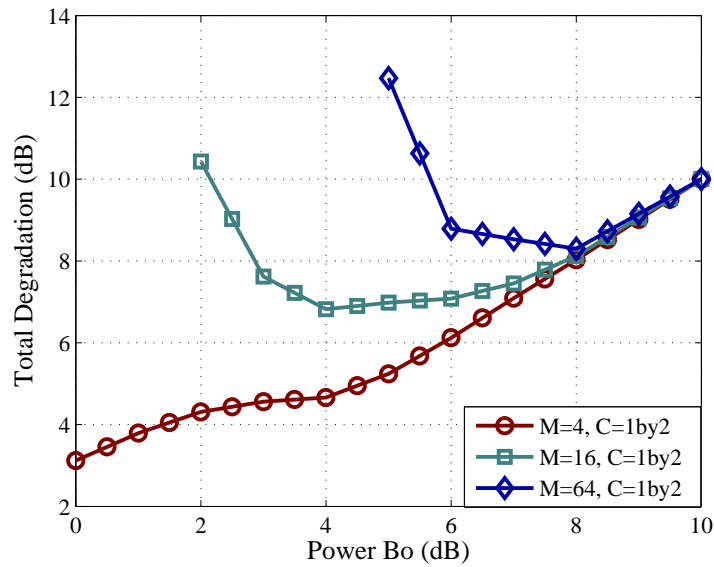


Figure 3.25: TD plot for $FEC = \frac{1}{2}$ with BLER Threshold= 0.1 in AWGN

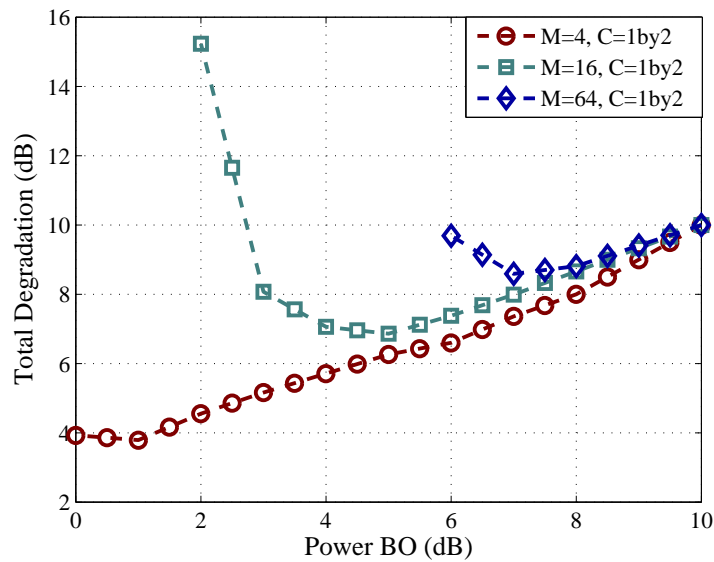


Figure 3.26: TD plot for $FEC = \frac{1}{2}$ with BLER Threshold= 0.05 in AWGN

Total Degradation Plot

Modulation and coding rate shows different behavior at various BO. So the choice of suitable BO or different modulation and coding are different. Also it is highly complex, if not impossible, to change the BO power frequently with the change in modulation and coding rate in link adapted system. So finding an optimum BO point considering modulation with coding rate becomes necessary for optimum performance.

Total Degradation (TD) for a certain BLER threshold is defined as the amount of BO plus the SNR degradation due to non-linearity in BLER performance as compared to the performance in basic system [31].

TD curve is very useful to find this optimum operating BO. The Table 3.1 shows how the TD values are calculated. For a certain value of BER or BLER, the corresponding required SNR to reach that level for ideal system (i.e system without HPA) is noted and used as the basic reference point as shown in the second column of the table. Then required SNR to reach the same BLER threshold for the system with HPA at various BO is noted. The difference between these values and basic reference values represent the degradation. Finally these degradation values are added to the corresponding BO values to get the Total Degradation (TD). Third row of the Table 3.1 shows the TD values.

Figure 3.25 and Figure 3.25 represents the TD curve for BLER threshold of 0.1 and 0.05 respectively. From this curve the minimum total degradation point can easily be obtained. For 4QAM, 16QAM and 64QAM, the best BO points are 0 dB, 4 dB and 7 dB respectively.

The amount of degradation can vary for different modulation, coding as well as for BLER threshold. From Figure 3.25, we can see that for 64 QAM, 16QAM and 4-QAM, optimum BO is 6 dB, 4 dB and 0 dB respectively. So TD Curve at different modulations and coding for different threshold becomes crucial to select optimum BO.

Table 3.1: Table for Calculation of Total Degradation in dB

BO Values	Ideal	10	8	6	5	4
Measured SNR	5.1	5.67	5.7	5.79	5.91	6.33
Degradation	0.0	0.57	0.6	0.69	0.91	1.33
TD	-	10.57	8.60	6.69	5.91	5.33

3.5.2 Performance in Fading Channel

With the knowledge of the system performance in AWGN channel, the system is now investigated in the fading channel to see its behavior under practical channel impairments. The nature of the performance of fading channel is very much similar except additional degradation due to multipath fading.

In the following sections the results for fading channel with uncoded system is presented which followed by the results for the coded system with $FEC = \frac{1}{2}$. The results obtained for the other code rates are available in the appendix.

The performance is shown in terms of BLER versus POST-SNR. For each transmitted SNR, due to channel variation in the fading channel, different channels go through different fade, and thus received SNR for different subchannel varies even though the transmit SNR remains same. So if BLER performance is plotted against *PRE-SNR*, it will represent average performance of subchannels which experienced different received SNR during that transmission. Clearly, it will not exhibit the appropriate behavior of the system. To get the performance based on the received SNR, in the simulator, some beans were created for different SNR values. For example if the received SNR ranges from 5 to 25 dB, then it can be subdivided in to 5 different equally spaced beans. Each bean is represented by a central value of that bean. i.e. if a bean is spaced between 5 to 11 dB then it is represented by 8 dB. For each transmission received SNR is measured for each subchannel and necessary information is saved in the bean to which it belongs to. Finally BLER is calculated for each bean and plotted. Obviously this technique will give much more realistic view. However to ensure enough number of samples in each bean, number of simulations required was quite high. The details of the performance is described below.

3.5.2.1 Uncoded System

In practical systems uncoded systems are used vary rarely. However the BER performance is presented so that performance improvement due to coding system can be compared if needed.

The Figure 3.27, 3.28 and 3.29 shows the BER performance for 4QAM, 16QAM and 64QAM modulation scheme respectively. It can be seen from the figures that for 4QAM, a

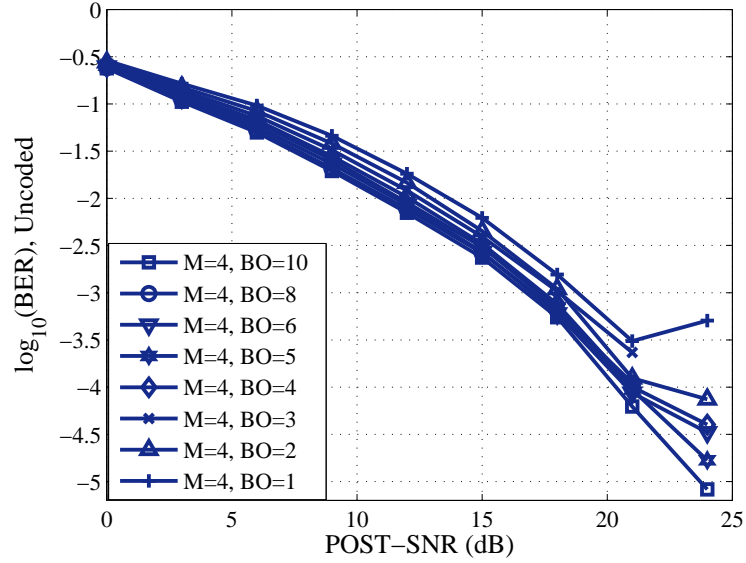


Figure 3.27: BER vs SNR curve for $M=4$, uncoded system in Fading Channel

little gain is possible by using power BO. By introducing 10 dB BO power, only around 2.5 dB of BER performance gain is achieved as compared to 1 dB of BO. However for 16QAM, there is quite a good performance improvement for adding BO power until 5 dB. After 5 dB no significant improvement is found. 64QAM modulation is most severely affected by the HPA and performance improvement is possible until 8 dB of BO power implementation.

So, the amount of BO required for optimum performance varies with modulation scheme. However, even in worse case, employing BO equal to the value of median of cdf of PAPR is enough to restore the performance.

3.5.2.2 Coded System

As mentioned earlier, coded system performance is shown in terms of BLER instead of BER in order to make it closer to the practical systems. In this section performance in terms of BLER and spectral efficiency has been shown and analyzed for all three modulation rate at different BO power. $FEC = \frac{1}{2}$ is used in all cases and result for other FEC coding rates are available in appendix.

The Figure 3.30 and 3.31 shows the BLER performance and corresponding SE performance for 4QAM modulation. Here almost no effect of BO is visible. Since constellation

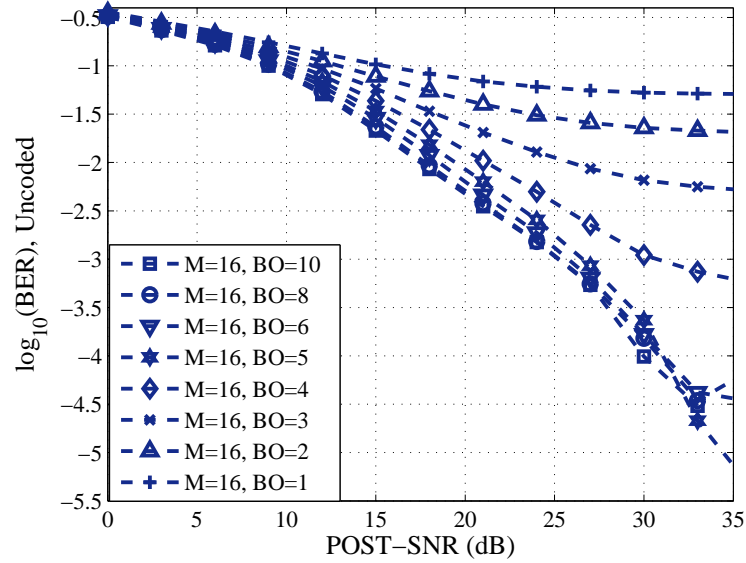


Figure 3.28: BER vs SNR curve for $M=16$, uncoded system in Fading Channel

points are quite far from one another, with 1 dB of BO it requires only 11 dB SNR to reach the BLER level of 10^{-1} . Whereas with 10 dB BO, 8 dB of SNR is required to reach the same level. Thus a BO difference of 9 dB is required to gain 3 dB of BLER performance gain at threshold 10^{-1} which is not practical at all. If the result is compared with the performance in AWGN channel, it can be seen that the nature is same, i.e. not much gain is achievable by employing large BO, but the performance degrades due to multipath fading. To reach BLER of 10^{-1} , 5 dB and 8 dB of SNR is required in AWGN and fading channel respectively. However, to reach BLER of 10^{-2} , around 8 dB and 14 dB of SNR is required in AWGN and fading channel respectively. With decreasing BLER level, impact of multipath fading increases. As it is obvious from the uncoded scenarios, the BO is not giving any improvement, it is better to use minimum BO and since coding reduces the spectral efficiency significantly, minimum coding rate should be chosen to achieve the high spectral efficiency for 4QAM modulation.

The Figure 3.32 and 3.33 represent the BLER and SE performance for 16QAM modulation. It can be seen from the figures that BLER performance is more dependant on BO compared to the 4QAM modulation. Impact of BO is not that much significant if it is 4 dB or more. However if BO is less than 4 dB then impact is quite significant. To reach

Chalmers University of Technology

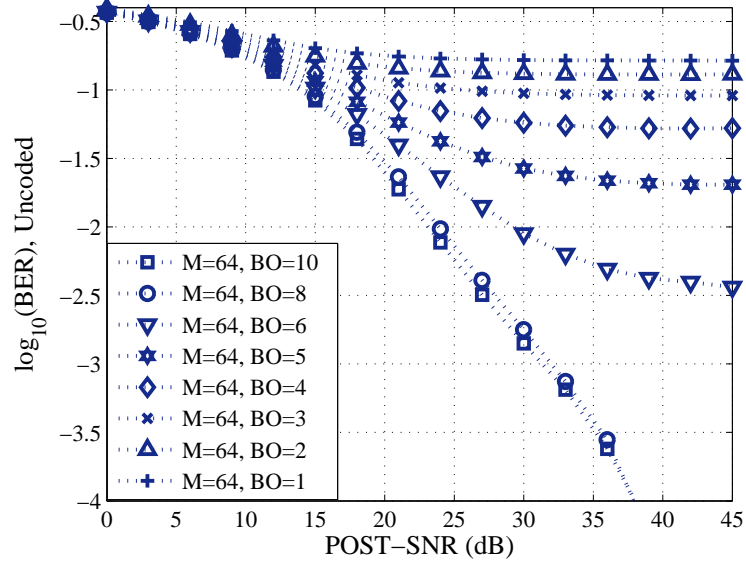


Figure 3.29: BER vs SNR curve for $M=64$, uncoded system in Fading Channel

the BLER level of 10^{-1} , difference in required SNR for the system with 2 dB and 3dB BO is 5 dB. Situation is even worse if 1 dB BO is considered. And SE also severely degrades in case of 1 dB BO power.

Like AWGN channel, most severely affected modulation among the schemes considered in this study is 64QAM. The Figure 3.34 and 3.35 represents the performance of 64QAM modulation. Effect of HPA can be suppressed only if BO equal to or greater than the median value of cdf of PAPR is applied. In order to reach BLER level of 10^{-1} , at least 5 dB BO necessary. Based on the level of BLER needs to be reached, some BO scheme even become unusable. Since the curves shows that to reach the level of 10^{-2} , we need BO power of at least more than 6 dB, the BO of 1 to 5 dB is not usable in this case. The BO has severe impact on SE performance as well. For BO of 5 dB and 10 dB, difference in SE is nearly 1 b/s/Hz at 30 dB of SNR. If the amount of BO employed is equal to or less than 3 dB, almost no SE is achievable. So, to achieve lower BLER and higher SE, around 8 dB of BO needs to be employed which is again the median value. However employing this amount of BO will cause a huge reduction of cell coverage.

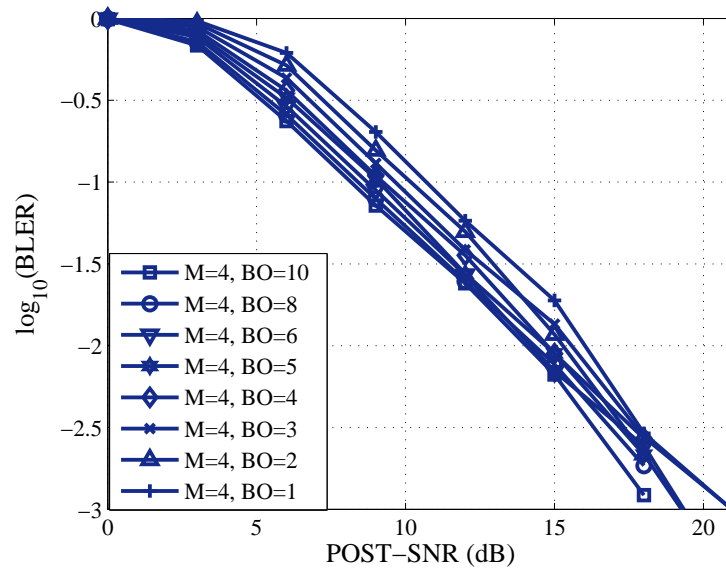


Figure 3.30: BLER vs SNR curve for $C = \frac{1}{2}$ and $M=4$ in Fading Channel

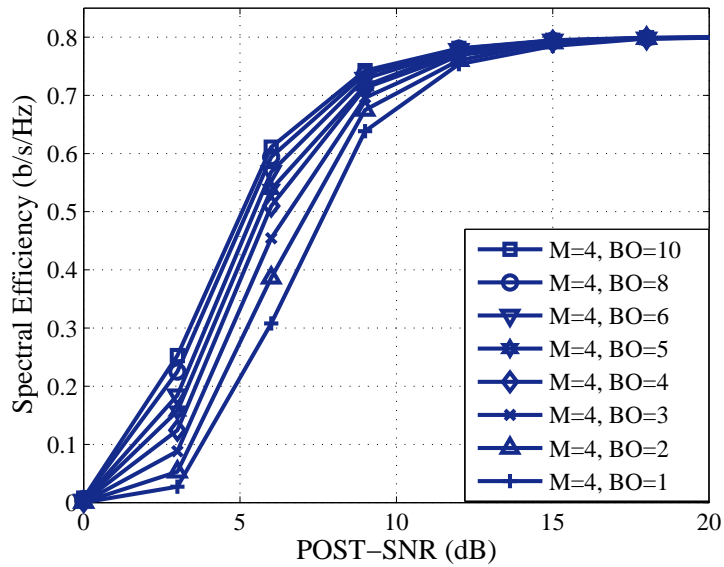


Figure 3.31: Spectral Efficiency vs SNR curve for $C = \frac{1}{2}$ and $M=4$ in Fading Channel

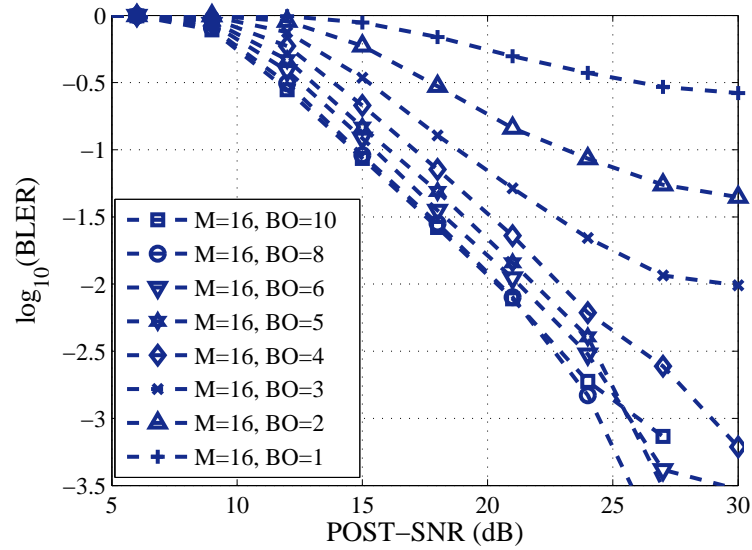


Figure 3.32: BLER vs SNR curve for $C = \frac{1}{2}$ and $M=16$ in Fading Channel

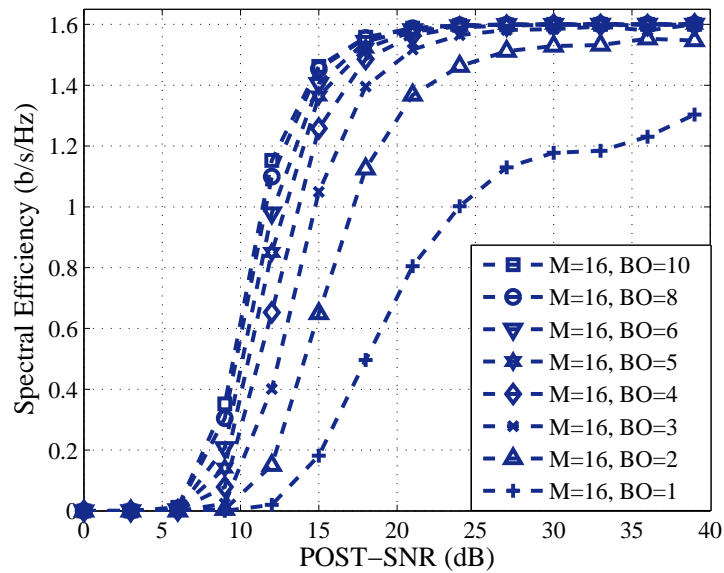


Figure 3.33: Spectral Efficiency vs SNR curve for $C = \frac{1}{2}$ and $M=16$ in Fading Channel

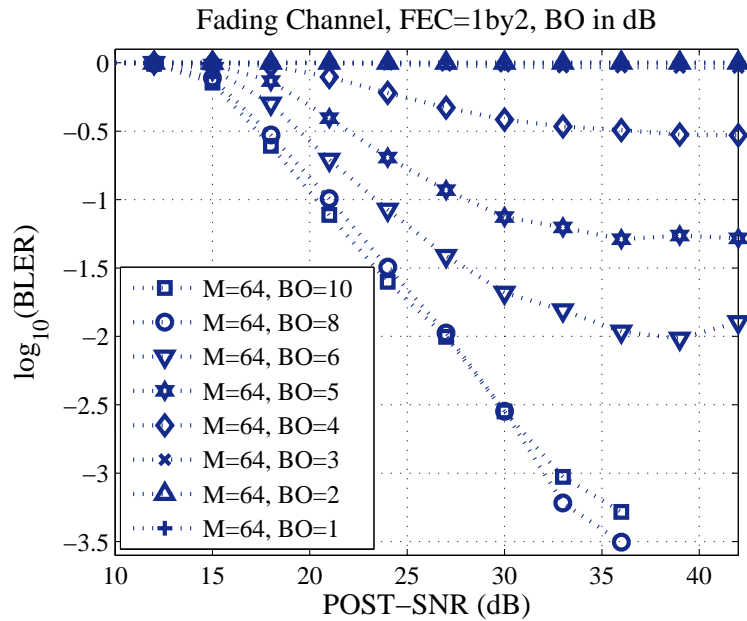


Figure 3.34: BLER vs SNR curve for $C = \frac{1}{2}$ and $M=64$ in Fading Channel

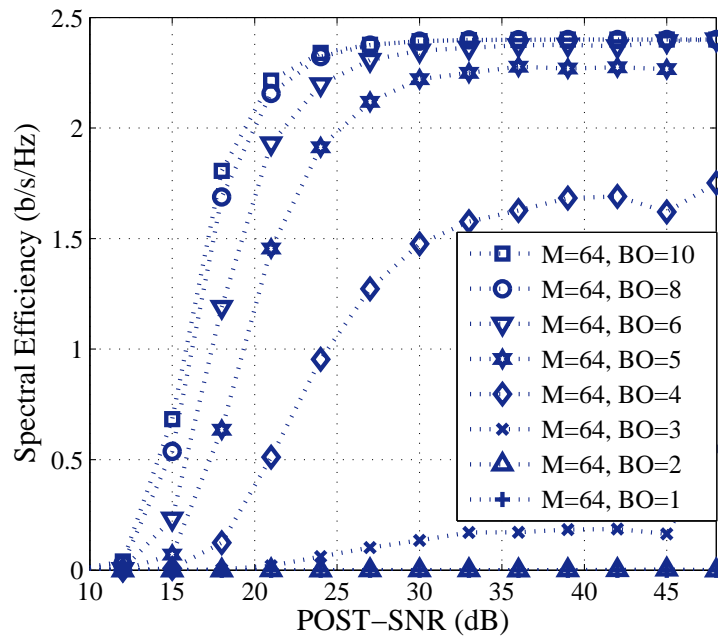


Figure 3.35: Spectral Efficiency vs SNR curve for $C = \frac{1}{2}$ and $M=64$ in Fading Channel

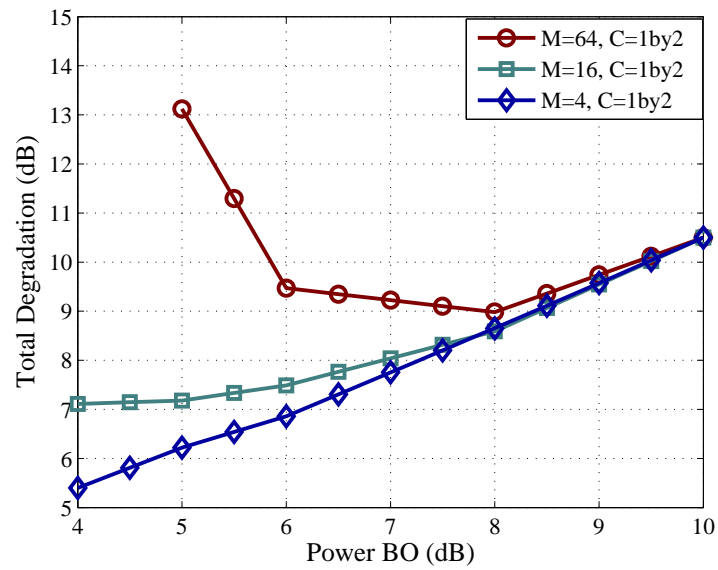


Figure 3.36: TD plot for $FEC = \frac{1}{2}$ with BLER Threshold = 0.1 in Fading Channel

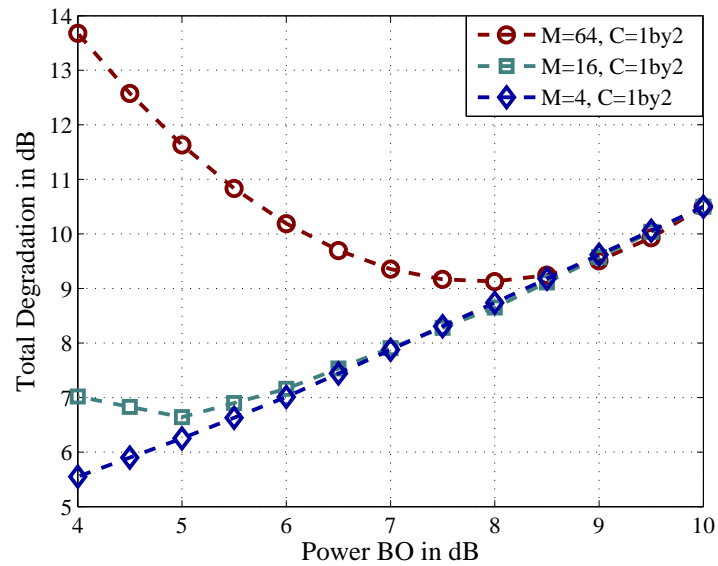


Figure 3.37: TD plot for $FEC = \frac{1}{2}$ with BLER Threshold = 0.05 in Fading Channel

Total Degradation Plot

The Figure 3.36 and 3.37 shows the total degradation curve for BLER threshold of 0.1 and 0.05 respectively. As mentioned earlier, this curve is very useful in determining which BO is to be selected for optimum performance. Similar to AWGN channel, optimum BO is different for different modulation level. Even it can change depending on the level BLER to maintain. For 64 QAM modulation, in both cases optimum BO is 8 dB which is the mean of the cdf of PAPR for the OFDM symbol with 512 subcarrier. Interestingly, for 16QAM modulation to get minimum total degradation different BO is needed for different BLER threshold. From the figures it can be seen that required BO is 4 dB and 5 dB to get the minimum degradation for of BLER threshold 0.1 and 0.05 respectively. For 4QAM, no BO is required at all.

3.6 Conclusion

In this chapter, the impact of HPA has been analyzed from different angles. Beginning with HPA model, cdf of PAPR is generated to see the nature of distribution of peaks in the symbol which also gives us the preliminary idea about the influence of BO required to reduce the nonlinearity due to HPA. The impact on signal level was investigated by generating spectrum plot. Then impact on constellation diagram was also studied. SDNR plots are generated which gives a further insight to the problem. It helps us to decided about range of SNR that are suitable for use.

In order to investigate the effect of HPA on system performance initially AWGN channel is studied with above mentioned impairments. The study is finally extended to the fading channel to include the multipath effect and also to see the performance under real environment scenarios. It has been found that there is significant impact of HPA on system performance which varies with modulation and coding rate. Though the impact is not very significant for low modulation rate, it becomes severe for higher modulation rates. BO is employed to reduce the effect of nonlinearity. However, the amount of BO power required to reduce the effect of nonlinearity to an acceptable level varies with modulation and coding

and coding rate becomes very important. And since LA system changes modulation and coding rate adaptively, investigation of LA system is also necessary. The result for LA system is presented in the next chapter.

Chapter 4

Influence of PAPR on Link Adaptation

4.1 Introduction

The condition of wireless channel is constantly changing. The change is more rapid if there is relative motion between transmitter and the receiver. A channel with a very good condition at one instant may experience a deep fade at the next instant. This fluctuation in received signal strength makes it extremely difficult to achieve very high data rate while maintaining a QoS constraint.

Link Adaptation (LA) is a technique which ensures efficient use of available spectrum. Adaptation of modulation, power and coding rate or any combination of these are done by exploiting channel dynamics. The main issues for such a link adaptation mechanism are the choice of parameter or parameters to be used for link quality estimation (e.g. packet error rate, signal to noise ratio, received signal strength, carrier to interference ratio, etc.), and how to select the appropriate rate from measurements of the selected parameter [36]. This selection usually varies based on the application for which link adaptation is done.

In this chapter basic LA concept with LA system model is described which is followed by a brief description to the LA algorithm used in the study. Finally, simulation results and performance comparison for different scenarios in both AWGN and fading channel is presented.

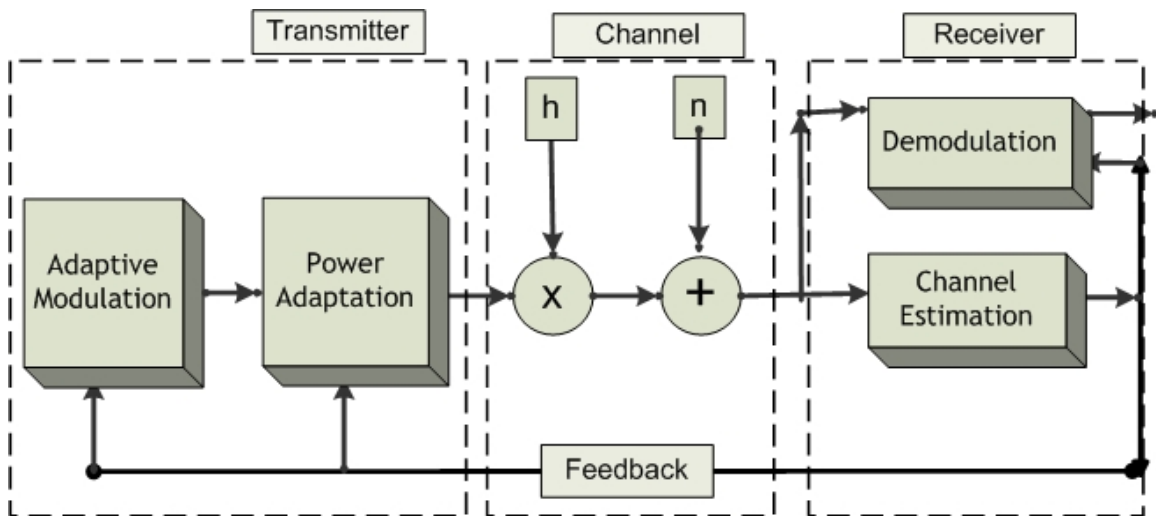


Figure 4.1: Basic Link Adaptation system employing adaptive modulation

4.2 Link Adaptation Concept

The Figure 4.1 shows the block diagram of a single carrier link adapted system. This model can be extended for multicarrier system simply by including channels for N subcarrier.

Link adaptation is done based on the feedback from the receiver. Some predefined known signal is transmitted in some of the subcarriers of OFDM symbol which is referred to as pilot and the subcarrier used to carry this signals are known as pilot subcarriers. In an OFDM transmission system, pilots are usually distributed in both time and frequency as shown in Figure 4.2. This pilot signal is estimated at the receiver and measured information is sent back to the transmitter which is referred to as Channel State Information (CSI). More frequently the pilot is sent, more accurate the CSI is. Since these pilot subcarriers do not carry any data, effective system throughput decreases with the increase in number of pilot subcarrier. On the other hand, too few pilots may make the CSI information obsolete and as a consequence LA system may fail due to erroneous and invalid feedback information. although the effective throughput increases. The amount of doppler shift also have impact on validity of CSI. Higher the doppler shift, faster the channel variation and more pilot is needed to get valid CSI. So a trade off must be made between efficiency of the system and accuracy of CSI while taking other parameters into account.

The Figure 4.4 shows how the LA system works considering the Spectral Efficiency

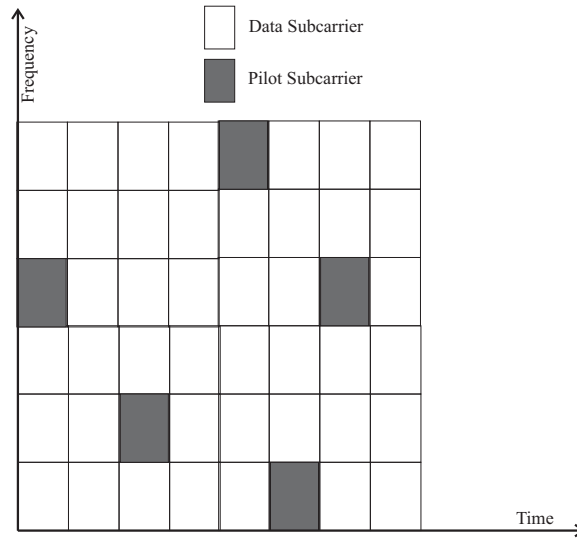


Figure 4.2: Pilot Subcarrier for CSI

(SE). The curves with different markers represent the SE performance of different modulation and coding. Now, if LA system is applied then with the increasing SNR the system will choose the modulation and coding rate, which has the best SE performance at that SNR. For example, from 0 to 3 dB, the only option is 4QAM with $FEC = \frac{1}{2}$ rate and the system will transmit with this scheme. However, until 8 dB there are two options, one is 4QAM with $FEC = \frac{1}{2}$ and other is 16QAM with $FEC = \frac{1}{3}$. The system will opt the previous one since it has the better spectral efficiency. At the value close to 8 dB the SE performance of 16QAM with $FEC = \frac{1}{3}$ crosses that of 4QAM with $FEC = \frac{1}{2}$ and immediately the system will switch to 16QAM with $FEC = \frac{1}{3}$. The dashed curve with maroon color represents the SE performance of this system.

Table 4.1: Switching Threshold for Link Adaptation

Modulation & FEC	M=0, C=0	M=4, C= $\frac{1}{2}$	M=16, C= $\frac{1}{3}$	M=16, C= $\frac{1}{2}$	M=16, C= $\frac{2}{3}$	M=64, C= $\frac{1}{2}$
SNR (dB)	0	8.2	10.9	14.7	18.4	20.4

QoS requirements varies based on the applications. Voice data tolerates low BLER, whereas file transfer application does not have strict BLER requirement. However, if some QoS constraint is imposed to meet the requirement of particular application, the LA concept described above will change slightly. For example if a system needs to maintain certain

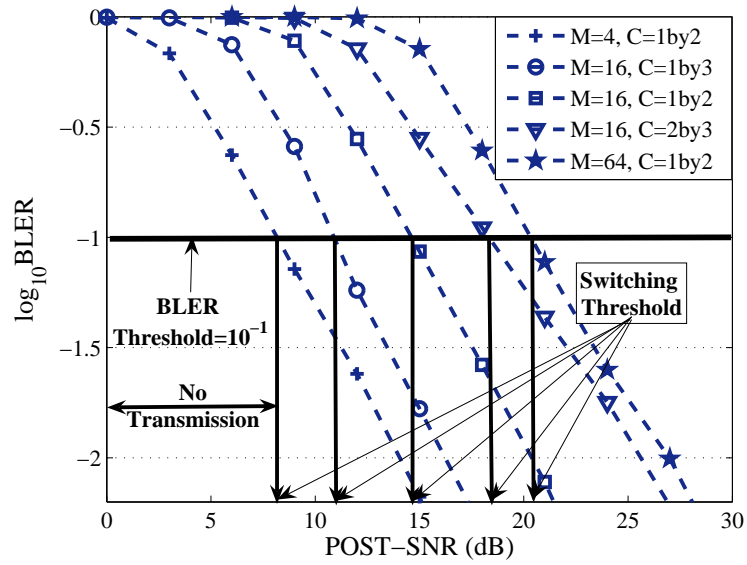


Figure 4.3: BER Threshold Points for LA System

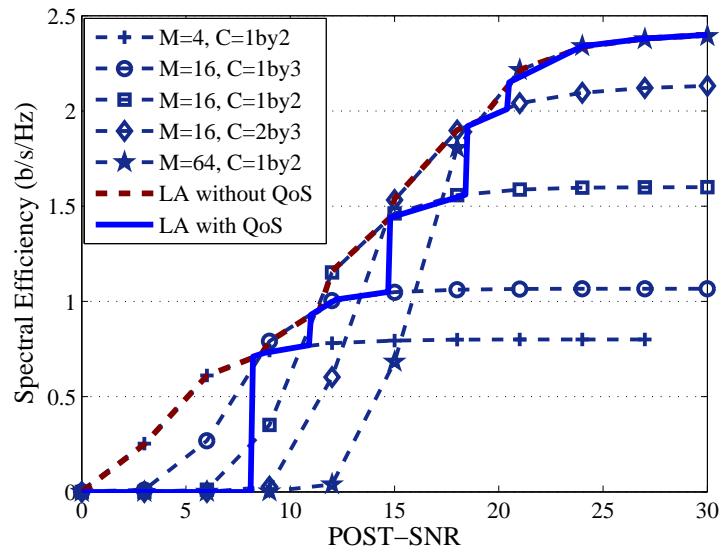


Figure 4.4: Spectral Efficiency Gain for LA System

BLER, it first strictly considers the BLER requirement and upon meeting this condition it considers the option which maximizes the SE performance. The Figure 4.3 shows the threshold points when the system can change from one modulation and coding scheme to another while maintaining the BLER constraint of 10^{-1} . To maintain this QoS, the system will not transmit until it reaches to 8 dB SNR even there was some SE much earlier. And it will switch to the next modulation and coding rate only if BLER constraint is met. Continuous blue curve in Figure 4.4 shows the performance of QoS constrained LA system.

4.2.1 LA with PAPR

OFDM signal, a expressed in Eq. 3.5 and whose PAPR is expressed by Eq. 3.4, is fed to the input of the HPA. The output of the HPA depends on the nonlinearity parameter p given by the equation 3.3. Output of the HPA can be written as:

$$y(t) = \alpha \cdot |x(t)|^2 \cdot e^{j\angle x} + n(t) = f(|x|^2, \alpha) \quad (4.1)$$

where, α is an attenuation constant depending on power BO value and $x(t)$ and $n(t)$ are uncorrelated.

Variance of the distortion caused by the amplifier is given by,

$$\sigma_D^2 = E[|x(t)|^2 - f(|x|^2, \alpha)]. \quad (4.2)$$

The SDNR can be expressed as:

$$SDNR = \frac{f(|x|^2, \alpha)}{\sigma_D^2 + \sigma_w^2} \quad (4.3)$$

where σ_w^2 is the variance of white gaussian noise.

For LA based system, threshold are the function of SNR distribution[37]. And since the Eq.(4.3) clearly shows that the SDNR is function of α which depends on amount of BO. So thresholds are also become dependent on α . This means the LUT, which contains the threshold values for different modulation and coding rate at certain BLER constraints, needs to be updated. For uncoded system, it is possible to obtain analytical expression

for revised threshold. However, this is not applicable to coded system. Since almost all practical system, as well as system under investigation, i.e. 3GPP-LTE and WiMAX, uses FEC coding, analytical expression obtained for uncoded system will not be usable.

Therefore, computer based simulations are used in this work in order to find the additional margin needed to update LUT for maintaining the QoS constraint.

4.3 Link Adaptation Algorithm

There are several LA algorithms available for OFDM systems. A very complex algorithm, is derived in [38], which achieves high spectral efficiency. Another algorithm is designed in [39] which is simpler in implementation but have lower throughput. The authors in [8] developed an algorithm which has the highest possible throughput of the two algorithms referred, while the complexity is between the two and is referred to as Simple Adaptive Modulation and Power Distribution Algorithm (SAMPDA). In SAMPDA, greedy approach is used, but unlike the Adaptive Power Distribution Algorithm (APDA) which starts from 0 power and 0 bits at the beginning, the algorithm is initiated with equal power for all sub-carriers. Then by comparing received SNR with the SNR-lookup table, loaded bits for each subcarrier can be found, and power required for each subcarrier is recalculated. Detailed performance results related to SAMPDA can be found in [8][16].

SAMPDA algorithm has been used in this work with some minor modification. In the original algorithm subcarrier based allocation with power redistribution was proposed. However, in 3GPP-LTE subchannels are considered instead of subcarrier for all allocation. A subchannel is formed by grouping few subcarriers together. So in this study an average power of subcarriers in a subchannel is used. In the original algorithm after bit allocation based on the expected received SNR, power of each subcarrier is reduced to the threshold level and it was preserved in a power sink. Also the power initially assigned to the subchannels that are excluded due to too bad condition is also added to the power sink. Then another iteration was done to redistribute the power to the subcarriers if there was any chance to increase the bit loading. To make the work simpler, power redistribution is excluded in our work. The modified algorithm is shown in Figure 4.5

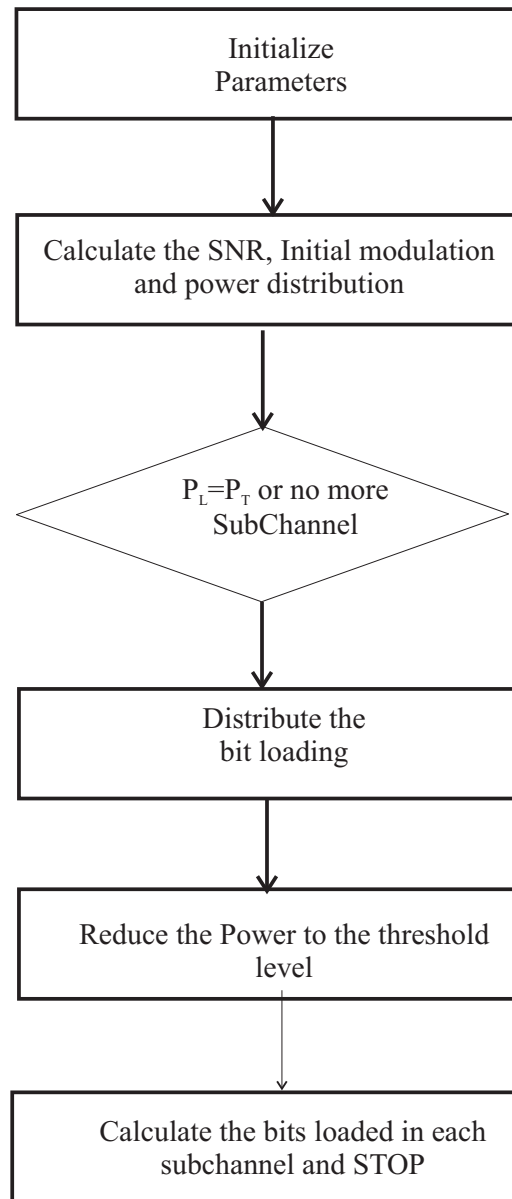


Figure 4.5: Link Adaptation Algorithm

4.4 Performance of LA based OFDM System

Performance of LA system has been investigated for both AWGN and fading channel. From the basic BLER vs SNR curve for different BO values, the nature of performance degradation can be found. The basic LUT is prepared from the basic BLER vs SNR curves. All the result obtained for LA based system is for $FEC = \frac{1}{2}$. BLER threshold was set 0.1 for all the simulations. Simulation is done for different combination of important parameter such as power BO, SNR values etc to bring out the necessary measures that compensates for the performance degradation. The detail result is presented and analyzed in the following subsections.

4.4.1 CDF of PAPR for LA System

From the expression of cdf of PAPR as given in Eq. 3.7 and also from the Figure 3.3 [40] it is clear that PAPR depends on the number for subcarrier. The link adaptation system used in this work, first decides which sub channels have sufficient SNR to be selected for loading bits. Thus when input SNR varies, number of subcarrier loaded during link adaptation also varies. The relation between SNR and the number of loaded subcarriers can be found in [16].

However, interestingly, the PAPR distribution for LA based system doesn't show that it varies with the variation of SNR. The Figure 4.6 shows the comparison for OFDM with 128 and 512 subcarrier for different scenarios. The basic curve for 128 and 512 subcarrier is shown. Then LA system is simulated for 5 dB and 20 dB and for each case PAPR distribution for the same number of subcarrier are shown. There is hardly any difference in PAPR distribution recognizable between systems with and without LA though the number of subcarrier loaded with bits varies significantly. The reason might be that high PAPR occurs very rarely [8]. And when proportion of average power and maximum power changes at the same level, PAPR distribution doesn't change even the SNR varies a lot.

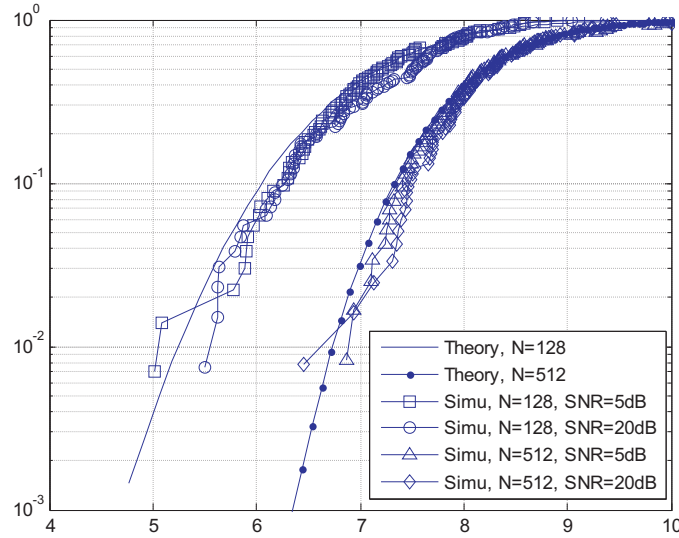


Figure 4.6: PAPR distribution for LA based OFDM system

4.4.2 Performance in AWGN Channel

The first row of the Table 4.2 shows the threshold for different modulation level when BLER constraint was set to 0.1. The Figure 4.7 shows the performance with the ideal scenario, i.e. when amplifier distortion is not taken into account. It clearly satisfies the BLER constraint. Figure 4.10 gives the corresponding SE performance. However when the power amplifier distortion is taken into account, it fails to satisfy the required BLER constraint, even though some back off power is employed which shifts the operating point to the more linear region. This is evident from Figure 4.8 that the performance of LA system also depends on amount of BO employed. With the same basic LUT, performance of the system with 5 dB BO is worse than that of with 6 dB BO. The Figure 4.10 shows how severely the throughput performance can be affected if PAPR is not taken care properly.

If 10 dB of BO is employed then it can accommodate most of the high peaks and performance is same as basic system as shown in Figure 4.7. However, this large amount of power back off drastically reduce the coverage. Obviously it can not be taken as the solution and some alternative method is required which compensates for the degradation. Section 4.2.1 suggests to modify the LUT by adding some extra margin which will compensate for

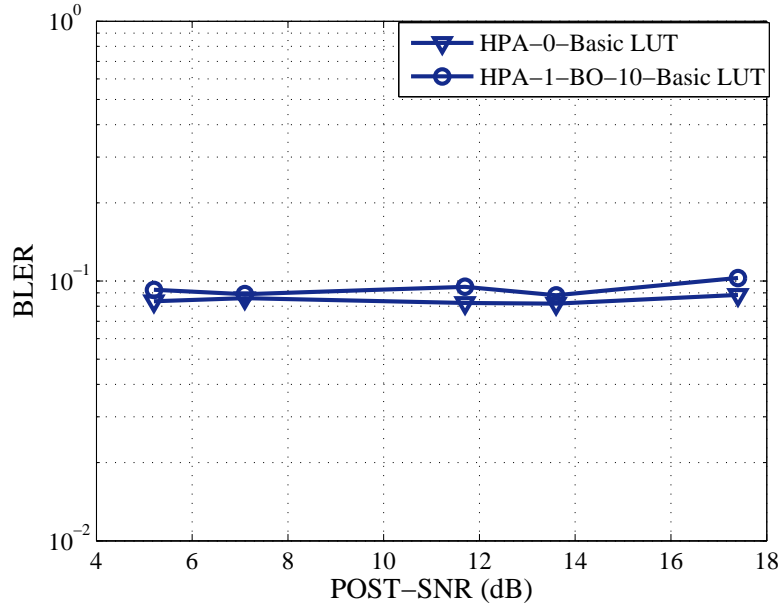


Figure 4.7: Performance of LA system with basic LUT when no power amplifier is applied

Table 4.2: LUT with basic and updated values for system with $FEC = \frac{1}{2}$ in AWGN Channel (Values in dB)

Power BO	None	QPSK	16QAM	64QAM
Ideal	0	5.1	11.6	17.3
6	0	5.1+0.5	11.6+0.9	17.3+2.9
5	0	5.1+0.8	11.6+1.5	17.3+7.1

the BLER degradation and thereby ensure maintaining the BLER constraint. The margin will be different for different amount of back off power employed. Less the amount of BO, more the distortion that results in more BLER performance degradation and hence more amount of threshold is needed. The Table 4.2 shows the ideal scenario as well as the added margin for non ideal cases with different BO power. And this is clear that more margin is needed if less BO is employed.

The Figure 4.9 shows that the system satisfies the QoS constraint when additional margin to the threshold is provided.. And the Figure 4.10 shows that spectral efficiency performance is restored to nearly the performance of the basic system.

There exists a zigzag nature in the curves in Figure 4.9 and in Figure 4.8 when HPA was used. This is due to the power adaptation algorithm used in the system. For each

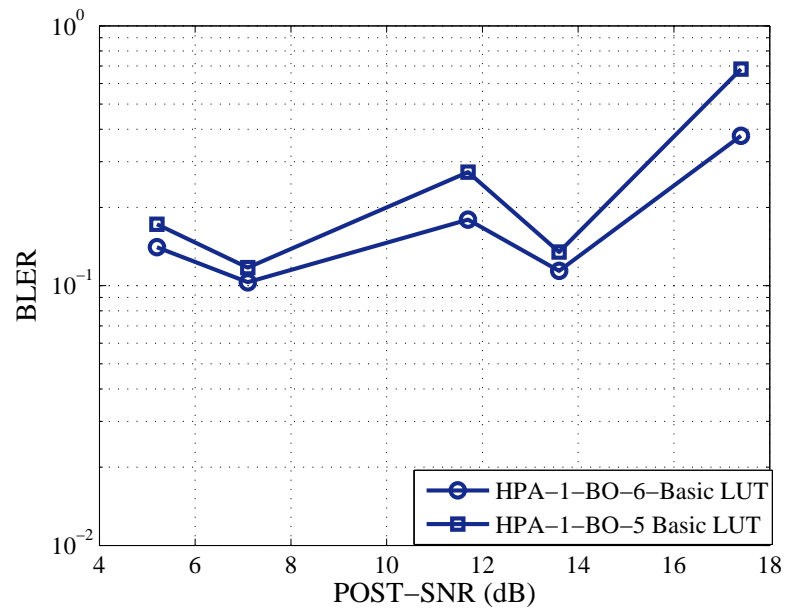


Figure 4.8: Performance of LA system with basic LUT when power amplifier is applied

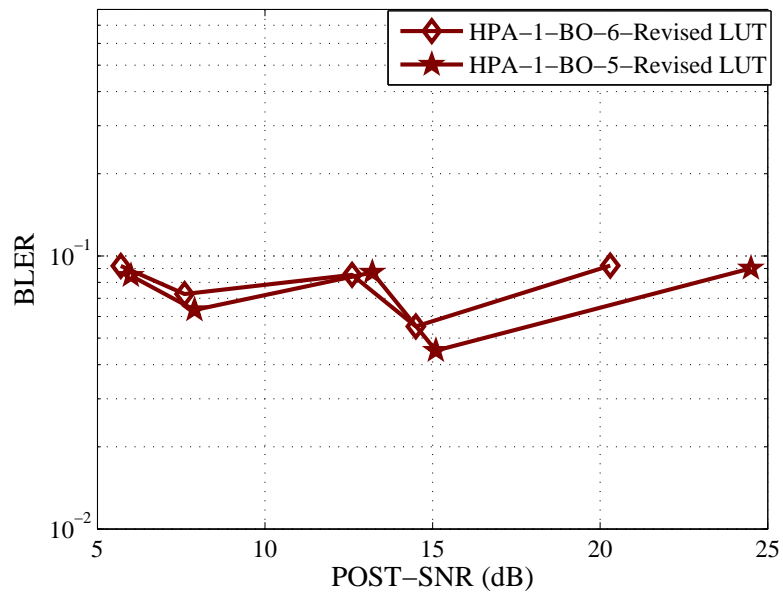


Figure 4.9: Performance of LA system with revised LUT when power amplifier is applied

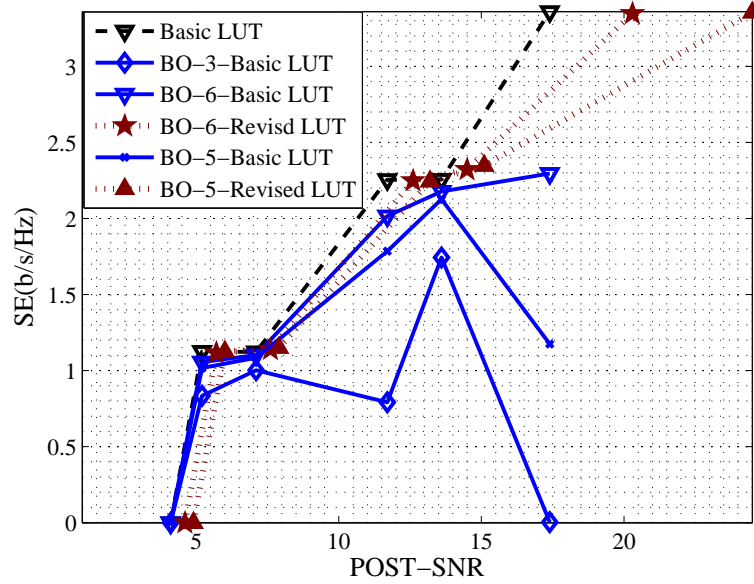


Figure 4.10: Spectral Efficiency comparison for LA system with and without PAPR consideration

subchannel, SNR is measured and checked which modulation scheme threshold it satisfies. And power for that subchannel is reduced to the threshold level. However, reducing power of the subchannel is in a way backing off power by certain amount which means it operates more in linear region that definitely improves the BLER performance. For two different operating SNR, amount of power reduction is different and therefore BLER performance for same LUT is different accordingly. That's why the zigzag nature is found in the figure.

4.4.3 Performance in Fading Channel

The discussion and results presented so far is based on AWGN channel. To use the results found for AWGN channel into the real system, it is very important to investigate the performance in the fading channel.

The study of link adaptation system is not so straight forward as in AWGN channel. For AWGN channel, there is no difference between $PRE-SNR$ and $POST-SNR$. So adaptation based on the $PRE-SNR$ was quite easy. Mostly it followed the BLER performance at different BO as found in the basic simulations.

In the previous chapter it was mentioned clearly how the performance based on

Table 4.3: LUT with basic values for system with $\text{FEC} = \frac{1}{2}$ in Fading Channel (Values in dB)

Power BO	None	QPSK	16QAM	64QAM
Ideal	0	8.46	14.76	20.58

POST-SNR is calculated. For link adapted system, for each PRE-SNR, subchannels can be loaded with different modulation rate depending on the estimated POST-SNR. In this case three different PRE-SNR 10, 20 and 25 dB were chosen. Finally calculations for different performance measures were done based on the received SNR.

To comply with the standard of 3GPP-LTE, subcarriers were grouped into subchannels. It is possible for the subcarriers of the same subchannel may experience some different fade. However, during measurement of the received SNR, an average of all the subcarriers in a subchannel were used. Definitely, there has been some inaccuracy due to averaging of information.

The table 4.3 shows the threshold of the basic system. System performance using the basic thresholds are shown in Figure 4.11 and 4.12 when 6 dB and 4 dB of BO was employed respectively. In both the cases system fails when 20 dB and 25 dB of transmit SNR was used and system satisfies when 10 dB of transmit SNR was used. Then using trial and error method, additional margins to satisfy the BLER constraint has been brought out. The Table 4.4, 4.5 and 4.6 gives the new LUT with additional margin required to satisfy the BLER constraint for 10, 20 and 25 dB of PRE-SNR. The performances with the revised LUT are shown in Figure 4.13 and 4.14.

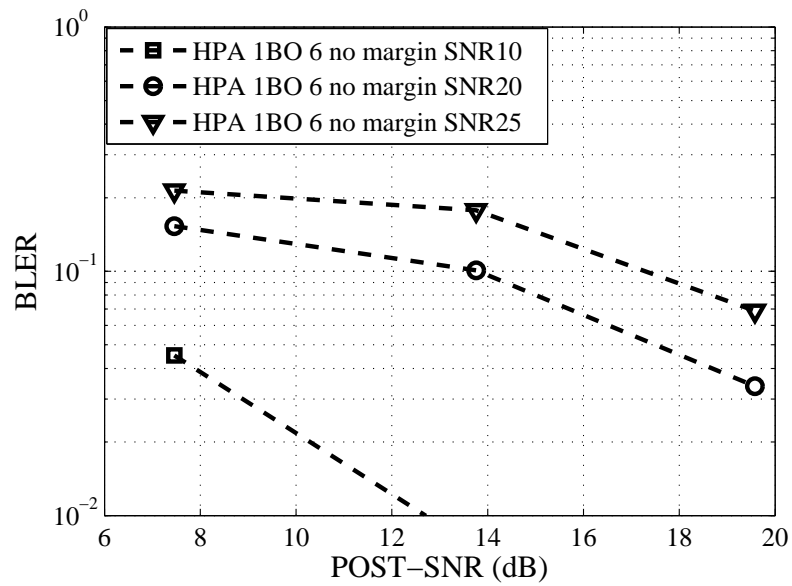


Figure 4.11: Performance of LA system with basic LUT for 6 dB of BO power

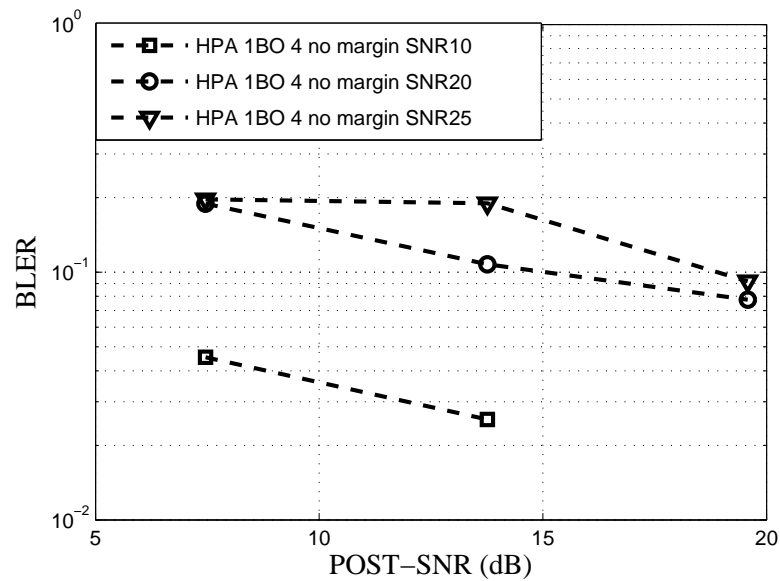


Figure 4.12: Performance of LA system with basic LUT for 4 dB of BO power

The above results give an interesting insight to the problem. When 10 dB of PRE–SNR was employed, which is slightly higher than the the switching threshold for 4QAM, the most of the subcarriers are loaded with 4QAM and few of the subcarrier may experience very good channel and are loaded with 16QAM. As seen from the performance presented in previous chapter that 4QAM is not that much affected by HPA so it satisfies the BLER level and the very few channels which are loaded with 16QAM are really good channel. So they also satisfy the performance and hence no additional margin is required.

Now for 20 dB of PRE–SNR, most of the subchannels are likely to be loaded with 16QAM and those experiencing very good channel conditions are loaded with 64 QAM. And the subchannels which experiences extremely worse channel condition get loaded with 4QAM. Even though they were loaded with 4QAM, due to their extremely bad channel condition, they are failed to satisfy the constraint. Hence, some additional margin is needed. And for 16QAM modulations due to HPA effect, they fails to meet the target BLER. And it can be seen from the Figure 4.13 and 4.13 that with additional margin they satisfy the BLER requirement. Since only very good subchannels are loaded with 64QAM, they meet the target BLER. The higher the BO, lower the additional margin required.

For 25 dB of PRE–SNR, it follows the same pattern but more margin is needed for different modulation scheme as compared to that of 20 dB PRE–SNR. The results give a very interesting insight to the problem. Depending on the PRE–SNR, the required threshold for switching of LA system changes. Also it is very tough to get the accurate solution for LA system when subchannels are considered instead of subcarriers. Because with the same average subchannel SNR, subcarriers of different subchannel may experience different fade and therefore the behavior will also be different which makes the decision extremely difficult. So, to make the system satisfy a set of LUT is required for different transmit SNR.

Table 4.4: LUT with updated values for system with $FEC = \frac{1}{2}$ and PRE–SNR of 10 dB in Fading Channel(Values in dB)

Power BO	None	QPSK	16QAM	64QAM
6	0	8.46+0	14.76+0	20.58+0
4	0	8.46+0	14.76+0	20.58+0

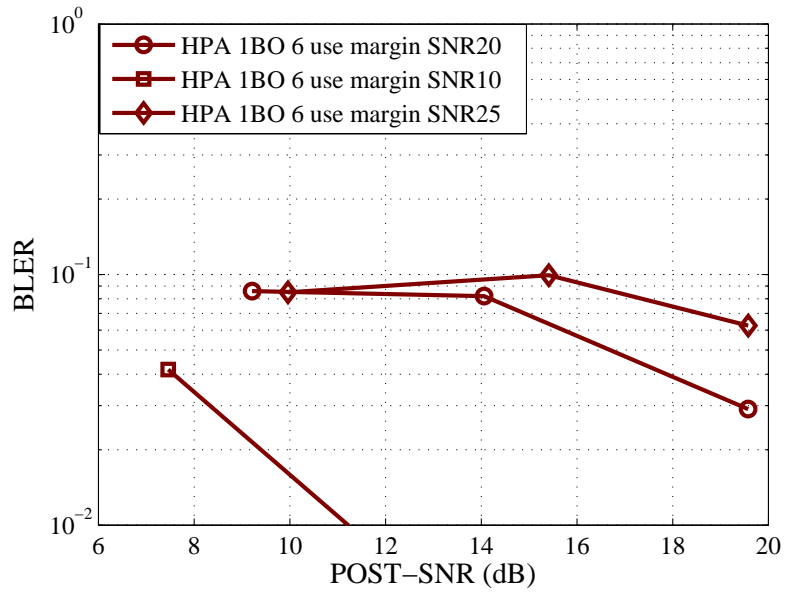


Figure 4.13: Performance of LA system with revised LUT for 6 dB of BO power

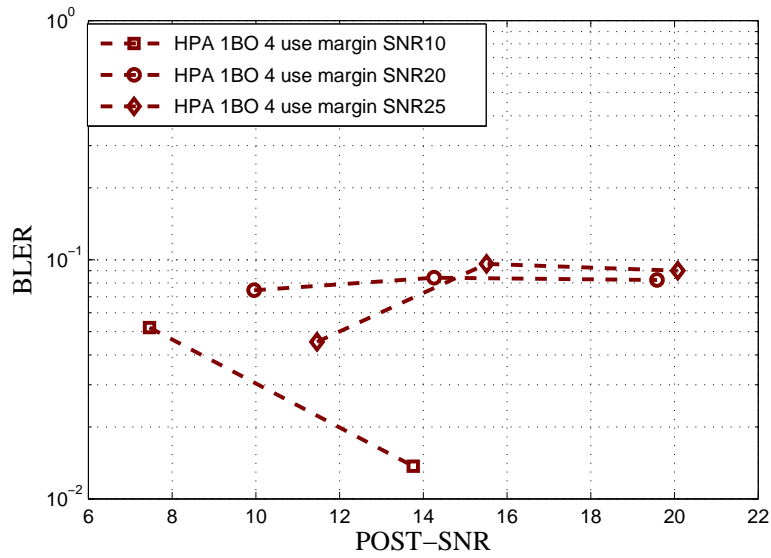


Figure 4.14: Performance of LA system with revised LUT for 4 dB of BO power

Table 4.5: LUT with updated values for system with $FEC = \frac{1}{2}$ and PRE-SNR of 20 dB in Fading Channel(Values in dB)

Power BO	None	QPSK	16QAM	64QAM
6	0	8.46++1.75	14.76+0.3	20.58+0
4	0	8.46+2.5	14.76+0.5	20.58+0

Table 4.6: LUT with updated values for system with $\text{FEC} = \frac{1}{2}$ and PRE-SNR of 25 dB in Fading Channel (Values in dB)

Power BO	None	QPSK	16QAM	64QAM
6	0	8.46+2.5	14.76+1.65	20.58+0
4	0	8.46+4.0	14.76+1.75	20.58+0.5

4.5 Conclusion

The above results for LA performance justifies the necessity of modifying existing LA algorithm in order to maintain the QoS. So, PAPR issue should be taken care properly. In this work only $\text{FEC} = \frac{1}{2}$ is considered. Results can be obtained for all other code rates in the same way. The LA system performance study considering PAPR in fading channel is extremely difficult due consideration of subchannels instead of subcarrier as in 3GPP-LTE standard. To get the accurate measures, all the impairments PAPR, ICI, feedback delay etc. need to be considered together. With the modified algorithm that finds the additional margin and updates the LUT to make the system maintain the BLER threshold we can generate several LUT for different combination of back off power and coding rate at different transmit SNR and use them where they fit best.

Chapter 5

Conclusion

5.1 Summary

The basic challenge of designing an efficient wireless system is to maintain certain quality of service by overcoming wireless channel fluctuations. All the impairment present in the system as well as in the environment should be considered very carefully. The Link adaptation techniques for OFDM based system needs to consider PAPR since it hampers the performance. The cumulative distribution function of PAPR in OFDM signal was studied in the beginning to see the nature of PAPR in OFDM symbol.

For both AWGN and Fading channel, performance was studied in terms of BER, BLER, Spectral Efficiency. In order to show the importance of PAPR consideration during design of link adaptation, a basic comparison has been done by simulating a system with HPA and without HPA. It shows significant performance difference exists in terms of BLER and Spectral Efficiency. Then impact of different power BO has also been studied. Power BO helps to reduce the effect of HPA by shifting operating point more to the linear region. With 10 dB of BO value, it is found that the nonlinear distortion is almost completely removed and it performs like a basic system. However, implementation of this large BO reduces the coverage drastically. All the basic performance is investigated for both AWGN and fading channel. Coded and uncoded system performance is also compared. FEC rate of $\frac{1}{2}$, $\frac{1}{3}$ and $\frac{2}{3}$ has been studied in conjunction with modulation scheme of 4-, 16- and 64-QAM.

Based on all of the above basic results we then investigated the performance existing algorithm of link adaptation systems. We found the existing system fails to maintain the target BLER which results in severe spectral efficiency degradation at high SNR. We proposed some modification of existing algorithm that modifies the LUT which was prepared based on the existing algorithm. When some additional margin is added to the LUT, the system again satisfies the target BLER and thereby maintains nearly the same spectral efficiency as of the basic system. Also we generated total degradation curves to find out the optimum power BO for each modulation and coding. With the consideration of PAPR now the system performance is quite satisfactory

5.2 Further Work

Since only a little attention is given to LA system with PAPR consideration, in a lot of ways this work can be further extended.

Quite a number of methods have been proposed so far to reduce the PAPR [7]. However, these methods also introduce some BER or BLER degradation. The main advantage of baseband processing is easier processing of signal in baseband than in RF domain.

Since the introducing BO means reduction in cell coverage. The study can be further extended to find out the impact on link adaptation considering cell coverage.

It would be an interesting area to investigate how this system performs in conjunction with different PAPR reduction mechanism. It may come out that some reduction mechanism along with the updated table gives better performance in terms of cell coverage, spectral efficiency and maintaining target BLER. In our work standard we followed was 3GPP-LTE. Since WiMAX proposes scalable OFDMA and support for distributed subcarrier allocation per subchannel, it offers a wide area to explore the impact of PAPR on link adaption in WiMAX like sytem.

The study was carried out with a fixed doppler frequency of 50 Hz. A comparative study can be done to find out the impact of different user speed. All other impairments can be combined together to get the big picture of LA system performance considering all the impairments.

The impact of PAPR on OFDM based 3GPP-LTE and WiMAX like systems can be incorporated with resource allocation algorithms to investigate how it affects overall system performance.

Appendix A

BLER and SE performance for Coded System

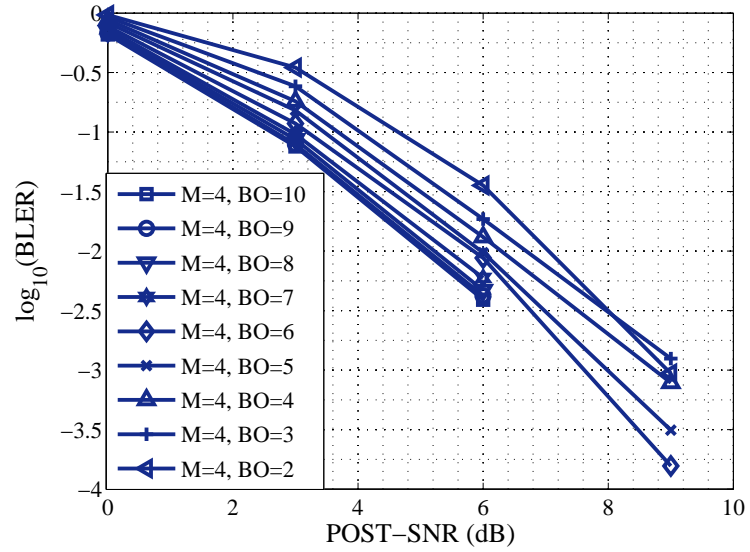


Figure A.1: BLER vs SNR curve for $C = \frac{1}{3}$ and $M = 4$ in AWGN

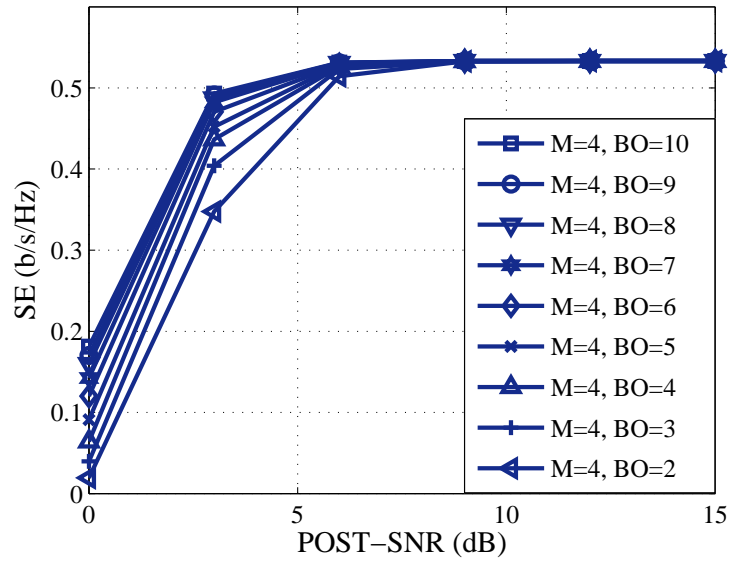


Figure A.2: Spectral Efficiency vs SNR curve for $C = \frac{1}{3}$ and $M = 4$ in AWGN

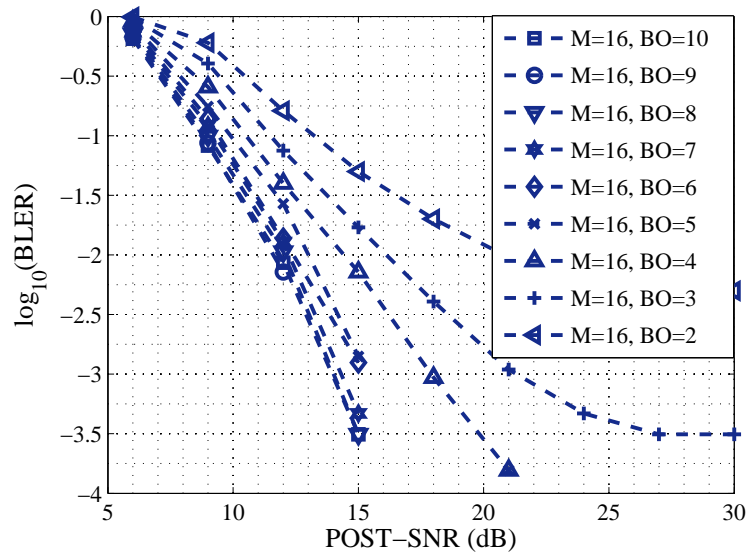


Figure A.3: BLER vs SNR curve for $C = \frac{1}{3}$ and $M=16$ in AWGN

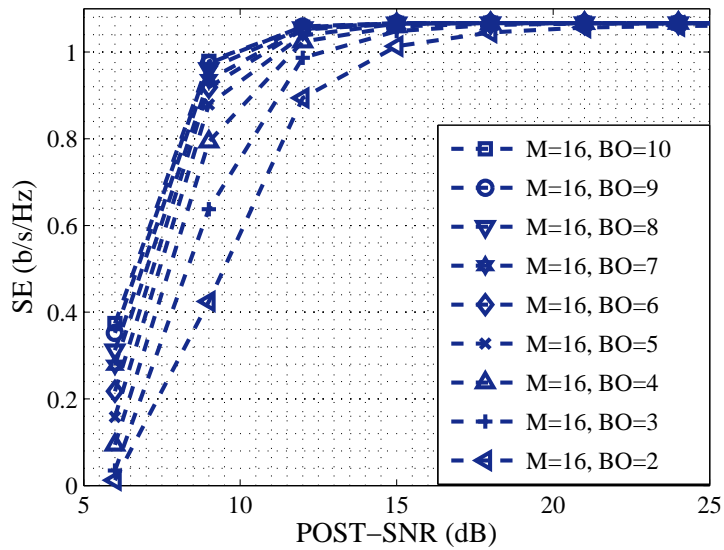


Figure A.4: Spectral Efficiency vs SNR curve for $C = \frac{1}{3}$ and $M=16$ in AWGN

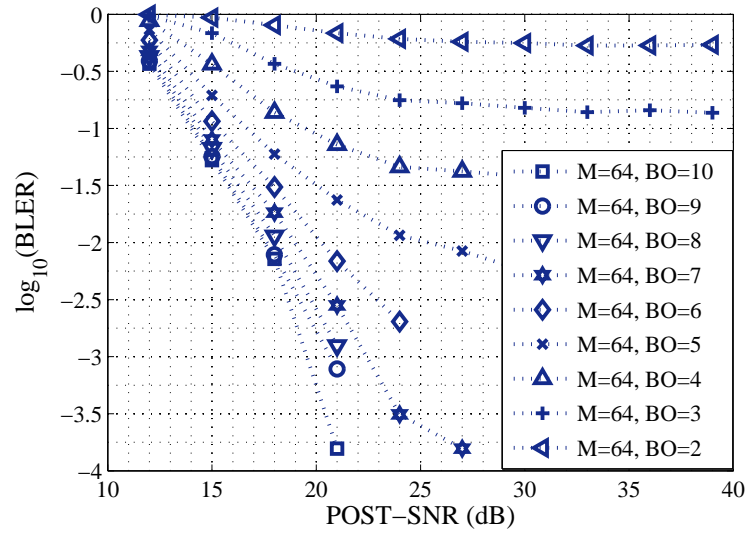


Figure A.5: BLER vs SNR curve for $C = \frac{1}{3}$ and $M = 64$ in AWGN

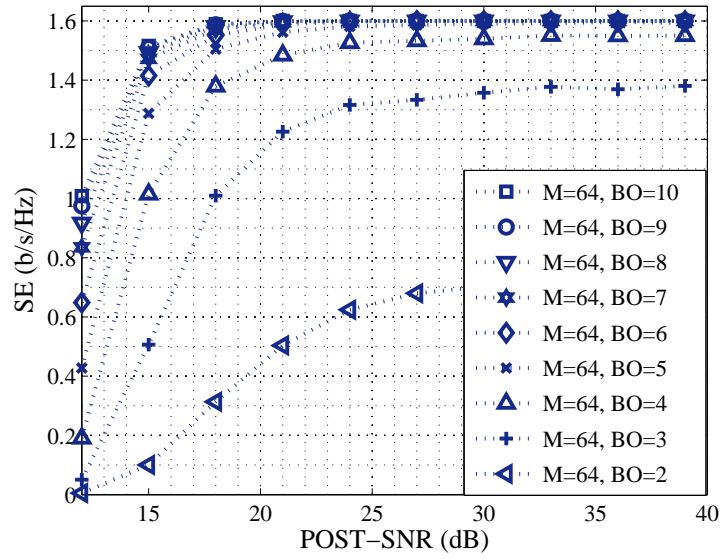


Figure A.6: Spectral Efficiency vs SNR curve for $C = \frac{1}{3}$ and $M = 64$ in AWGN

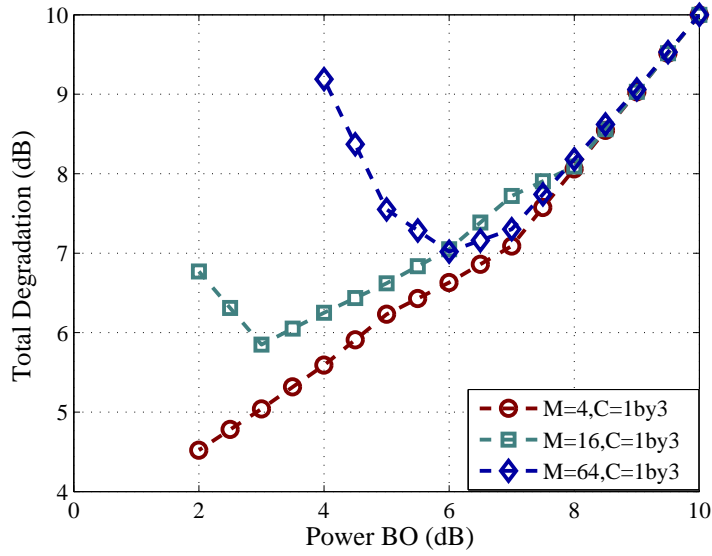


Figure A.7: TD plot for $FEC = \frac{1}{7}$ with BLER Threshold= 0.1 in AWGN

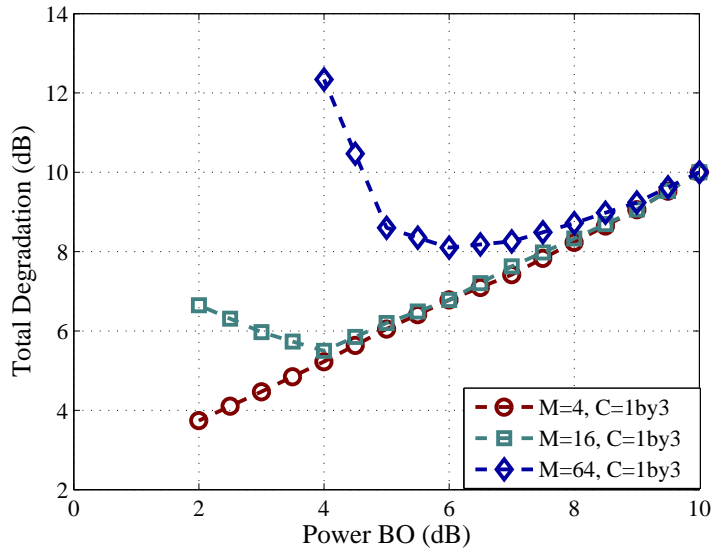


Figure A.8: TD plot for $FEC = \frac{1}{3}$ with BLER Threshold= 0.05 in AWGN

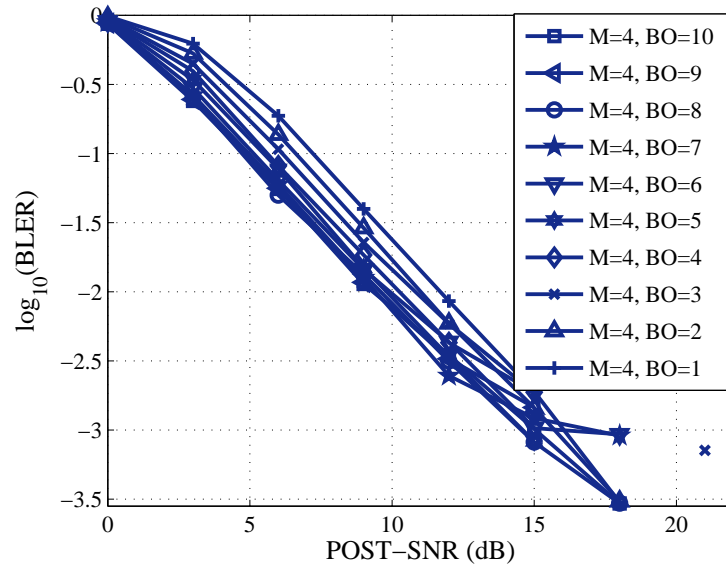


Figure A.9: BLER vs SNR curve for $C = \frac{1}{3}$ and $M=4$ in Fading Channel

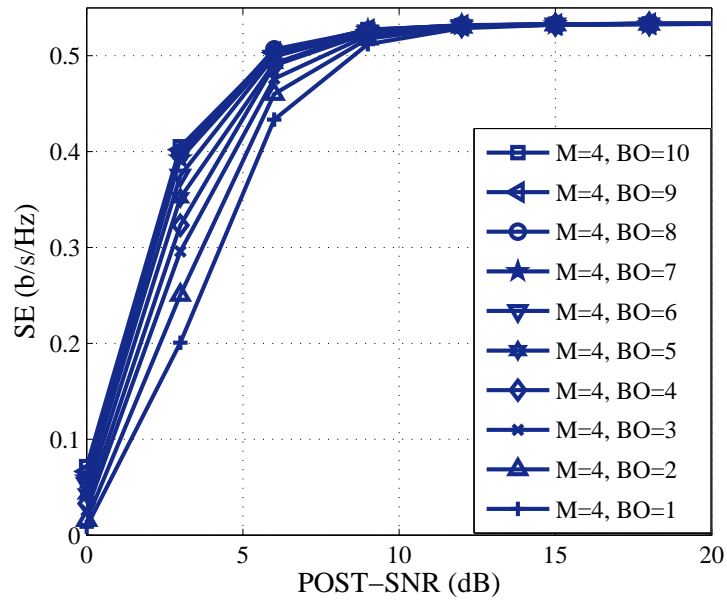


Figure A.10: Spectral Efficiency vs SNR curve for $C = \frac{1}{3}$ and $M=4$ in Fading Channel

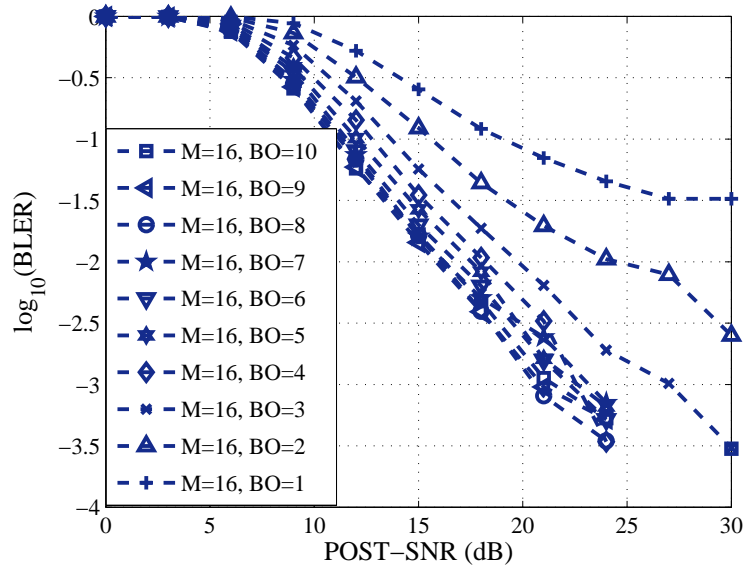


Figure A.11: BLER vs SNR curve for $C = \frac{1}{3}$ and $M=16$ in Fading Channel

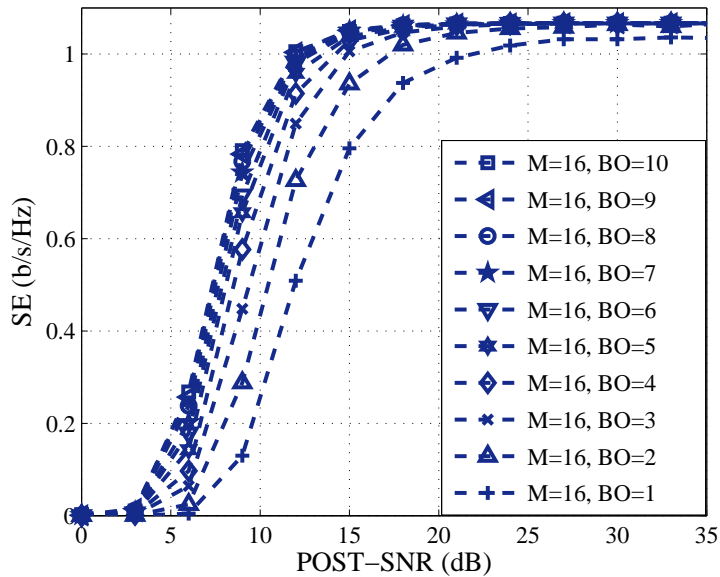


Figure A.12: Spectral Efficiency vs SNR curve for $C = \frac{1}{3}$ and $M=16$ in Fading Channel

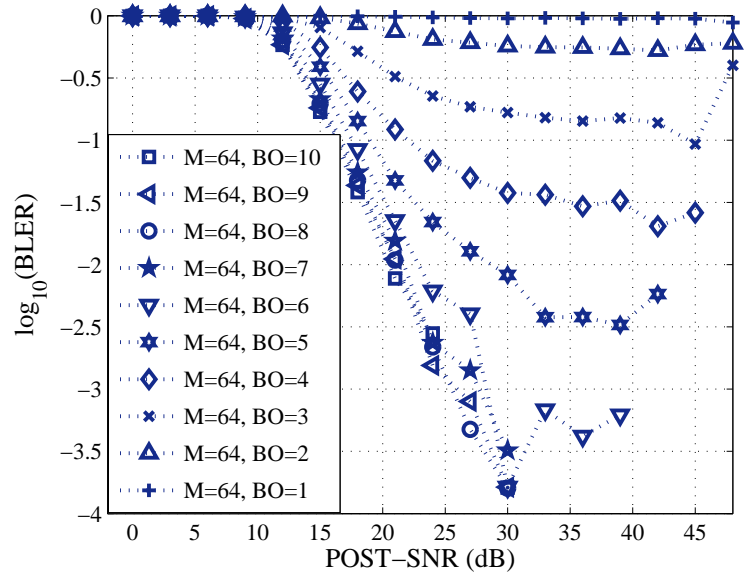


Figure A.13: BLER vs SNR curve for $C = \frac{1}{3}$ and $M=64$ in Fading Channel

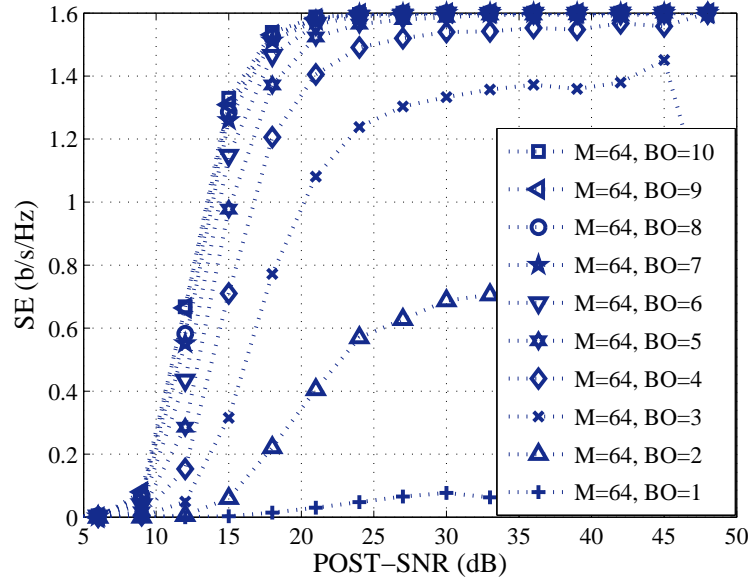


Figure A.14: Spectral Efficiency vs SNR curve for $C = \frac{1}{3}$ and $M=64$ in Fading Channel

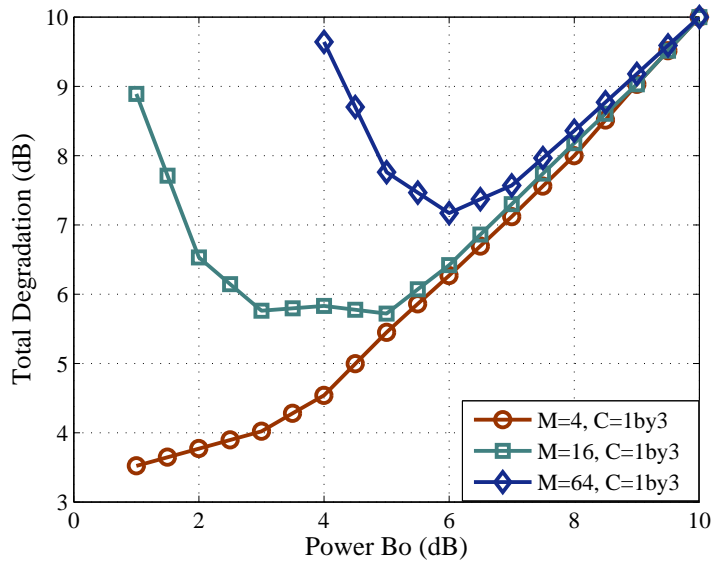


Figure A.15: TD plot for $FEC = \frac{1}{3}$ with BLER Threshold= 0.1 in Fading Channel

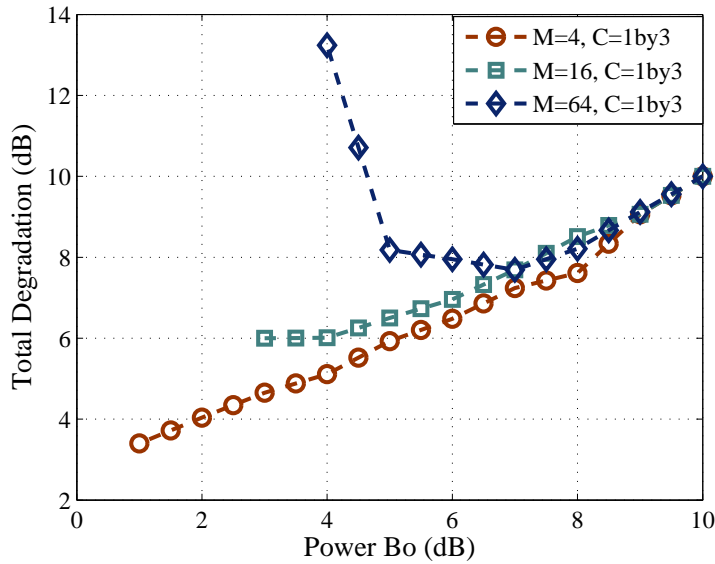


Figure A.16: TD plot for $FEC = \frac{1}{3}$ with BLER Threshold= 0.05 in Fading Channel

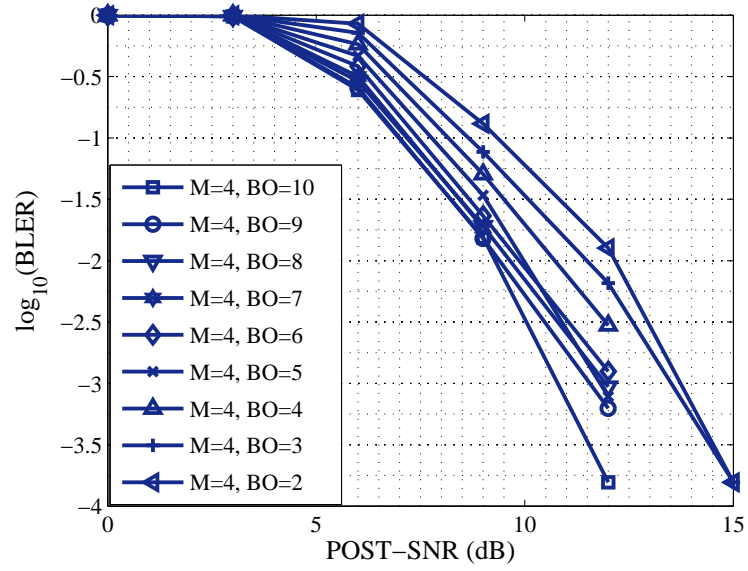


Figure A.17: BLER vs SNR curve for $C = \frac{2}{3}$ and $M = 4$ in AWGN

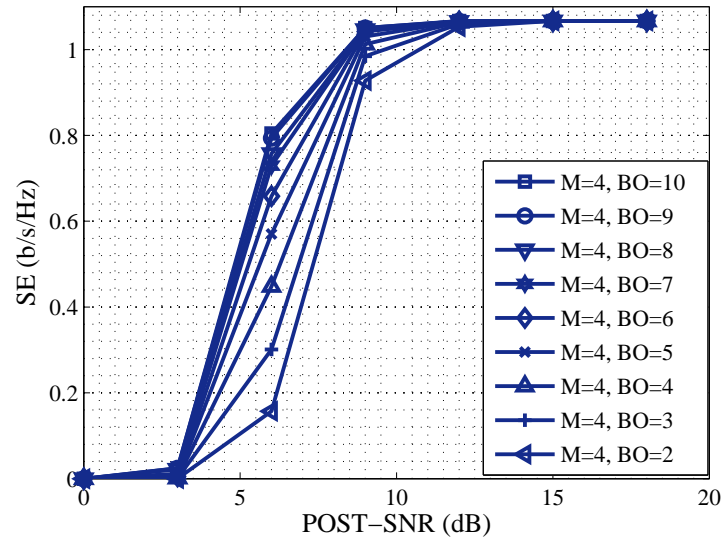


Figure A.18: Spectral Efficiency vs SNR curve for $C = \frac{2}{3}$ and $M = 4$ in AWGN

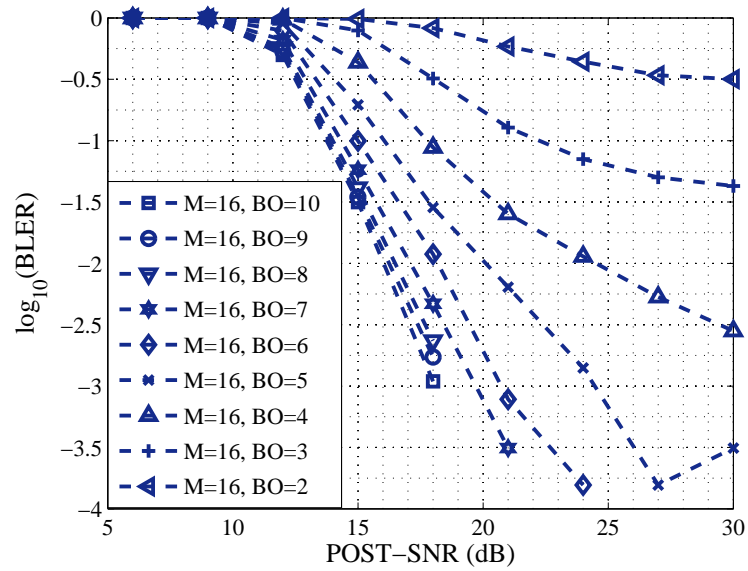


Figure A.19: BLER vs SNR curve for $C = \frac{2}{3}$ and $M = 16$ in AWGN

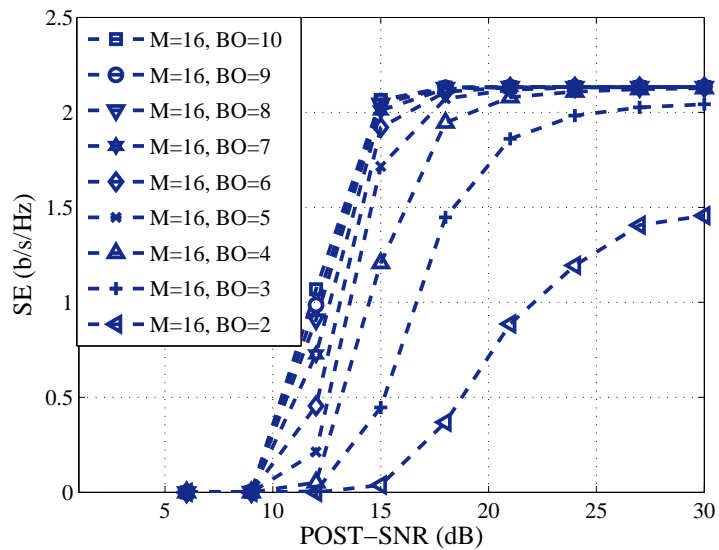


Figure A.20: Spectral Efficiency vs SNR curve for $C = \frac{2}{3}$ and $M = 16$ in AWGN

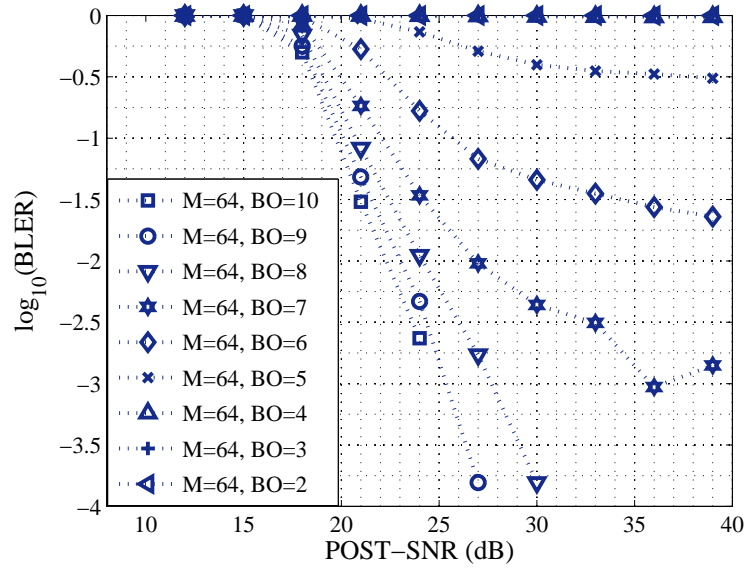


Figure A.21: BLER vs SNR curve for $C = \frac{2}{3}$ and $M= 64$ in AWGN

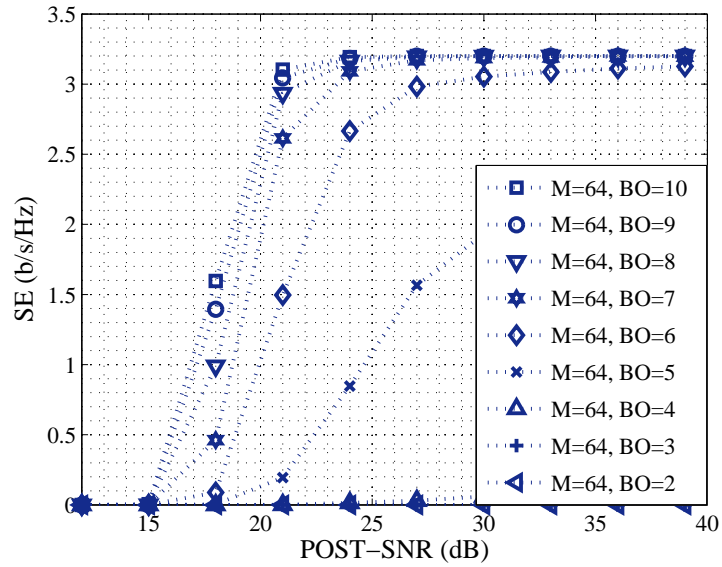


Figure A.22: Spectral Efficiency vs SNR curve for $C = \frac{2}{3}$ and $M= 64$ in AWGN

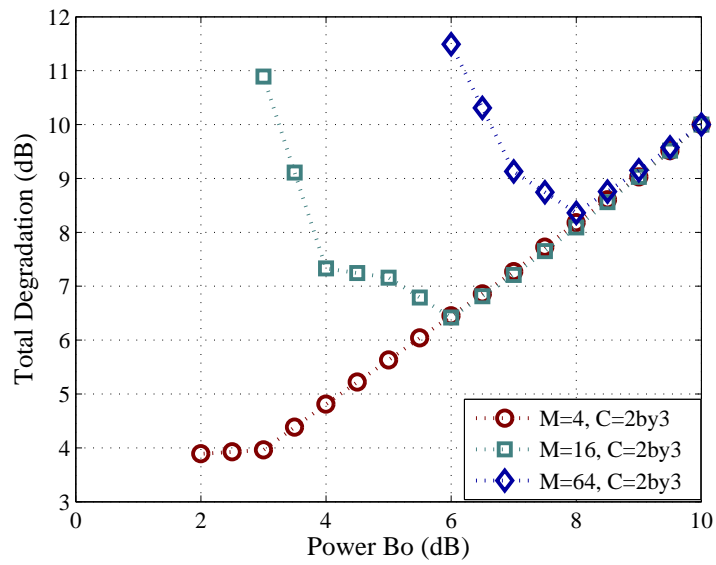


Figure A.23: TD plot for $FEC = \frac{2}{3}$ with BLER Threshold= 0.1 in AWGN

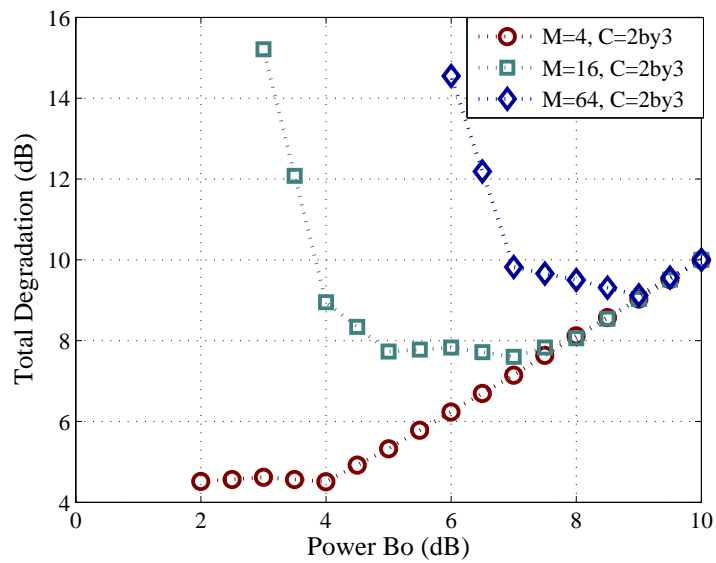


Figure A.24: TD plot for $FEC = \frac{2}{3}$ with BLER Threshold= 0.05 in AWGN

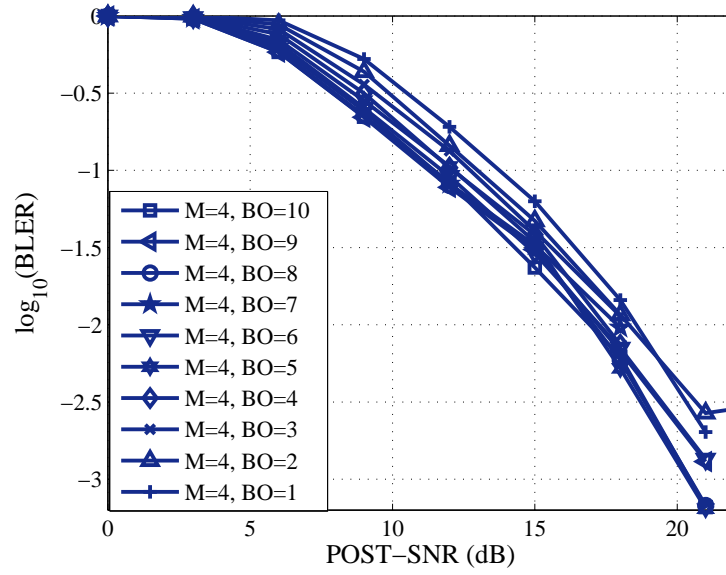


Figure A.25: BLER vs SNR curve for $C = \frac{2}{3}$ and $M=4$ in Fading Channel

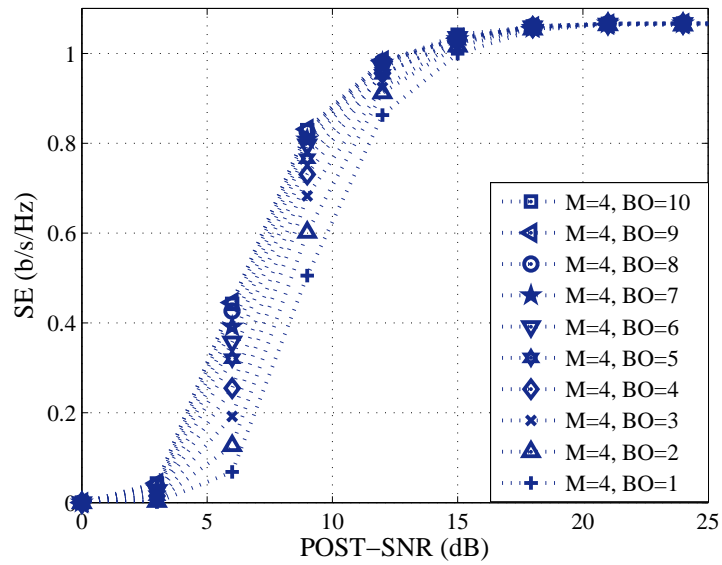


Figure A.26: Spectral Efficiency vs SNR curve for $C = \frac{2}{3}$ and $M=4$ in Fading Channel

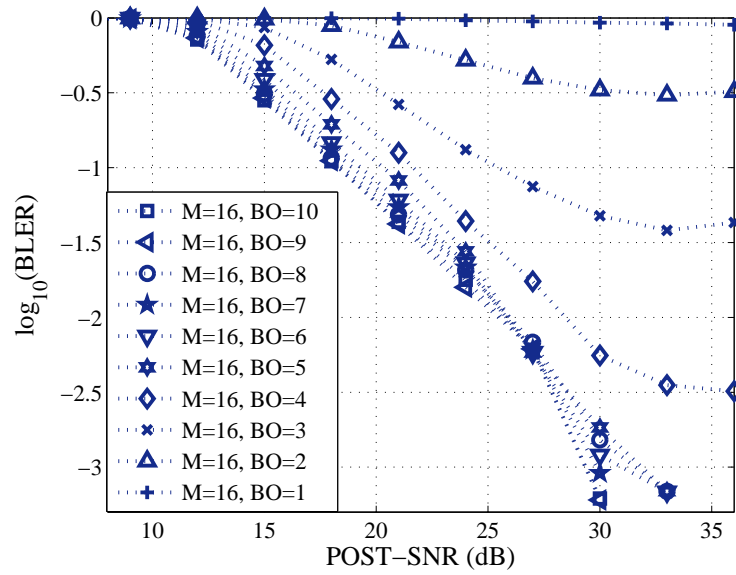


Figure A.27: BLER vs SNR curve for $C = \frac{2}{3}$ and $M=16$ in Fading Channel

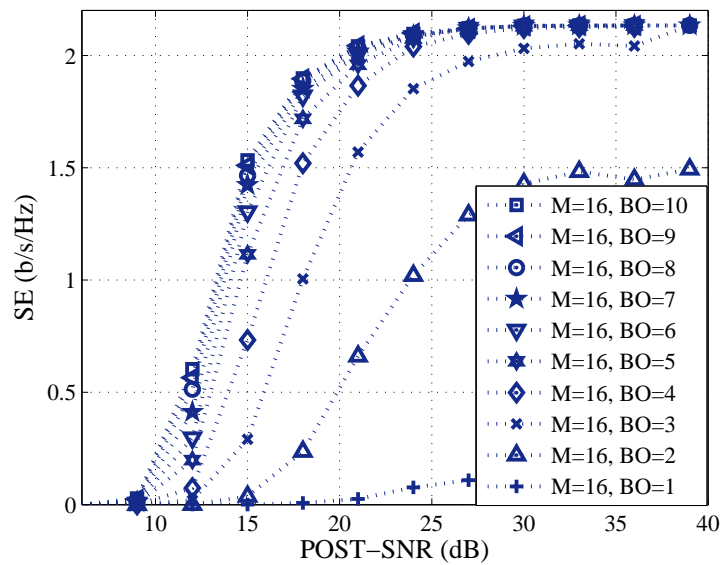


Figure A.28: Spectral Efficiency vs SNR curve for $C = \frac{2}{3}$ and $M=16$ in Fading Channel

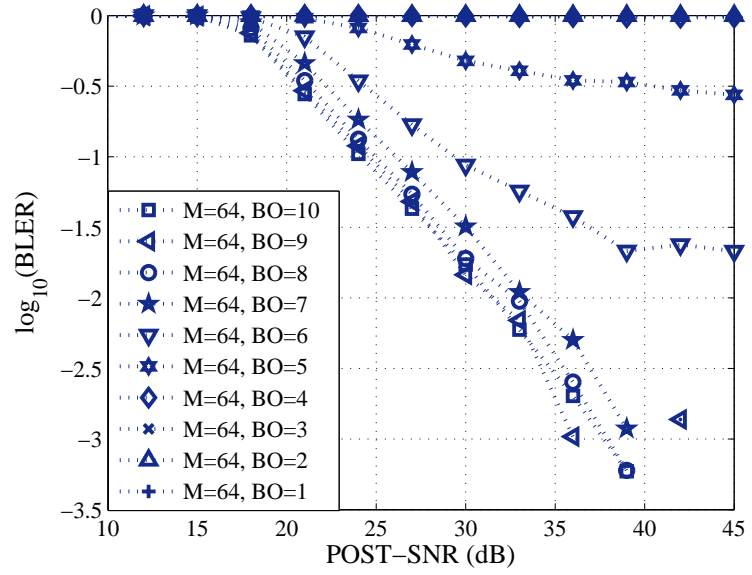


Figure A.29: BLER vs SNR curve for $C = \frac{2}{3}$ and $M= 64$ in Fading Channel

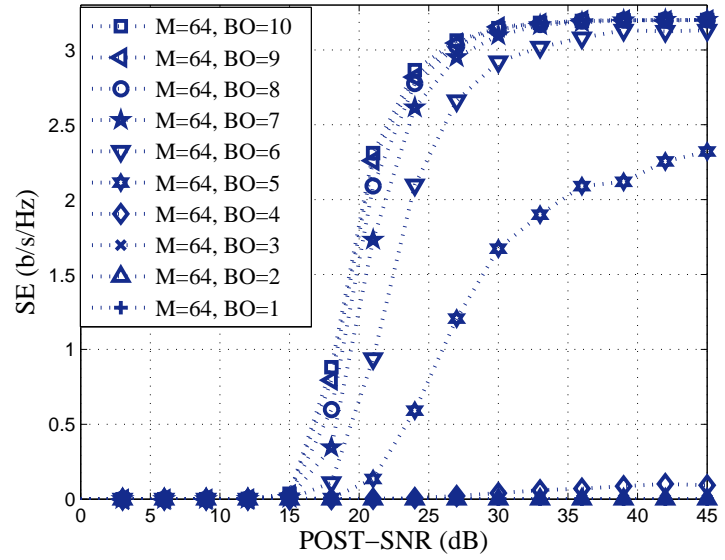


Figure A.30: Spectral Efficiency vs SNR curve for $C = \frac{2}{3}$ and $M= 64$ in Fading Channel

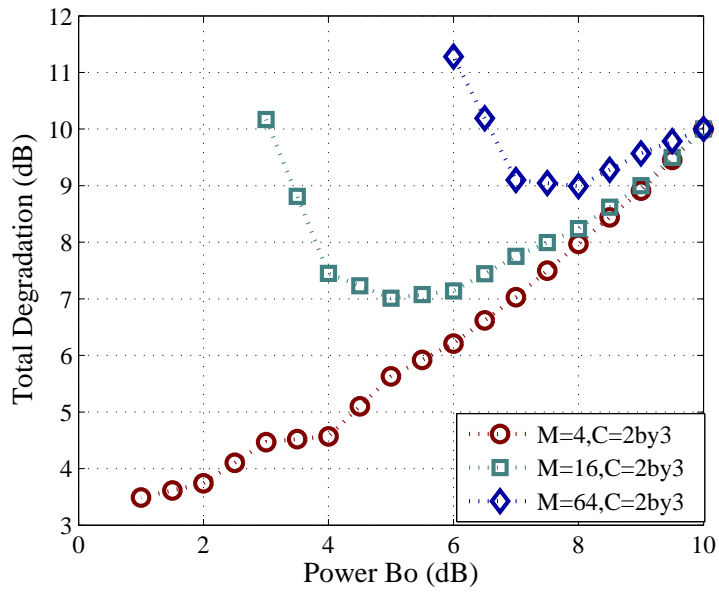


Figure A.31: TD plot for $FEC = \frac{2}{3}$ with BLER Threshold= 0.1 in Fading Channel

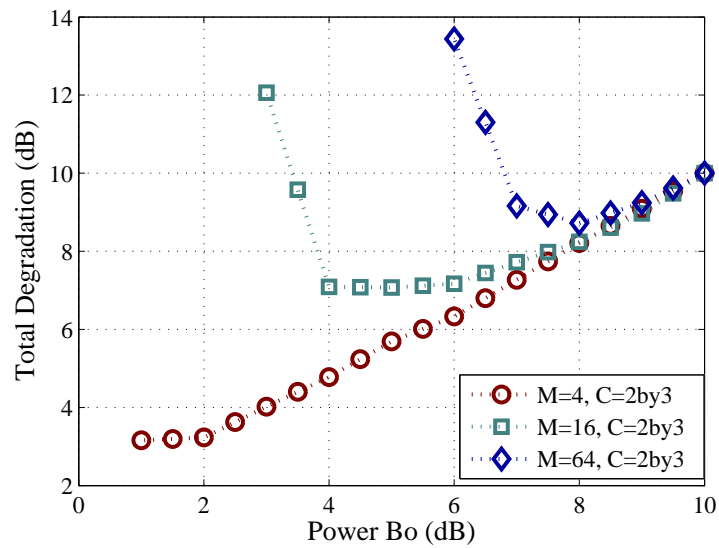


Figure A.32: TD plot for $FEC = \frac{2}{3}$ with BLER Threshold= 0.05 in Fading Channel

Appendix B

BER performance of Coded System

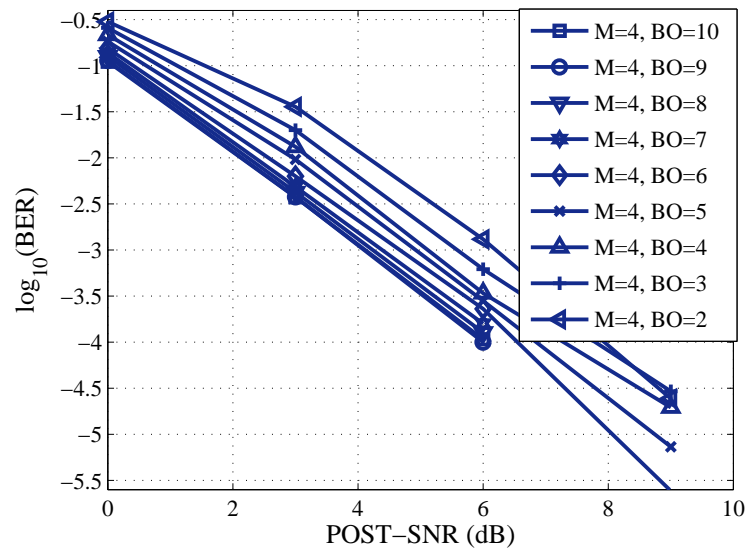


Figure B.1: BER vs SNR curve for $C = \frac{1}{3}$ and $M = 4$ in AWGN

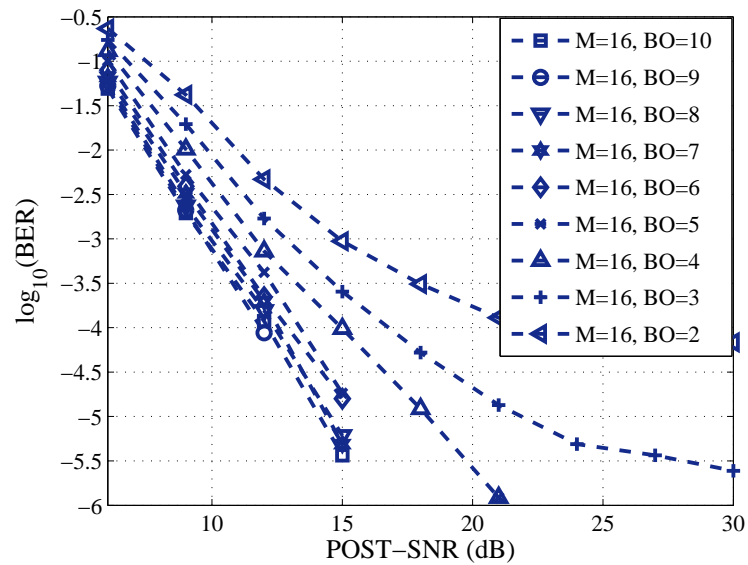


Figure B.2: BER vs SNR curve for $C = \frac{1}{3}$ and $M = 16$ in AWGN

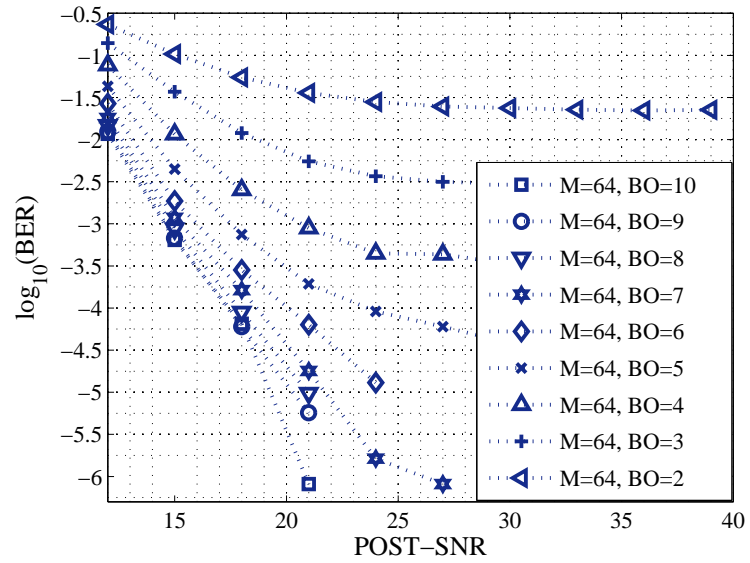


Figure B.3: BER vs SNR curve for $C = \frac{1}{3}$ and $M = 64$ in AWGN

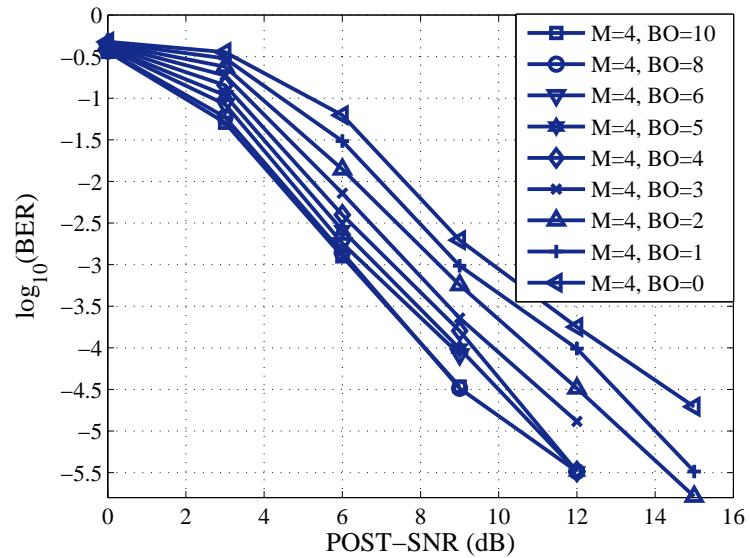


Figure B.4: BER vs SNR curve for $C = \frac{1}{2}$ and $M = 4$ in AWGN

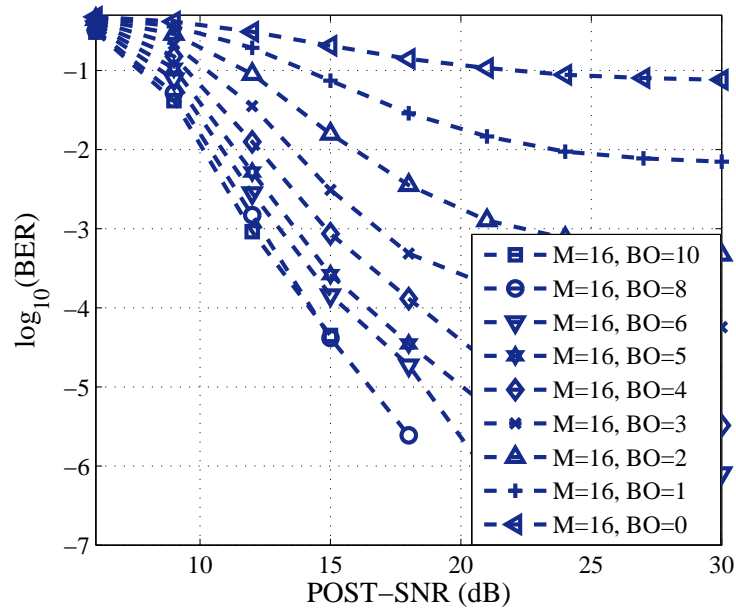


Figure B.5: BER vs SNR curve for $C = \frac{1}{2}$ and $M = 16$ in AWGN

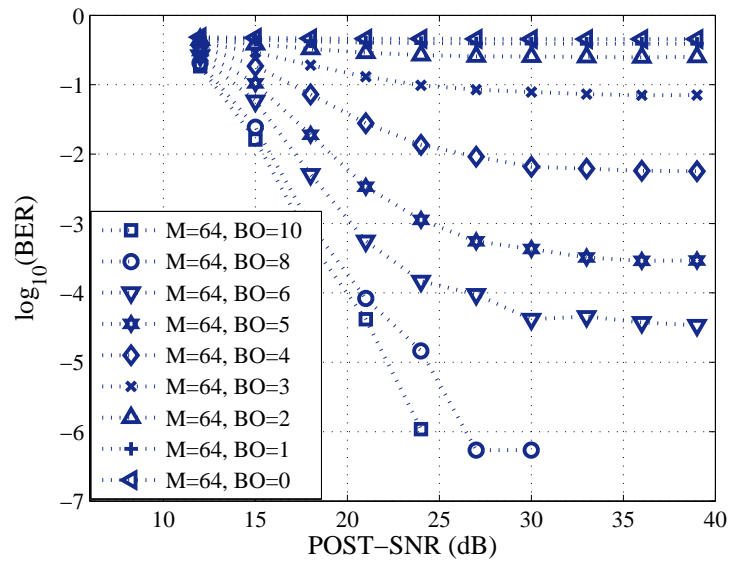


Figure B.6: BER vs SNR curve for $C = \frac{1}{2}$ and $M = 64$ in AWGN

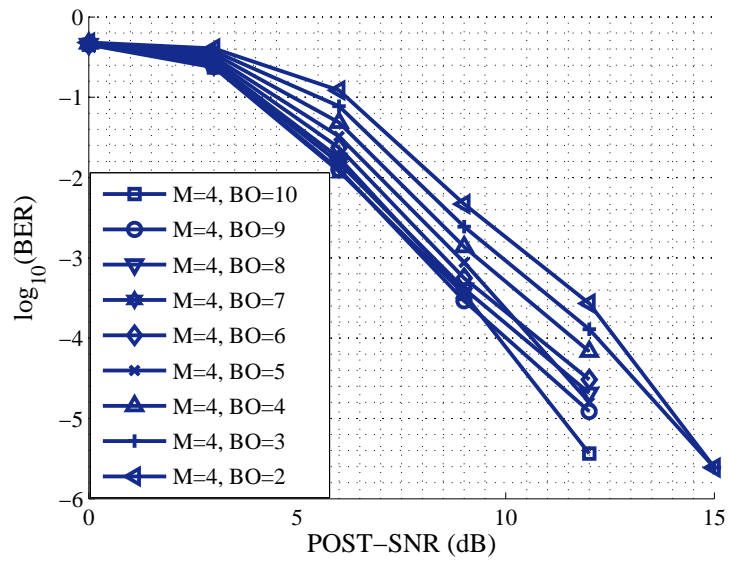


Figure B.7: BER vs SNR curve for $C = \frac{2}{3}$ and $M = 4$ in AWGN

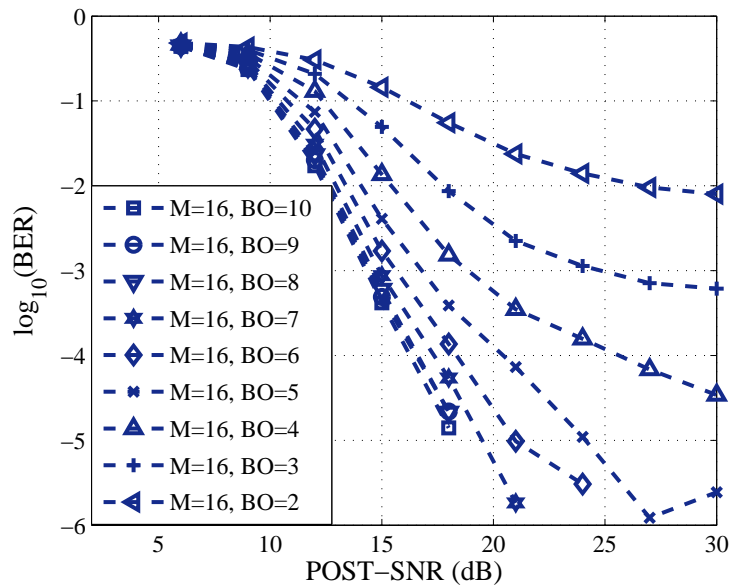


Figure B.8: BER vs SNR curve for $C = \frac{2}{3}$ and $M = 16$ in AWGN

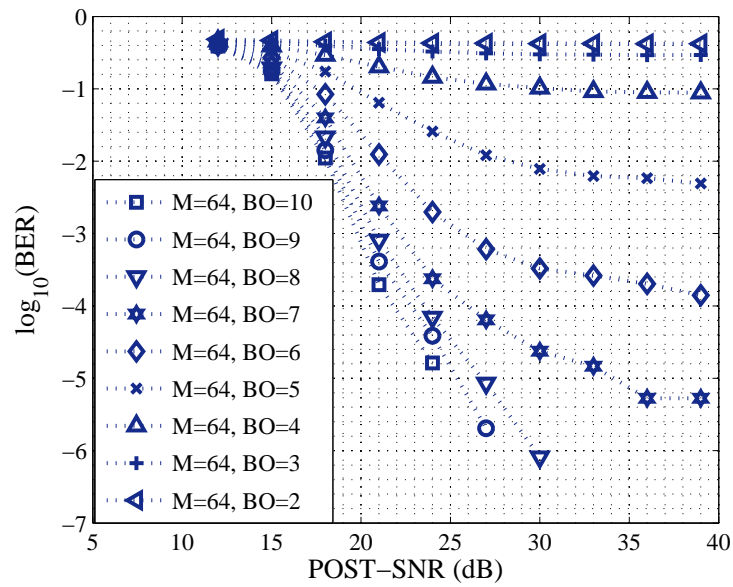


Figure B.9: BER vs SNR curve for $C = \frac{2}{3}$ and $M = 64$ in AWGN

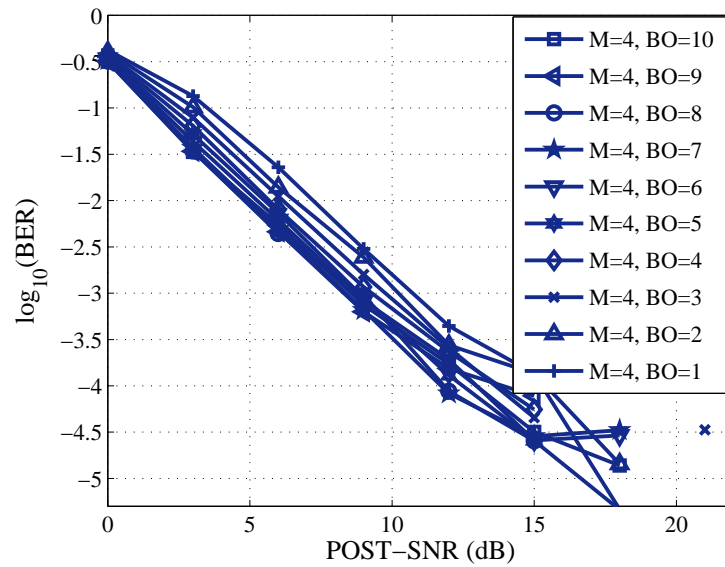


Figure B.10: BER vs SNR curve for $C = \frac{1}{3}$ and $M = 4$ in Fading Channel

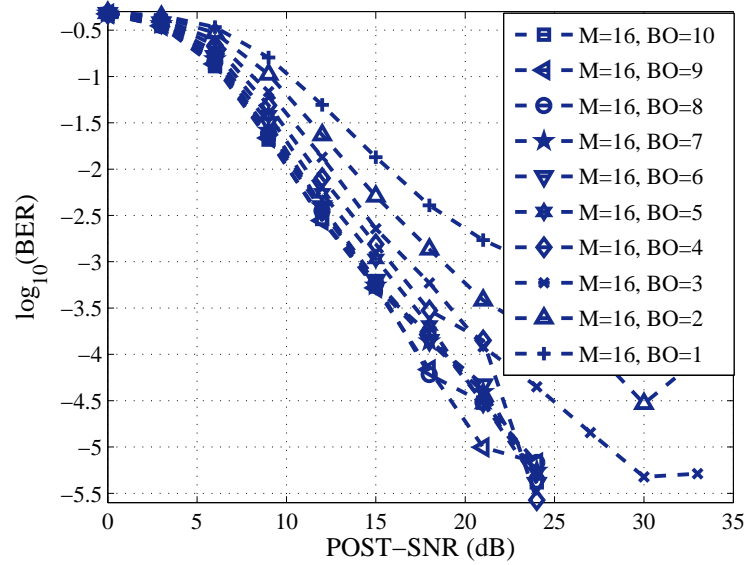


Figure B.11: BER vs SNR curve for $C = \frac{1}{3}$ and $M = 16$ in Fading Channel

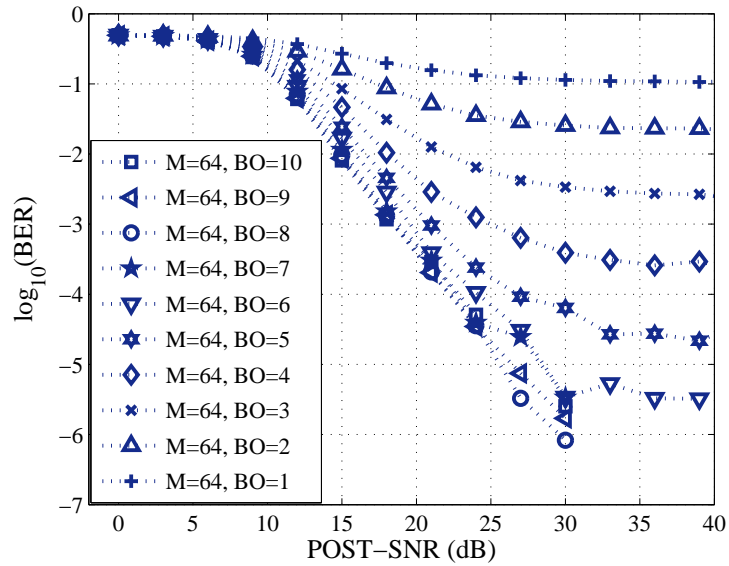


Figure B.12: BER vs SNR curve for $C = \frac{1}{3}$ and $M = 64$ in Fading Channel

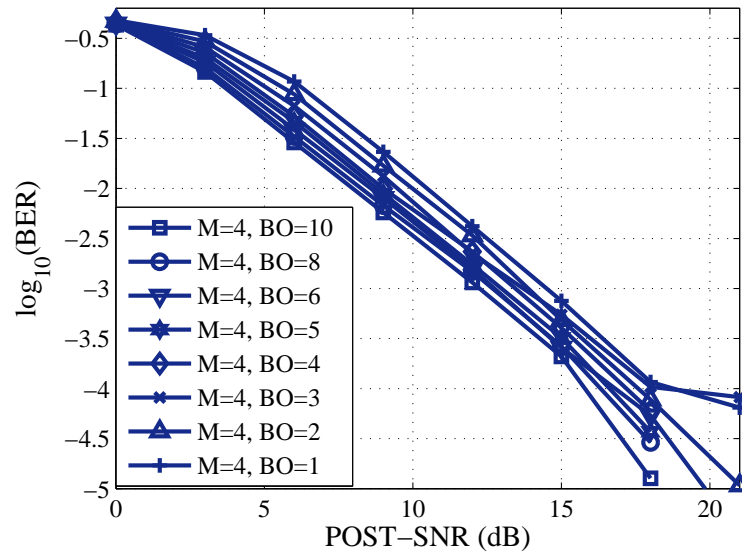


Figure B.13: BER vs SNR curve for $C = \frac{1}{2}$ and $M = 4$ in Fading Channel

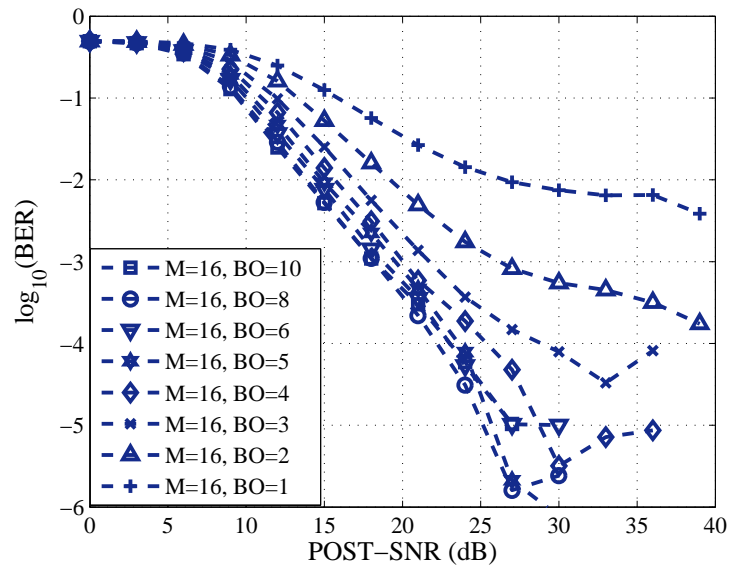


Figure B.14: BER vs SNR curve for $C = \frac{1}{2}$ and $M = 16$ in Fading Channel

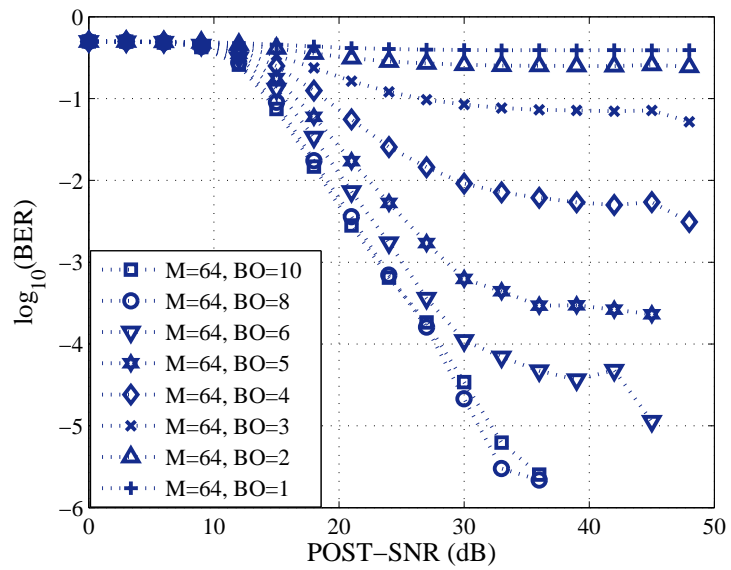


Figure B.15: BER vs SNR curve for $C = \frac{1}{2}$ and $M=64$ in Fading Channel

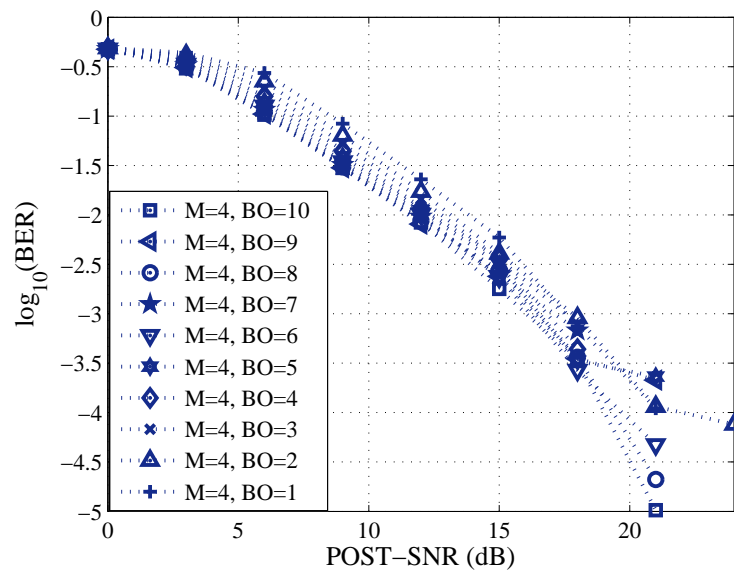


Figure B.16: BER vs SNR curve for $C = \frac{2}{3}$ and $M=4$ in Fading Channel

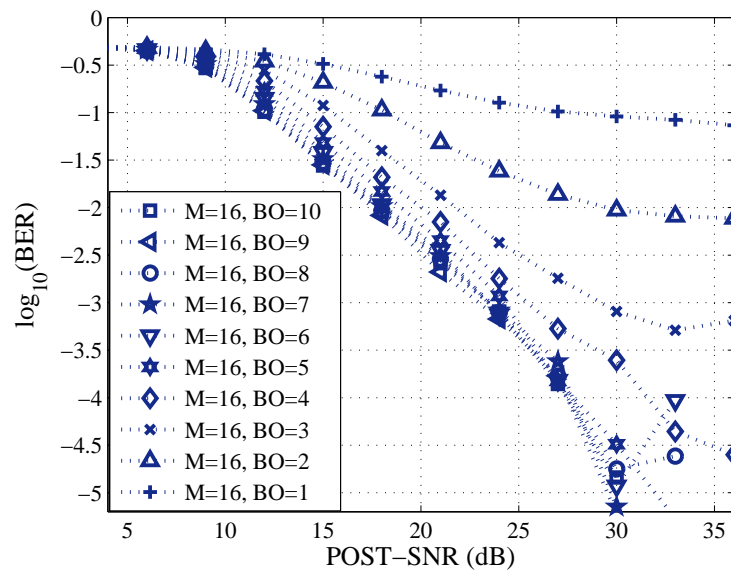


Figure B.17: BER vs SNR curve for $C = \frac{2}{3}$ and $M=16$ in Fading Channel

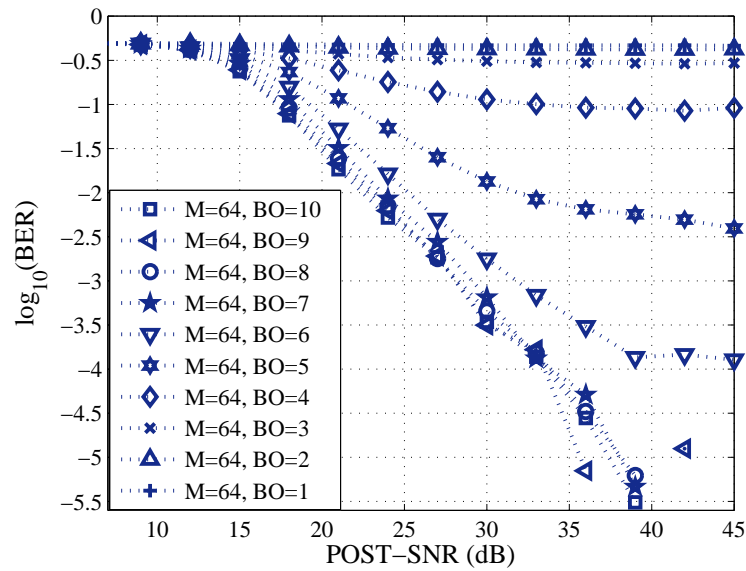


Figure B.18: BER vs SNR curve for $C = \frac{2}{3}$ and $M=64$ in Fading Channel

Bibliography

- [1] Ramjee Prasad , *OFDM for Wireless Communication*. Artech House Publishers, 2004.
- [2] S. Hara and R. Prasad, *Multicarrier Techniques for 4G Mobile Communications*. Artech House, 2003.
- [3] A. Goldsmith, *Wireless Communications*. Cambridge University Press, 2005.
- [4] T. S. Rappaport, *Wireless communications: Principles & practice*, 2nd ed. Prentice Hall, 2002.
- [5] M. I. Rahman, S. S. Das, and F. H. P. Fitzek, “OFDM Based WLAN Systems,,” Center for TeleInFrastruktur (CTIF), Aalborg University, Tech. Rep., 2004.
- [6] S. T. Chung and A. Goldsmith, “Adaptive multicarrier modulation for wireless systems,” *Thirty-Fourth Asilomar Conference on Signals, Systems and Computers*, vol. 2, pp. 1603 – 1607, Oct - Nov 2000.
- [7] S. H. Han and J. H. Lee, “An overview of peak-to-average power ratio reduction techniques for multicarrier transmission,” in *IEEE Wireless Communications*, vol. 12, no. 2, April 2005, pp. 56– 65.
- [8] S.S. Das, M.I. Rahman et al., “Influence of PAPR on Link Adaptation Algorithms in OFDM Systems,” in *IEEE VTC Spring’07*, Dublin, Ireland, 22-25 April 2007.
- [9] You Y.-H.; et al, “Training sequence design and channel estimation of OFDM-CDMA broadband wireless access networks with diversity techniques,” *IEEE Transactions on Broadcasting*, vol. 49, pp. 354–361.

- [10] Richard Van Nee and Ramjee Prasad, *OFDM Wireless Multimedia Communication*. Artech House Publishers, 2000.
- [11] S. B. Slimane, "Reducing the peak-to-average power ratio of OFDM signals through precoding," *IEEE Transactions on Vehicular Technology*, Apr. 2006.
- [12] A. Behravan and T. Eriksson, "PAPR and other measures for OFDM systems with nonlinearity," in *IEEE WPMC*, October 2003.
- [13] S. B. Slimane, "Peak-to-average power ratio reduction of OFDM signals using pulse shaping," in *Proceedings IEEE Global Telecommunications Conference*, vol. 3, Dec. 2000, pp. 1412 – 1416.
- [14] J. G. Proakis, *Digital Communications*. McGraw-Hill Book Co., 1995.
- [15] A. Molisch, *Wireless Communication*. IEEE Press, 2005.
- [16] B. A. Jati, C. F. Mayorga, Y. Wang, and N. H. Mahmood, "Exploiting channel dynamics for bit and power allocation," Aalborg Univeristy, Tech. Rep., 2006.
- [17] R. W. Chang, "Synthesis of Band Limited Orthogonal Signals for Multi-channel Data Transmission," in *Bell Syst. Tech. J.*, vol. 45, December 1966, pp. 1775–1796.
- [18] B. R. Salzberg, "Performance of an efficient parallel data transmission system," in *IEEE Trans. Comm.*, vol. 15, December 1967, pp. 805–813.
- [19] S. B. Weinstein and P. M. Ebert, "Data Transmission of Frequency Division Multiplexing Using The Discrete Frequency Transform," in *IEEE Trans. Comm.*, vol. 19, October 1971, pp. 623–634.
- [20] R. Peled and A. Ruiz., "Frequency Domain Data Transmission Using Reduced Computational Complexity Algorithms," in *IEEE International Conference on Acoustics, Speech, and Signal Processing*, Denver, USA, 1980, pp. 964–967.
- [21] D. Matic, "OFDM Synchronization and Wideband Power Measurements at 60 GHz for Future Wireless Broadband Multimedia Communications," Ph.D. dissertation, Aalborg University, Denmark, September 2001.

- [22] U.S. Jha, “Low Complexity Resource Efficient OFDM Based Transceiver Design,” Ph.D. dissertation, Aalborg University, Denmark, September 2002.
- [23] H. Rohling et al., “OFDM Air Interface for the 4th Generation of Mobile Communication Systems,” in *Proc. 6th International OFDM Workshop*, Hamburg, Germany, September 2001.
- [24] F. Alam, “Space Time Processing for Third Generation CDMA Systems,” Ph.D. dissertation, Virginia Polytechnic Institute & State University, November 2002.
- [25] 3GPP Technical Report, “Physical layer aspects for evolved Universal Terrestrial Radio Access (UTRA), (release 7),” 3GPP, Technical Report TR 25.814, v7.0.0 June,2006.
- [26] A. Toskala, H. Holma et al, “UTRAN Long Term Evolution in 3GPP,” in *proc. 17th IEEE PIMRC*, Helsinki, Finland, 9-11 September 2006.
- [27] N. Marchetti, E. Cianca & R. Prasad, “Low Complexity Transmit Diversity Scheme for SCFDE Transmissions over Time-Selective Channels,” in *proc. IEEE ICC (accepted for publication)*, Glasgow, Scotland, June 2007.
- [28] S. J. Vaughan-Nichols, “Achieving wireless broadband with wimax,” *IEEE Computer*, vol. 37, no. 6, pp. 10 – 13, 2004.
- [29] R. Baines, “The roadmap to mobile wimax,” *IEE Communications Engineer*, vol. 3, no. 4, pp. 30 – 34, Aug - Sept 2005.
- [30] H. Yaghoobi, “Scalable ofdma physical layer in ieee 802.16 wirelessman,” *Intel Technology Journal*, vol. 8, no. 3, pp. 201 – 212, 2004.
- [31] Paolo Banelli and Giuseppe Baruffa and Saverio Cacopardi, “Effect of HPA Non Linearity on Frequency Multiplexed OFDM Signals,” in *IEEE Transaction on Broadcasting*, vol. 47, no. 2, June 2001, pp. 123–136.
- [32] G Santella and F Mazzenga, “ A hybrid analytical-simulation procedure for performance evaluationin M-QAM-OFDM schemes in presence of nonlinear distortions,” in *IEEE Transactions on Vehicular Technology*, vol. 47, no. 1, February 1998, pp. 142–151.

- [33] Adel A. M. Saleh, "Frequency-Independent and Frequency-Dependent Nonlinear Models of TWT Amplifiers," in *IEEE Transaction on Communication*, vol. COM-29, no. 11, November 1981, pp. 1715–1720.
- [34] C. Rapp, "Effects of HPA-nonlinearity on a 4-DPSK/OFDM-signal for a digital sound broadcasting signal," in *ESA, Second European Conference on Satellite Communications (ECSC-2) p 179-184 (SEE N92-15210 06-32)*, Oct. 1991, pp. 179–184.
- [35] J. Thomas, "Overview of amplifier technology choices for ground based ka-band amplifiers," in *5th Ka Band Utilization Conference*.
- [36] Chevillat, P. Jelitto, J. Barreto, A.N. Truong, H.L., "A dynamic link adaptation algorithm for IEEE 802.11 a wireless LANs," in *IEEE International Conference on Communications*, May 2003.
- [37] S. Chung and A. Goldsmith, "Degrees of freedom in adaptive modulation: a unified view," in *IEEE Trans. Comm.*
- [38] M Lei and P Zhang and Harada Hiroshi and Wakana Hiromitsu, "An adaptive power distribution algorithm for improving spectral efficiency in OFDM," in *IEEE trans. broadcast.*, 2004, pp. 347–351.
- [39] A.T. Toyserkani et al., "Sub-carrier based Adaptive Modulation in HIPERLAN/2 System," *IEEE ICC'04*, vol. 6, pp. 3460 – 3464, June 2004.
- [40] Nidcha Pongsuwanich, "PAPR Issues in Link Adaptation for WiMAX like OFDM Systems," Aalborg Univeristy, Tech. Rep., 2006.

Vita

Faisal Tariq was born in Rajshahi, Bangladesh on July 22, 1977. He received his BSc and MSc degree in Applied Physics and Electronics from Rajshahi University, Bangladesh in 2000 and 2002 respectively. From 2002 he served as a lecturer in Information and Communication Engineering Department of the same university until he started the MS program at Chalmers University of Technology, Sweden in 2005. He worked as guest researcher at CTIF, Aalborg University from September 2006 to March 2007. His research interest includes Multi Antenna Multiple Access Technology for future Wireless Communication system, link adaptation and resource allocation, Network Coding and Information Theory etc. He is a student member of IEEE Sweden Branch.

Permanent Address: Department of Signals and Systems
Chalmers University of Technology
Sweden

This thesis was typeset with L^AT_EX 2_ε¹ by the author.

¹L^AT_EX 2_ε is an extension of L^AT_EX. L^AT_EX is a collection of macros for T_EX. T_EX is a trademark of the American Mathematical Society. The macros used in formatting this thesis were written by Dinesh Das, Department of Computer Sciences, The University of Texas at Austin, and extended by Bert Kay, James A. Bednar, and Ayman El-Khashab.